

March 2017

Design and Analysis of the Sphinx-NG CubeSat

Daniel James Pelgrift
Worcester Polytechnic Institute

Dong Hyun Ko
Worcester Polytechnic Institute

Matthew Francis Murphy
Worcester Polytechnic Institute

Samuel Adam Young
Worcester Polytechnic Institute

Steven Charles Laudage
Worcester Polytechnic Institute

Follow this and additional works at: <https://digitalcommons.wpi.edu/mqp-all>

Repository Citation

Pelgrift, D. J., Ko, D. H., Murphy, M. F., Young, S. A., & Laudage, S. C. (2017). *Design and Analysis of the Sphinx-NG CubeSat*. Retrieved from <https://digitalcommons.wpi.edu/mqp-all/30>

This Unrestricted is brought to you for free and open access by the Major Qualifying Projects at Digital WPI. It has been accepted for inclusion in Major Qualifying Projects (All Years) by an authorized administrator of Digital WPI. For more information, please contact digitalwpi@wpi.edu.

Design and Analysis of the Sphinx-NG CubeSat

A Major Qualifying Project Report
Submitted to the Faculty of the
WORCESTER POLYTECHNIC INSTITUTE
in Partial Fulfillment of the Requirements for the
Degree of Bachelor of Science
in Aerospace Engineering

by



Dong Hyun Ko



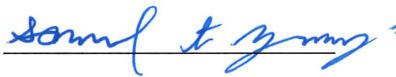
Steven Laudage



Matthew Murphy



Dan Pelgrift



Samuel Young

March 24, 2017

Approved by: 

Professor John J. Blandino, Advisor
Aerospace Engineering Program
WPI

Abstract

A CubeSat was designed to support a mission to perform solar and X-ray spectroscopy using the Sphinx-NG instrument. The work consisted of designing the electric power (EPS), telecommunication, computer and data handling (C&DH), and thermal control subsystems. C&DH system design included estimating memory and computational requirements for each operational mode. A power budget was generated for the spacecraft and the solar arrays were sized to generate a maximum power of 12.4 W. The telecommunication subsystem was designed supporting a downlink capability of approximately 101 Mb/day. A thermal model included time-dependent spacecraft illumination and internal power generation. Results were used to estimate the range of spacecraft temperatures and evaluate thermal control options.

"Certain materials are included under the fair use exemption of the U.S. Copyright Law and have been prepared according to the fair use guidelines and are restricted from further use."

Acknowledgements

We would like to thank the following individuals and groups for their help and support throughout the entirety of this project.

Project Advisor Professor Blandino

ADC Team Professor Demetriou
 Jack Agolli
 James Gadoury
 Andrew Rathbun

Mechanical Team Professor Gatsonis
 Emily Curci
 Jarrett Jacobson
 Weston Schlack
 Kelley Slabinski

Table of Authorship

Section	Author
<i>1 Introduction</i>	
1.0, 1.1	SL
1.2	DP
1.3	MM
1.4	SY
<i>2 Background</i>	
2.1	SL
2.2	DP
2.3	MM
2.4.1	SY
2.4.2	DK
2.4.3	DK
2.4.4	DK
<i>3 Methodology</i>	
3.1 (except 3.1.2: <i>CubeSat Functionality</i>)	SL
3.1.2: <i>CubeSat Functionality</i>	MM
3.2	DP
3.3	MM
3.4.1	DK
3.4.2	SY
3.4.3	DK
3.4.4	DK
<i>4 Results</i>	

4.1 (except 4.1.2: <i>CubeSat Functionality</i>)	SL
4.1.2: <i>CubeSat Functionality</i>	MM
4.2	DP
4.3	MM
4.4	DK
<i>5 Conclusions & Recommendations</i>	
5.1	SL
5.2	DP
5.3	MM
5.4	SY
<i>Appendix A</i>	MM
<i>Appendix B</i>	SL
<i>Appendix C</i>	SL
<i>Appendix D</i>	DP
<i>Appendix E</i>	DP
<i>Appendix F</i>	DP

Table of Contents

Abstract	0
Acknowledgements	1
Table of Authorship	2
Table of Contents	4
List of Figures	7
List of Tables	10
Executive Summary	11
1 Introduction	13
1.1 The CubeSat MQP	13
1.2 Project Goals and Objectives	15
1.3 Command and Data Handling Subsystem Objectives	15
1.4 Power Subsystem Objectives	16
1.5 Telecommunications Subsystem Objectives	17
1.6 Thermal Control Subsystem Objectives	17
2 Background	19
2.1 Command and Data Handling Subsystem	19
2.1.1 Previous WPI Research.....	20
2.1.2 Hardware and Software.....	21
2.1.3 Data Interfacing	23
2.2 Power Subsystem	28
2.2.1 CubeSat MQP 2013 Final Power Budget	28
2.2.2 Power Subsystem Hardware	29
2.2.3 Power Subsystem Related Interface Control Document (ICD) Requirements	32
2.3 Telecommunications Subsystem	35
2.3.1 Interface Control Document (ICD) Requirements.....	35
2.3.2 Hardware.....	36
2.3.3 Ground Stations	39
2.4 Thermal Control Subsystem	41
2.4.1 Thermal Environment	41
2.4.2 Thermal Limits.....	43
2.4.3 Thermal Controls	44
2.4.4 COMSOL Multiphysics	49
3 Methodology	50
3.1 Command and Data Handling Subsystem	50
3.1.1 System Requirements.....	50

3.1.2	Hardware & Software Definition.....	51
3.1.3	Computing Profile Modeling.....	58
3.2	Power Subsystem	62
3.2.1	Power System Evaluation.....	62
3.2.2	Power Component Selection.....	63
3.2.3	Power System Distribution.....	64
3.2.4	Telemetry Communication.....	68
3.2.5	Power Profile Modeling.....	68
3.3	Telecommunications Subsystem.....	69
3.3.1	Ground Station Network Analysis.....	69
3.3.2	Second Mobile Ground Station Case Study.....	72
3.3.3	STK Analysis.....	74
3.4	Thermal Controls Subsystem	79
3.4.1	STK Analysis.....	79
3.4.2	CubeSat CAD Model.....	82
3.4.3	COMSOL Multiphysics.....	87
3.4.4	Iterative Thermal Analysis and Design.....	101
4	Results.....	103
4.1	Command & Data Handling Subsystem	103
4.1.1	System Requirements.....	103
4.1.2	Hardware & Software Definition.....	104
4.1.3	Computing Profile Modeling.....	116
4.2	Power Subsystem	127
4.2.1	Final Hardware Configuration.....	127
4.2.2	Final Wiring Results.....	131
4.2.3	Power Profile Results.....	133
4.3	Telecommunications Subsystem.....	142
4.3.1	Mission Modeling and Timelines.....	142
4.3.2	Communication Hardware.....	147
4.4	Thermal Subsystem	147
4.4.1	CubeSat Thermal Limits.....	147
4.4.2	Initial Result.....	148
4.4.3	Surface Finishes.....	155
4.4.4	Recommended Thermal Control System Design.....	160
5	Conclusions & Recommendations.....	161
5.1	Command & Data Handling Subsystem	161
5.2	Power Subsystem	162
5.3	Telecommunications Subsystem.....	162
5.4	Thermal Subsystem.....	163

Works Cited.....	167
Appendices.....	173
Appendix A: GENSO Ground Stations [34].....	173
Appendix B: Subsystem and Sensor Computing Requirements.....	176
Appendix C: Subsystem Commands	180
Appendix D: Subsystem and Sensor Data Processing Calculations.....	181
Appendix E: CubeSat Main Header Connections.....	186
Appendix F: CubeSat Wiring Diagrams.....	188

List of Figures

FIGURE 1: SPHINX-NG CUBESAT	13
FIGURE 2: CLYDE SPACE ON-BOARD COMPUTER [14] COPYRIGHT 2016 © CLYDE SPACE LTD.....	21
FIGURE 3: CUBESAT STACK [7].....	24
FIGURE 4: INTER-INTEGRATED CIRCUIT BUS [17] COPYRIGHT © 2016 I2C INFO.....	25
FIGURE 5: SERIAL PERIPHERAL INTERFACE BUS [18] COPYRIGHT © 2006 COLIN M.L. BURNETT	26
FIGURE 6: SOLAR ARRAY CURRENT VS. VOLTAGE [23]. COPYRIGHT © 2016 CLYDE SPACE LTD.....	30
FIGURE 7: EPS POWER FLOW	31
FIGURE 8: LOCATION OF DEPLOYMENT SWITCHES [24] COPYRIGHT © 2011 CAL POLY SLO.....	33
FIGURE 9: LOCATION OF ACCESS PORT FOR 3U CUBESAT [24] COPYRIGHT © 2011 CAL POLY SLO	34
FIGURE 10: TELECOMMUNICATIONS SUBSYSTEM BLOCK DIAGRAM	37
FIGURE 11: ISIS UHF/VHF TRANSCEIVER [32] COPYRIGHT © 2017 CUBESATSHOP.COM.....	38
FIGURE 12: ISIS DIPOLE DEPLOYABLE ANTENNA [35] COPYRIGHT ©2017 INNOVATIVE SOLUTIONS IN SPACE.	39
FIGURE 13: 2014 CUBESAT GROUND COVERAGE MAP [1].....	41
FIGURE 14: SURFACE ABSORPTIVITY AND EMISSIVITY OF VARIOUS TYPES OF MATERIALS [41] COPYRIGHT © 2017 THE AEROSPACE PRESS	45
FIGURE 15: SCHEMATIC OF LOUVER ASSEMBLY [42] COPYRIGHT © 2002 AIAA	48
FIGURE 16: SCHEMATIC OF HEAT PIPE SYSTEM [42] COPYRIGHT © 2002 AIAA	48
FIGURE 17: C&DH BLOCK DIAGRAM EXAMPLE.....	52
FIGURE 18: MISSION PHASES	54
FIGURE 19: UNIVERSITY OF MICHIGAN FUNCTIONAL MODEL METHODOLOGY [45] © IEEE 2012	55
FIGURE 20: SYSTEM STATE MODEL	59
FIGURE 21: VOLATILE MEMORY STORAGE MODEL.....	60
FIGURE 22: NON-VOLATILE MEMORY STORAGE MODEL.....	61
FIGURE 24: EXAMPLE SOLAR ARRAY CONFIGURATION SA1-3 [23] COPYRIGHT © 2016 CLYDE SPACE LTD.	65
FIGURE 25: EPS BOARD POWER FLOW	67
FIGURE 26: STK GROUND STATION GROUND TRACK	70
FIGURE 27: BUILT UNIVERSITY OF HAWAII AT MANOA MOBILE GROUND STATION [50]	71
FIGURE 28: SECOND MGS CASE STUDY STK SCENARIO	73
FIGURE 29: SAMPLE LINK BUDGET REPORT.....	76
FIGURE 30: STK ACCESS TIME REPORT	78
FIGURE 31: ACCESS TIME VS. TIME OF YEAR.....	79
FIGURE 32: CUBESAT BODY COORDINATE SYSTEM USING THE RHR [1] COPYRIGHT © 2013 WPI	81
FIGURE 33: ILLUSTRATION OF <i>SUN ALIGNMENT WITH NADIR CONSTRAINT</i> ORIENTATION	81
FIGURE 34: 2013 MQP CUBESAT SOLAR PANEL HINGE [1] COPYRIGHT © 2013 WPI.....	84
FIGURE 35: CLYDE SPACE HINGE FOR MOUNTING SOLAR PANELS TO CUBESAT BODY [7] COPYRIGHT © 2016 CLYDE SPACE LTD.	84
FIGURE 36: SIMPLIFIED HINGE FOR MOUNTING CUBESAT TO BODY.....	85
FIGURE 37: MQP SIMPLIFIED SOLAR PANEL AND CELLS	85
FIGURE 38: MQP SIMPLIFIED EXTERNAL STRUCTURE	86
FIGURE 39: SIMPLIFIED CIRCUIT STACK WITH HEAT DISSIPATING COMPONENTS	87
FIGURE 40: VIEW FACTOR AS A FUNCTION OF B AND ALTITUDE [52].....	89
FIGURE 41: FRONT VIEW OF CUBESAT IN COMSOL	91
FIGURE 42: REAR VIEW OF CUBESAT IN COMSOL	91
FIGURE 43: OPERATION OF THE HEATER [58] © 2016 CLYDE SPACE LTD.....	98
FIGURE 44: BOUNDARIES SELECTED FOR SURFACE-TO-SURFACE RADIATION	99
FIGURE 45: ITERATIVE PROCESS OF THERMAL ANALYSIS AND DESIGN	101

FIGURE 46: SPHINX-NG MISSION OPERATIONAL STATES	104
FIGURE 47: P-POD DEPLOYMENT OPERATIONAL STATE	105
FIGURE 48: DETUMBLE OPERATIONAL STATE.....	107
FIGURE 49: INITIAL ATTITUDE DETERMINATION AND SUN ACQUISITION OPERATIONAL STATE.....	108
FIGURE 50: ROUTINE OPERATIONAL STATE	110
FIGURE 51: SYSTEM DEACTIVATION & ORBIT DECAY OPERATIONAL STATE	111
FIGURE 52: REQUEST PAYLOAD DATA DIAGRAM	112
FIGURE 53: REQUEST TELEMETRY DIAGRAM.....	113
FIGURE 54: TOTAL FUNCTION LIST [45].....	114
FIGURE 55: COMMAND AND DATA HANDLING SUBSYSTEM BLOCK DIAGRAM	115
FIGURE 56: SUN AND GROUND STATION EXPOSURE	118
FIGURE 57: SUBSYSTEM AND SENSOR STATES	120
FIGURE 58: SIMULATION OF INDIVIDUAL USERS OF MRAM.....	123
FIGURE 5918: SIMULATION OF SUM OF ALL USERS OF MRAM	124
FIGURE 60: SIMULATION OF INDIVIDUAL USERS OF FLASH MEMORY	125
FIGURE 61: SIMULATION OF SUM OF ALL USERS OF MRAM	126
FIGURE 62: CLYDE SPACE 3U EPS [23] COPYRIGHT © 2016 CLYDE SPACE LTD.	128
FIGURE 63: CLYDE SPACE 40 W-HR CUBESAT BATTERY [59] COPYRIGHT © 2016 CLYDE SPACE LTD.	129
FIGURE 19: PUMPKIN CUBESATKIT PROTOBOARD [61] COPYRIGHT © 2007 PUMPKIN INC.	132
FIGURE 65: RADIO & SPHINX-NG POWER STATES	134
FIGURE 66: SUM OF TOTAL CURRENT DRAW (30 W-HR).....	135
FIGURE 67: SUM OF TOTAL CURRENT DRAW (40 W-HR).....	135
FIGURE 68: SOLAR PANEL TEMPERATURE.....	137
FIGURE 69: SOLAR PANEL POWER PRODUCTION	137
FIGURE 70: SUM OF CONSTANT POWER CONSUMPTION	139
FIGURE 71: BATTERY CHARGE VS. TIME.....	140
FIGURE 72: ALTERED RADIO & SPHINX-NG STATE VECTORS	141
FIGURE 73: BATTERY CHARGE (ALTERED SPHINX-NG STATE VECTOR)	141
FIGURE 74: ANNUAL ACCESS TIME PER GROUND STATION	142
FIGURE 75: ANNUAL ACCESS TIME PER STATION	143
FIGURE 76: ANNUAL DOWNLINK PER STATION	143
FIGURE 77: FINAL ANNUAL DOWNLINK BUDGET PER STATION	146
FIGURE 78: FINAL ANNUAL ACCESS TIME PER STATION.....	146
FIGURE 79: SNAPSHOT OF 3-D EXTERNAL TEMPERATURE GRAPH (T = 10476 SEC)	149
FIGURE 80: SNAPSHOT OF 3-D EXTERNAL TEMPERATURE GRAPH (T = 13130 SEC)	149
FIGURE 81: SNAPSHOT OF 3-D CIRCUIT STACK TEMPERATURE GRAPH (T = 10476 SEC).....	150
FIGURE 82: SNAPSHOT OF 3-D CIRCUIT STACK TEMPERATURE GRAPH (T = 13130 SEC).....	150
FIGURE 83: AVERAGE TEMPERATURE VS. TIME FOR EXTERNAL DOMAINS	152
FIGURE 84: AVERAGE TEMPERATURE VS. TIME FOR CIRCUIT BOARDS	152
FIGURE 85: AVERAGE TEMPERATURE VS. TIME FOR COMPONENTS	153
FIGURE 86: TEMPERATURE RANGE AND LIMITS.....	154
FIGURE 87: AVERAGE TEMPERATURE VS. TIME FOR EXTERNAL DOMAINS (E = 0.3).....	156
FIGURE 88: AVERAGE TEMPERATURE VS. TIME FOR EXTERNAL DOMAINS (E = 0.5).....	157
FIGURE 89: AVERAGE TEMPERATURE VS. TIME FOR EXTERNAL DOMAINS (E = 0.7).....	157
FIGURE 90: AVERAGE TEMPERATURE VS. TIME FOR EXTERNAL DOMAINS (E = 0.9).....	158
FIGURE 91: TEMPERATURE RANGE AND LIMITS (E = 0.3).....	158
FIGURE 92: TEMPERATURE RANGE AND LIMITS (E = 0.5).....	159
FIGURE 93: TEMPERATURE RANGE AND LIMITS (E = 0.7).....	159
FIGURE 94: TEMPERATURE RANGE AND LIMITS (E = 0.9).....	160

FIGURE 95: BETA ANGLE OF SATELLITE [70]. COPYRIGHT © 2005 COLORADO CENTER FOR ASTRODYNAMICS RESEARCH 165

FIGURE 96: BETA ANGLE EFFECT ON ILLUMINATION OF SPACECRAFT [71]. COPYRIGHT © 2016 NASA ENGINEERING AND SAFETY CENTER 165

List of Tables

TABLE 1: FINAL POWER BUDGET FROM 2013 CUBESAT MQP [1]. COPYRIGHT © 2013 WORCESTER POLYTECHNIC INSTITUTE.....	28
TABLE 2: LIST OF UNIVERSITY OF MICHIGAN SUBSYSTEM FUNCTIONS [45] ©IEEE 2012	56
TABLE 3: TRANSMITTER ATTRIBUTES	74
TABLE 4: ANTENNA ATTRIBUTES	75
TABLE 5: GROUND STATION ATTRIBUTES	75
TABLE 6: ORBITAL PARAMETERS OF CUBESAT [7].....	80
TABLE 7: DEFINED GLOBAL PARAMETERS	88
TABLE 8: VARIABLE NAME AND POSITION IN FILE FOR EACH REPORT.....	90
TABLE 9: MATERIALS CHOSEN FOR CUBESAT THERMAL MODEL	92
TABLE 10: MANUALLY DEFINED MATERIAL PROPERTIES	93
TABLE 11: DEFINED Q0 FOR EACH SURFACE	95
TABLE 12: POWER USAGE OF SELECTED COMPONENTS	95
TABLE 13: PTOT OF COMPONENTS	97
TABLE 14: PTOT OF OBC AND EPS.....	97
TABLE 15: THERMAL CONTACT PAIR SETTINGS [5].....	100
TABLE 16: C&DH SUBSYSTEM MEMORY CAPACITY	116
TABLE 17: C&DH SUBSYSTEM COMPONENTS.....	117
TABLE 18: OPERATIONAL STATE ESTIMATED TIME SPANS	118
TABLE 19: MRAM USER INFORMATION	122
TABLE 20: NON-VOLATILE DATA PRODUCER INFORMATION	124
TABLE 21: CUBESAT POWER BUDGET.....	130
TABLE 22: POWER HARDWARE COST	131
TABLE 23: SIMULATION INDIVIDUAL COMPONENT POWER CONSUMPTION	138
TABLE 24: MOBILE GROUND STATION COST.....	144
TABLE 25: ADDED ACCESS TIME AND DOWNLINK BUDGET	145
TABLE 26: OPERATIONAL AND SURVIVAL TEMPERATURE RANGE²	147
TABLE 27: STEADY-STATE TEMPERATURES OF COMPONENTS	153
TABLE 28: SURFACE FINISH SIMULATION SUMMARY	156

Executive Summary

The WPI CubeSat Design Project at WPI began in 2010; since then the SphinX-NG mission design process has seen significant progress toward funding and an eventual launch in the near future. The Mechanical, Power, and Thermal CubeSat Major Qualifying Project (MQP) 2013 [1] worked to create a preliminary hardware selection and created a model in COMSOL Multiphysics (COMSOL Inc., Burlington, MA) for internal, external, and “Lab Option” simulations. This year, the project got even closer to reality through hardware finalization and breaking ground in the command and data handling subsystem.

Previously, no dedicated research had been performed on the command and data handling subsystem of the CubeSat. Accordingly, this opportunity was used to create a far more robust understanding of the subsystem and its operations. Information was gathered from all subsystem leaders regarding the potential functionality of their devices and requirements for the subsystem, and used to define the operational states of the entire spacecraft throughout its mission. The states of individual components and the memory capacity of the system were additionally modeled using a MATLAB (The MathWorks Inc., Natick, MA) simulation.

With respect to the electric power subsystem, an existing power budget was updated and used to ensure there will be enough power supplied to all hardware on board the CubeSat throughout its mission. As changes were made to on-board hardware, the budget was updated with the respective required power supply data. A power profile simulation was created and used to evaluate the CubeSat power hardware. The power connections to the main CubeSat bus were defined in detail and shared with the CubeSat Structural team.

Another major area investigated was the telecommunications subsystem, including both the on-board components and the ground station hardware. A list of ground stations were identified

for CubeSat communications, including a hypothetical ground station at Worcester Polytechnic Institute (WPI). Using this information, access and link budgets were made in Systems Tools Kit (STK) (Analytical Graphics Inc., Exton, PA) which were essential in characterizing the data transferred. Also, a case study was performed to determine the cost and best location for a mobile ground station (MGS) to fit in the already established ground network.

The thermal subsystem maintains the spacecraft temperature within acceptable limits. The group evaluating this subsystem was responsible for conducting thermal analysis over five representative orbits using spacecraft-sun vectors generated using STK and finite element model created in COMSOL. The model included external thermal environment as well as internal heat dissipation. Over the five representative periods, average temperatures of the external structure and components of interest were calculated. Results were analyzed and appropriate thermal controls were recommended to guarantee that the temperature of the components on board the CubeSat remained within specified limits.

1 Introduction

1.1 The CubeSat MQP

This Major Qualifying Project (MQP) is a part of a larger group of students that has been performing the conceptual design of a 3U CubeSat which carries the Solar Photometer in X-rays-Next Generation (Sphinx-NG) instrument. The Space Research Center (SRC) at the Polish Academy of Sciences is leading the design of the Sphinx-NG instrument as a miniaturized version of the SphinX-NG, which flew onboard the Coronas-Photon spacecraft. WPI has been undergoing the design of the Sphinx-NG CubeSat with a series of MQPs reviewed later in this section. The overall goal of the mission is to place the CubeSat into a polar, sun-synchronous orbit at an altitude of 450-650 km so the Sphinx-NG can perform solar and extraterrestrial X-ray spectroscopy. The SphinX-NG CubeSat design is shown in Figure 1.

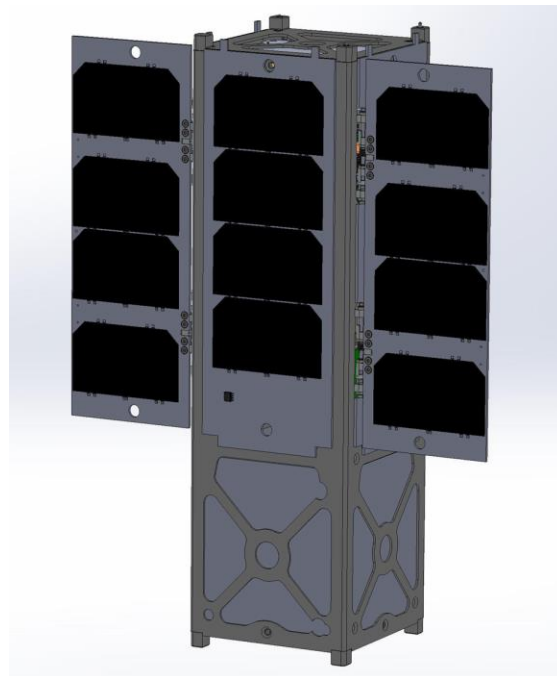


Figure 1: SphinX-NG CubeSat

During the 2011-12 academic year, WPI began its relationship with the Polish Academy of Sciences in Poland and NASA's Goddard Space Flight Center to develop a 3U CubeSat which could house the SphinX-NG [2]. The 2011-12 group consisted of 16 students divided into three MQP teams. Dopart et al. [2] presents orbital and decay analysis using Systems Tool Kit (STK), the selection of the GPS and the magnetometer, ambient and induced environment analysis using COMSOL, and a preliminary discussion on command and data handling and the on-board computer. Farhead et al. [3] presents the hardware selection of the gyroscope, sun sensors, and magnetorquers, attitude determination algorithms, and control policies. Bauer et al. [4] presents environmental and component-induced thermal analysis, component and assembly design, preliminary stress analysis, and power generation and management.

The version of the CubeSat that served as the baseline for this project's work was developed by sixteen students separated into three groups during the 2012-13 academic year. Billings et al. [5] presents the mechanical design, orbital analysis using STK, and an analysis of electromagnetic interference induced by the magnetorquers. Dawson et al. [6] presents the selection of sensor, actuator, and processor hardware, the attitude control algorithm using MATLAB, and the preliminary design of an attitude control test-bed stand. Hanley et al. [1] presents the analysis of the CubeSat power budget, a preliminary wiring diagram, thermal analysis using STK and COMSOL, and telecommunications analysis using STK.

To continue advancing the SphinX-NG CubeSat design during the academic year 2016-17, a group of twelve aerospace engineering majors constituted the Systems Engineering Group (SEG). The SEG was split into three separate teams (and MQPs) addressing the various subsystems and mission operations of the CubeSat:

- mechanical, structural, orbital, and environmental [7]

- command and data handling, power, telecommunications, and thermal [8]
- attitude determination and control [9]

Each team carried out its respective tasks independently and presented its progress at a weekly meeting of the SEG. The success of the project depended on how well the teams communicated with one another to share important mission details. To accomplish this, teams also used the SEG meetings to ask other teams for required information or create action items for other teams to complete.

1.2 Project Goals and Objectives

The goal of this project was to create refinements to the CubeSat subsystems that have been developed over the past few years through WPI studies of the mission. The subsystems of concern for the present study are of critical importance for the control of the spacecraft and the achievement of its mission: the electrical power subsystem (EPS), the command and data handling (C&DH) subsystem, the telecommunications subsystem, and the thermal control subsystem. In previous years, dedicated research had been performed in each of these except the command and data handling subsystem [1, 2, 3]. Sufficient analysis of these subsystems was required in order to assure a spacecraft design capable of supporting the Sphinx-NG instrument and any associated future CubeSat proposal.

1.3 Command and Data Handling Subsystem Objectives

The command and data handling (C&DH) subsystem controls all of the computational tasks that a satellite must accomplish in order to successfully operate and achieve its mission

objectives. With the CubeSat's on-board computer (OBC) as its core element, this subsystem commands other subsystems and sensors aboard the spacecraft to function as desired, and collects, stores, and operates upon data gathered from them. To define the C&DH subsystem, the first objective of this project was to identify all computational and data storage requirements required of other subsystems, outlining the expected baseline capacity of the C&DH subsystem in support of the CubeSat. The next objective was to select hardware and software components to fulfill the C&DH needs of the spacecraft, finding compromise between the demands of other subsystems whenever possible. Moreover, the team had to define hardware and software interfaces between the OBC and other subsystems in order to assure their proper integration into the C&DH subsystem. The last objective was to model the command and data storage profiles of the C&DH subsystem over several orbits in order to assure that the subsystem could operate as desired during the actual implementation of this mission. These goals were iterative in that continual refinements made by other subsystems would necessitate reassessment of the C&DH subsystem, from which feedback could be generated regarding the feasibility of such suggested changes.

1.4 Power Subsystem Objectives

The power subsystem on board a satellite is responsible for generating, conditioning, storing, and distributing electrical power throughout the spacecraft. One major objective of this MQP with regards to the power subsystem was to extend the work done as part of the 2013 CubeSat MQP [1] by creating a power budget to ensure the EPS meets the needs of all components aboard the CubeSat. Another objective was to identify, evaluate, and select components to generate, store, and distribute power, as well as to define the specific hardware and software interfaces between them, the on-board computer (OBC), and the other "power users." The final objective for the power

subsystem was to create a detailed power profile that would define how and when power is individually distributed to each user throughout a number of representative orbits.

1.5 Telecommunications Subsystem Objectives

The telecommunications subsystem of a satellite receives commands from ground stations on Earth, and sends telemetry and payload data from the CubeSat to Earth. To define the hardware needed to accomplish this function, several objectives regarding the telecommunications subsystem had to be met. The first objective was to characterize the uplink and downlink budgets for the CubeSat by analyzing the daily ground coverage of the CubeSat by ground stations. Using this, the next objective was to quantify the daily data budget that the CubeSat can support and provide the information to the rest of the CubeSat team. The third objective was to define the software and hardware interfaces with the on-board computer. The last objective was to generate recommendations for the telecommunications subsystem hardware to carry out mission requirements.

1.6 Thermal Control Subsystem Objectives

The central goal of a satellite's thermal control subsystem is to ensure that all components of the spacecraft remain within their operational temperature limits while operating, and that these components always remain within their survivable temperature limits. To define the thermal control system, three primary objectives were addressed. The first objective was to construct a model of external heating of the spacecraft from sources such as the sun using information from one of the previous CubeSat MQP studies, and from the orbital model created by the orbital

analysis team. The second objective was to create a model of the heating experienced by internal components due to the heat that they themselves produce, that which is conducted to them by other parts of the spacecraft, and that which radiates to them from the body of the craft. The third and final objective was to use the information from objectives one and two to identify and recommend thermal control methods to ensure that thermal constraints are met.

2 Background

2.1 Command and Data Handling Subsystem

The command and data handling or C&DH subsystem of any space vehicle is critical to its operation. The C&DH system is responsible for controlling what operations all subsystems of the spacecraft are performing at all times, thus determining the operational states of the spacecraft throughout its lifespan. At the center of the C&DH subsystem is a spacecraft's on-board computer (OBC), which instructs the other subsystems to execute certain actions depending upon mission requirements and current conditions, and performs the computations required for these other subsystems to operate. Therefore, the C&DH subsystem and its central OBC must be computationally robust in order to perform these actions as needed. Additionally, the C&DH subsystem gathers data from each of the spacecraft's subsystems and sensors, in order to allow ground controllers to assess the status of the vehicle's operations over time. As such, there must be sufficient data storage available on the spacecraft, to allow data to accumulate before it can be processed onboard or transmitted to Earth.

A spacecraft C&DH subsystem is unique in that its components are not necessarily located on the spacecraft itself. Ground computers serve to carry out computations which are not time-sensitive, and collect information sent from the satellite's telecommunications system to ground stations on Earth. Such information includes data collected by the payload instrument, in addition to spacecraft and payload health data, which can be used to ensure the proper operation of all systems or diagnose problems that may arise. Since this health information and the data produced by the payload may require some human interaction and are not critical to processes performed by the OBC, they are sent to Earth for analysis and action.

2.1.1 Previous WPI Research

Previously, no dedicated research on the C&DH subsystem of a CubeSat supporting the SphinX-NG instrument had been performed as part of a Major Qualifying Project (MQP) at WPI, though these student groups have given some input into the development of the subsystem. In a 2014 WPI Report, the C&DH system of such a CubeSat was described, and identified components from the Scotland-based CubeSat components company, Clyde Space, for use on the satellite [13]. Previously, MQP groups had identified various models of OBCs for use in support of the SphinX-NG instrument, including those from companies such as Pumpkin, GomSpace, and Tyvak [2, 3, 13]. As is common in the computer industry, however, the computer models identified in the 2012 and 2013 MQP reports were no longer available for purchase at the outset of this project, and so comparable updated OBC models from these companies would be required [2, 3]. Additionally, other subsystem studies have suggested the use of Clyde Space components for their systems [2, 3]. A benefit of using computing hardware components mostly obtained from a single company is improved compatibility. This is the case with Clyde Space, from which the various CubeSat component boards stack neatly using interlocking bus headers, thus requiring no rewiring for each board to operate properly. Most notably, the 2014 report suggested the use of the then current Clyde Space Mission Interface Computer Grande FM as the OBC for the satellite, and as such, Clyde Space's computer elements served as the baseline for further development of the C&DH system in this project [13]. The more current model of Clyde Space's OBC products, their Nanosatellite On-Board Computer, is shown in Figure 2.



Figure 2: Clyde Space On-Board Computer [14] Copyright 2016 © Clyde Space Ltd.

In order to transfer data to ground stations, mission data must be packetized, or formatted into groups of information, according to international standards [13]. Previous WPI graduate research has identified the use of the Consultative Committee for Space Data Systems (CCSDS) Packet Telemetry Standards in encoding the information, which the OBC sends to the telecommunications subsystem for relaying to Earth [15]. The CCSDS standards benefit from their universality: space agencies around the world collaborated to form the CCSDS, so that the recommendations it created could apply across each of them. The hardware in each of these nations' ground stations accordingly are now capable of handling data from any satellites that also conform to CCSDS standards.

2.1.2 Hardware and Software

The hardware and software components of the C&DH subsystem must comply with the requirements set by the other subsystems on the spacecraft, and its components must accordingly be sufficient to carry out these tasks. The C&DH subsystem must be able to effectively command

other subsystems' operations and must have sufficient memory in order to store software and collected data [16].

On-Board Computer (OBC)

To quantify the processing power of a computer, it is important to consider its clock speed, measured in cycles per second, or Hertz. The clock speed can give an accurate idea of the performance of the computer, when considered in conjunction with the amount of clock cycles certain tasks take to complete. This results in a measure of processing time known as the “throughput” of a computer, usually given in terms of millions of instructions per second, or MIPS (thousands of instructions per second are referred to as KIPS) [16]. The throughput capabilities of a potential OBC, when compared to the estimated throughput requirements for the spacecraft's operation, can give one an idea of how suitable that OBC could be for that mission.

Memory

The memory available on board a satellite limits the amount of data that can be collected by the CubeSat's sensors and systems. If the spacecraft's payload and health sensors create data faster than existing data can be operated upon and replaced, the C&DH subsystem will not be able to perform its duties for the mission. Two types of memory are primarily used in computing: volatile and non-volatile memory [16]. Non-volatile memory retains stored information when the system is turned off and back on, and accordingly is used for the storage of mission critical software, which will remain necessary throughout the life of the spacecraft. Examples of non-volatile memory include read-only memory (ROM), and flash memory. Volatile memory does not retain data if unpowered, and is accordingly used for the running of programs and short-term storage of data on the spacecraft. One example of volatile memory is random-access memory (RAM). Data stored for downlink to Earth is commonly stored in non-volatile memory to prevent

erasure in a fault, while sensor data used in OBC calculations are temporarily stored in volatile memory.

Software

The software loaded onto a computer determines the functions that it is capable of carrying out in support of mission objectives. Firmware is software, which is permanently needed throughout the life of a mission, and thus must be stored in a computer's non-volatile memory [16]. Various commercial software packages are available on the market, which can be tailored to suit a particular mission's needs. These software packages are often available as base-model systems, which can be configured by the end user to control the various C&DH operations of a CubeSat, thus achieving its mission objectives. The memory required to store software can be estimated by comparing one's expected computational operations to those that have already been developed and put into use on previous missions.

2.1.3 Data Interfacing

While there may be other computer boards incorporated into the C&DH system of a satellite, as is the case with this CubeSat, the on-board computer acts as the "Master" computer to each of the other "Slave" computer boards. For example, the electrical power system (EPS) board of the power subsystem can perform computational tasks, but does so when commanded to do so by the OBC. In order to receive these tasks from the OBC, there must be some connections between the OBC and its various dependents. Most often, these connections are made through the spacecraft bus header, which can be seen as the large rectangular element at the right-rear of Figure 3.

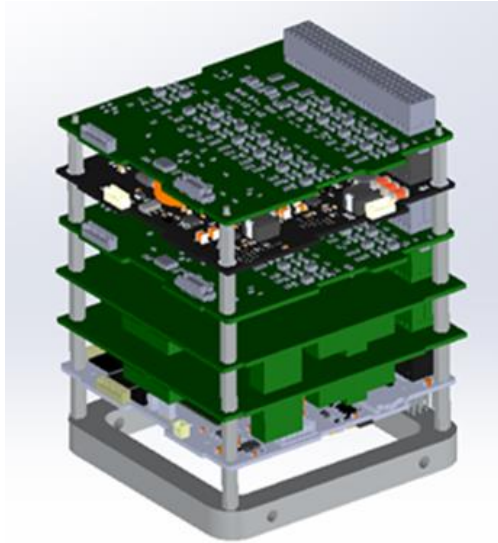


Figure 3: CubeSat Stack [7]

The header consists of a bank of male pins, which protrude out of the bottom of each board, which connect to a corresponding bank of female sockets on the top of the board below it. In this way, a set of boards can all be connected to one another to form a set of pins which run continuously through all boards in what is collectively referred to as a “stack,” as seen in Figure 3. In this way, each of the boards of the stack has digital access to each other board, and data can be transmitted among them.

The protocols of data transfer among these systems can take many forms, but a few notable examples are most often used.

Inter-Integrated Circuit (I²C) Bus

The Inter-Integrated Circuit (I²C) Bus uses only two wires in order to communicate between as many subsystems as required. As shown in Figure 4, the master and slave computers connect via

1. a serial data line (SDA), and
2. a serial clock line (SCL).

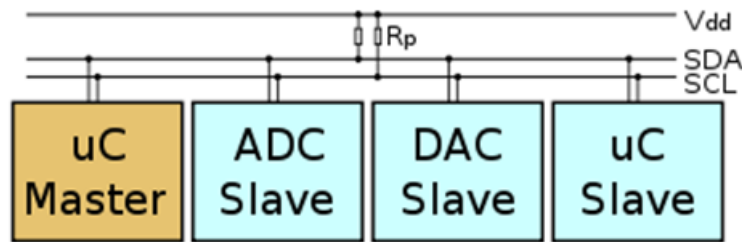


Figure 4: Inter-Integrated Circuit Bus [17] Copyright © 2016 I2C Info

These two interfaces are sufficient for the master to control a system of all connected slave devices. The SDA line is used for data transfer, while the SCL line is used to control the speed of data transfer along the other line, ensuring that both the receiver and transmitter of a signal can be synchronized to send each bit of information successfully. Each component can communicate along shared pathways for data transfer due to the serial nature of the system. The power supply voltage V_{dd} serves to “pull up” the signal on a line, or bring the voltage on that line to a certain default level, should there be no activity on it. If the signal on the line is “up,” it serves to indicate to each system connected to the I²C bus that there is in fact no activity currently being carried out on it [17]. Each computer connected to the line can “pull down” the voltage on line in order to indicate that it is using it currently. To indicate that it seeks a certain slave to perform an action, the master sends a “Start” condition by first pulling the SDA line and then the SCL line low, followed by a specific command for a slave’s action along the same line. The command is then performed by the slave, after which a “Stop” condition is sent, by pulling the SCL line and then the SDA line high, in order to acknowledge that the task is complete and other operations can commence.

Serial Peripheral Interface (SPI) Bus

Similar to the I²C bus in that it allows for several slave computers to be connected to a master, the Serial Peripheral Interface (SPI) uses four wires to transmit information. As shown in Figure 5, these computers connect via

1. a serial clock line (SCLK),
2. a master output, slave input line (MOSI),
3. a master input, slave output line (MISO), and
4. a slave select line (SS) for each slave.

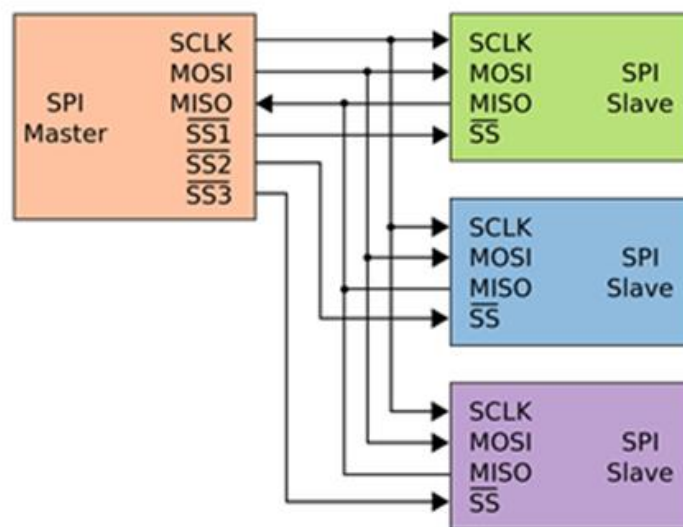


Figure 5: Serial Peripheral Interface Bus [18] Copyright © 2006 Colin M.L. Burnett

Instead of “Start” and “Stop” conditions as used in I²C, in this case, the master uses the particular SS line to address a certain slave for action [19]. This is followed by the master sending its command along the MOSI line to the slaves, where only the slave of concern considers the data. In turn, the slave then returns a signal via the MISO line to the master until communication is

complete between the two. Finally, the master deactivates that slave's SS line to indicate the task has been completed.

Universal Asynchronous Receiver/Transmitter (UART) Transmission

Universal Asynchronous Receiver/Transmitter (UART) is another method used widely in modern computing devices for simple serial interfacing. Similarly to the I²C bus, a UART device uses data lines to transfer information from its source to its target, however no clock line is used to ensure that the two devices remain synchronized. Thus, it is important for these two communicating devices operate at the same transmission speed beforehand, so that they can effectively relay information. Each UART device has a receiving line (RX) and a transmitting line (TX) connected to other UART devices, though it is possible that a certain UART device be capable of only receiving and not transmitting data [20]. The receiving and transmitting data lines are “pulled up” when not in use, until the transmitter of a signal pulls its transmitting line low to indicate the beginning of a message. Then, data is transferred between devices, where one device can either transmit all of its data at once, or take turns receiving and transmitting data with its partner device.

General Purpose Input/Output (GPIO)

General Purpose Input/Output (GPIO) pins on a bus header can be configured as required for implementation by the end-user of a system. In this way, GPIO pins are free for use and definition by the designer of the C&DH system, and can be customized to suit a particular subsystem when other types of data bus setups are not possible. GPIO interfaces are commonly used for devices, which do not have their own computing capabilities. For example, the analog voltage produced by a thermocouple sensor can simply be fed through an analog-to-digital

converter (ADC) and then directly into a GPIO pin which has been configured to accept such an input voltage.

2.2 Power Subsystem

2.2.1 CubeSat MQP 2013 Final Power Budget

Power is one of the most important resources in any spacecraft, and the miniaturized nature of a CubeSat severely limits the power available to all power consumers. The 2013 Thermal, Telecommunications, and Power Major Qualifying Project (MQP) team produced a final power budget based on the components that were selected for that mission. Table 1 shows the final power budget generated by the 2013 group [1].

Table 1: Final Power Budget from 2013 CubeSat MQP [1].
Copyright © 2013 Worcester Polytechnic Institute

Component	Part Number	Peak Pwr (W)	Nominal Pwr (W)	Quiescent Pwr (W)	Current (mA)	Voltage (V)
GPS	SGR-05U	0.080	0.080	0.080	16	5
OBC	Pumpkin	0.300	0.300	0.000	TBD	TBD
Magnetorquers (3)	Zarm Technik AG MTO 2.1 (Optimized)	0.420	0.420	0.420	28	5
Sun Sensor	ComTech AeroAstro	0.050	0.050	0.050	3.5	N/A
Gyro	ADXRS450	0.030	0.030	0.030	6	Variable
Magnetometer	Honeywell HMC5883L	0.001	0.001	0.000	0.25	3.6 (max)
Instrument		8.000	8.000	1.000	TBD	TBD
EPS Board	ClydeSpace	0.1	< 0.1	< 0.1	TBD	TBD
PDM Board	ClydeSpace	0.160	0.160	0.160	TBD	TBD
PPM	ARM922T	0.180	0.180	0.180	TBD	TBD
UHF Transceiver		2.000	2.000	0.000	TBD	TBD
Total		11.321	11.321	2.020		
Total Available		12.520	12.520	12.520		
Margin		1.199	1.199	10.500		

The budget in Table 1 is not complete as it does not take into account inefficiencies within the power components and circuitry that reduce the total available power. Because of these inefficiencies, the actual power available to satellite systems falls below the ideal amount produced by a satellite's solar panels, typically by 10-15% [22].

2.2.2 Power Subsystem Hardware

The power subsystem serves three main functions: to generate and store power, to condition and distribute that power, and to protect the CubeSat in the case of an electrical fault. On most CubeSat missions, power generation and storage is performed by a combination of solar cells which provide power while in view of the Sun, and batteries which provide power during eclipse. Power conditioning and distribution is done by a series of power conditioning modules (PCMs) and power distribution modules (PDMs) in the form of circuits located on the main EPS board. In this case, power conditioning refers to the conversion of power to specific voltages and currents as needed by individual power users and distribution refers to the routing of power to those users as they require it. Electrical faults, in which excessive current can damage electronics, can potentially cripple satellite hardware and must be mitigated as much as possible. Fault protection is accomplished by safeguards built into the PCMs and PDMs, which monitor the flow of current to prevent damage to other components. The PDMs and their safeguards can operate independently of the OBC to ensure that power continues to flow in the event of an OBC malfunction or reboot. In such an event, the EPS would continue to supply power for as long as it had been previously instructed.

Solar Array

Due to the plentiful solar energy available in orbit around Earth, power generation on CubeSats and other small Earth-orbiting satellites is primarily carried out by small, light solar arrays. Solar cells for these small arrays are typically composed of gallium-arsenide (Ga-As) photovoltaic cells due to their high-efficiency, attached to a lightweight substrate of fiberglass, aluminum, carbon fiber, or other composite [22].

The total power generated by the solar arrays is determined by their area, efficiency, temperature, and angle of incidence of sunlight on the panels. Due to the Sun-observing nature of this CubeSat’s mission, the solar arrays are assumed to be pointed directly towards the sun and the angle of incidence is a negligible factor in our power estimates. Of the remaining factors in power production, which include array size, array efficiency, solar flux, and temperature, only temperature will change considerably over time, and as such the panels must be optimized for the temperature range that the CubeSat will experience throughout its lifetime. Solar cells operate more efficiently at lower temperatures, so the thermal profile of the CubeSat will need to be taken into account to insure the solar panels can dissipate heat effectively [22]. There is also an optimal point in the relationship between a solar panel’s voltage and current outputs such that its power output is maximized. This is known as the peak power point or maximum power point and its location on the current-voltage curve changes based on the temperature of the solar panels as shown in Figure 6 [23].

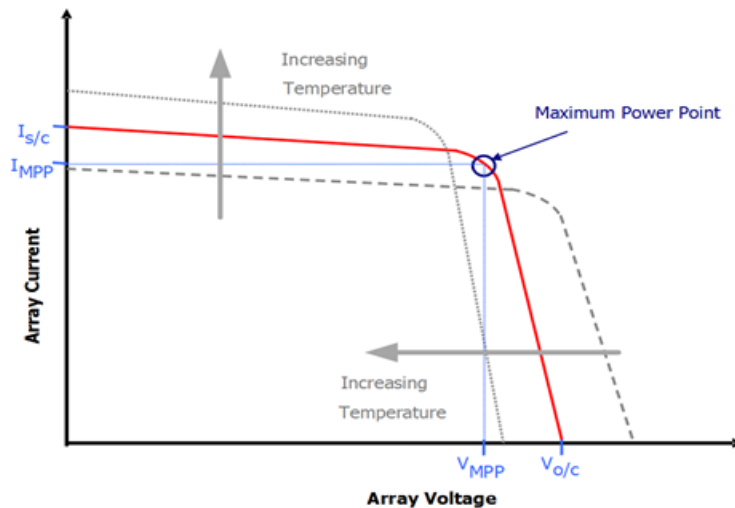


Figure 6: Solar Array Current vs. Voltage [23]. Copyright © 2016 Clyde Space Ltd.

Previous MQP teams chose to use a three-panel system for power generation, utilizing a single body-mounted 2U solar panel flanked by a pair of single-deployed 2U solar panels on each side [1,4] as can be seen in Figure 1. The same solar array arrangement was selected for this study.

Electrical Power System (EPS) Board

The main electrical power system (EPS) hardware is typically mounted on a single, discrete circuit board. The EPS board interfaces with and controls the entirety of the power subsystem. It directly interfaces with the solar panels, battery, OBC, and all other powered components onboard the CubeSat. It is responsible for monitoring and regulating the power from the solar arrays, as well as both to and from the battery. In addition, the EPS board controls the flow of power to the OBC and other components through its integrated PDMs, as well as communicates with and receives commands from the OBC. The EPS is also responsible for maintaining the solar panels at their peak power point. Figure 7 demonstrates the flow of power through the EPS.

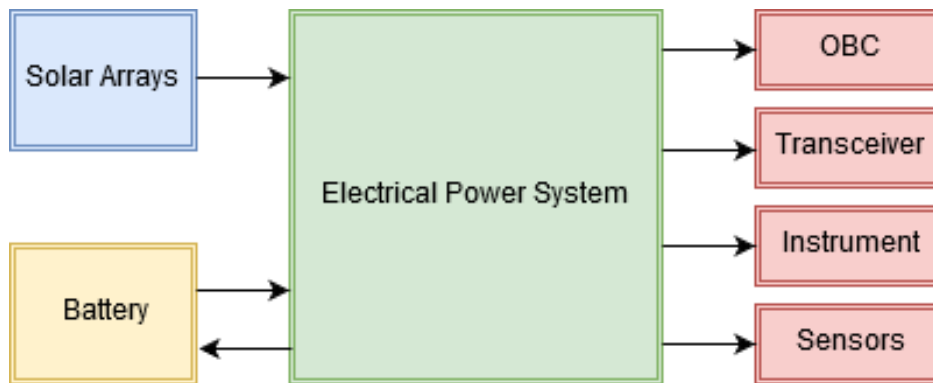


Figure 7: EPS Power Flow

The 2012 MQP team selected a Clyde Space EPS board (model number CS-3UEPS2-NB), which has since been discontinued [4]. As such, a new EPS board needed to be considered.

Battery

Batteries allow solar powered spacecraft to maintain operation during eclipse and help to supplement the arrays at peak power usage. Lithium-ion (Li-ion) and lithium-polymer (Li-Po) cells are often used in such applications due to their high energy density, resulting in a high capacity compared to their size. However, they tend to become unstable at extreme temperatures and as such they must be constantly monitored and kept within their acceptable temperature threshold (typically -10 to 50 degrees Celsius) [22]. This temperature is maintained using the thermal controls of the spacecraft as well as an integrated heater on certain batteries. Additionally, to maximize battery life, the power drain should be managed so as to never cause the battery to exceed its recommended depth of discharge (DoD), a measure of the percentage of the battery's total capacity has been discharged, which is typically around 20% to 30% for batteries typically used on CubeSats and other satellites that operate in low Earth orbit [22]. The 2012 MQP team chose a Clyde Space 30 Watt-hour battery that is no longer available for purchase [4]. As such, a different battery had to be considered for this study.

2.2.3 Power Subsystem Related Interface Control Document (ICD) Requirements

The requirements outlined in the “Launch Services Program: Program Level Poly-Picosatellite Orbital Deployer (P-POD) and CubeSat Requirements Document” [24] state that “No electronics shall be active during launch so as to prevent any interference from either electrical or RF sources with the launch vehicle and primary payloads” [24]. The CubeSat must also have a remove before flight (RBF) pin, which when installed must cut all power to the CubeSat bus and must be removed after the CubeSat is integrated with the Poly-Picosatellite Orbital Deployer (P-POD). The P-POD deployment system is a specialized launcher tube that acts as the interface between the CubeSat and launch vehicle and is responsible for ejection of the CubeSat. If an RBF

pin is not present, the satellite must launch with its batteries fully discharged. The CubeSat must also have at least one deployment switch located on the -z face of the CubeSat as shown in Figure 8. The deployment switch must keep the satellite powered off while it is actuated. Once the satellite is deployed, the deployment switch will no longer be actuated and this will start a deployment timer which ensures that no mechanical structures or appendages are deployed until 30 minutes after the satellite is ejected from the P-POD and that no transmissions are generated until 45 minutes after the satellite is ejected from the P-POD [24]. The deployment switch must also be able to reset the deployment timer if the switch is toggled from the actuated state and then actuated again. After the CubeSat is loaded into the P-POD, it can then be charged through access ports located on the P-POD as shown in Figure 8. However, P-POD requirements state that the total stored energy in the battery after charging must be no more than 100 Watt-hours during launch.

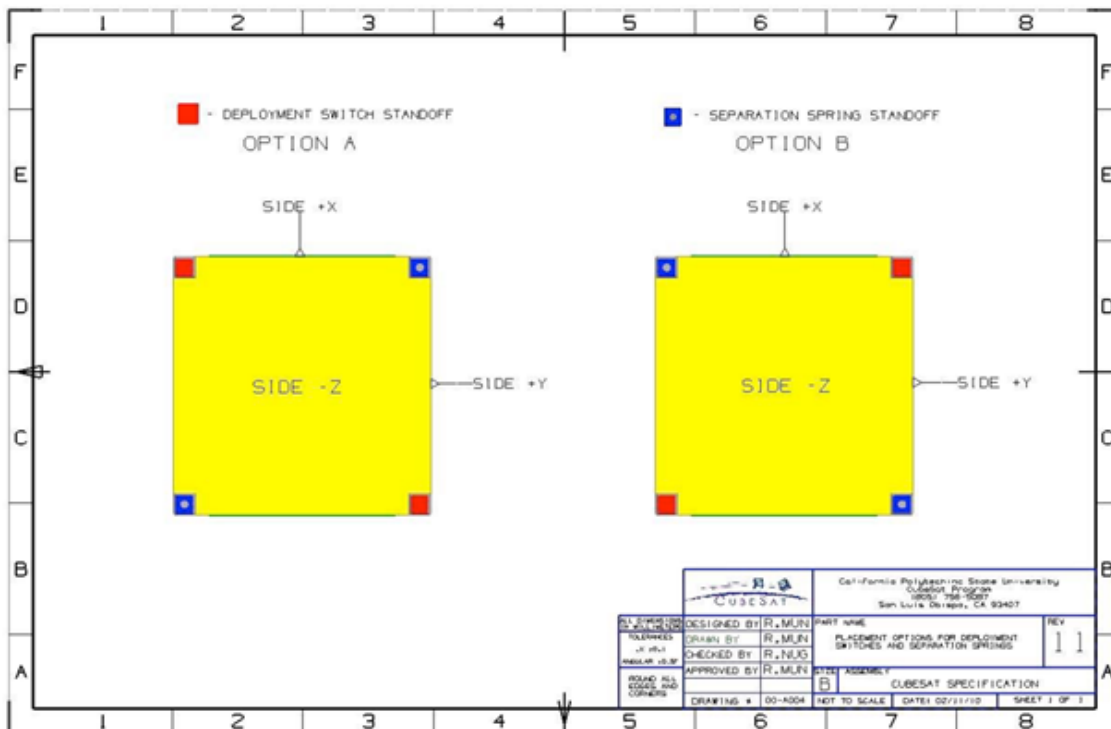


Figure 8: Location of Deployment Switches [24] Copyright © 2011 Cal Poly SLO.

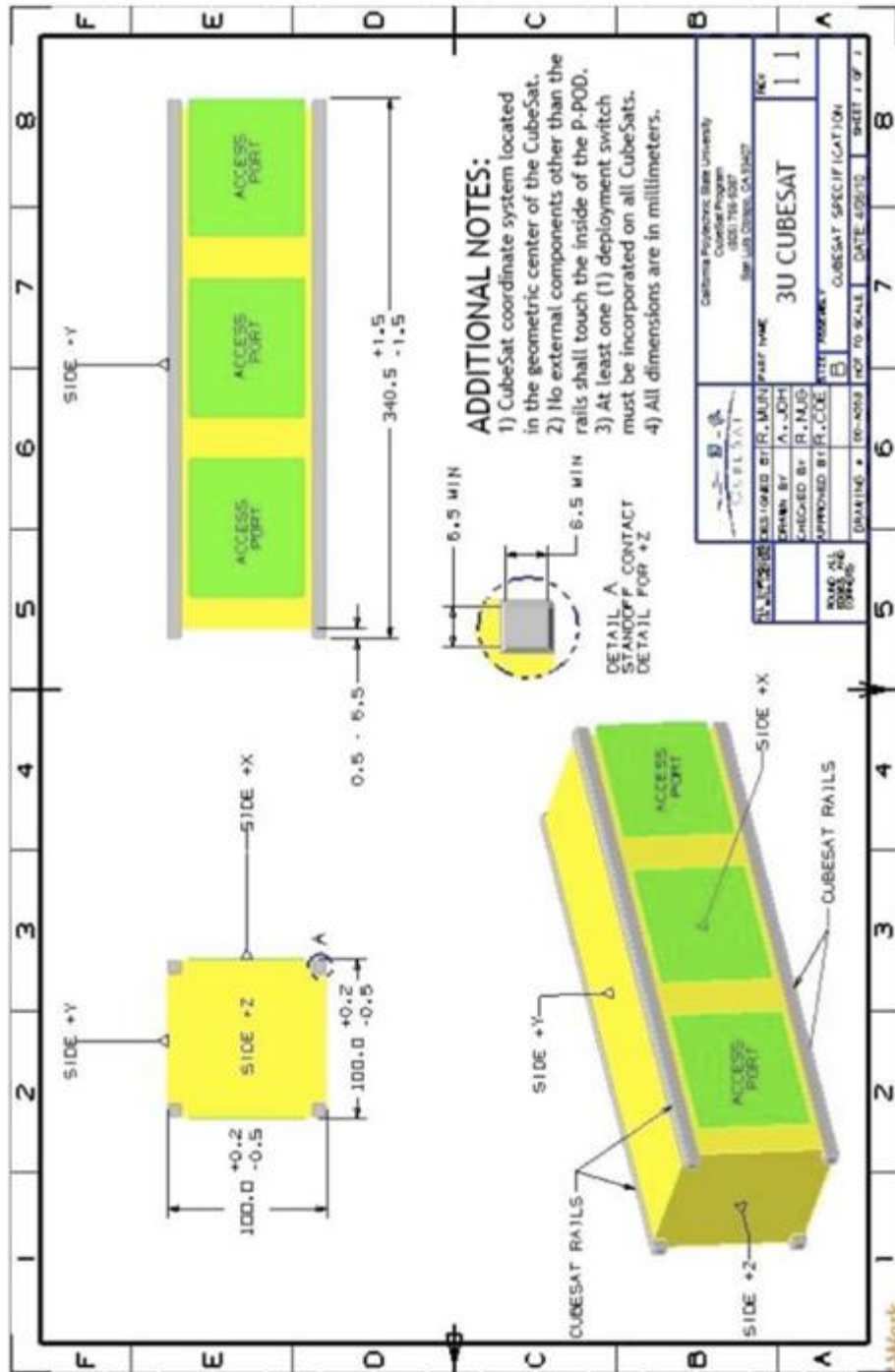


Figure 9: Location of Access Port for 3U CubeSat [24] Copyright © 2011 Cal Poly SLO

According to the NASA document “Standard Materials and Processes Requirements for Spacecraft”: “The CubeSat shall also be self-contained, providing its own power, sequencing and

wiring” [25]. The requirement that the CubeSat be able to provide its own sequencing means it must be able to carry out its tasks without constant commands from a ground station. “The electrical wiring of the satellite, specifically its insulation, shall also be inspected for flammability prior to its launch” [25]. If the wire insulation is chemically and physically similar to a material found to be acceptable by NASA-STD-(I)-6001 (a NASA technical standard which establishes requirements for the selection, testing, and evaluation of materials intended for use in space vehicles), then the material may be used without testing and justified on an approved Material Usage Agreement (MUA) that shall be submitted for approval as described in NASA-STD-6016 [25]. One major part of CubeSat testing involves a thermal bakeout test, where the CubeSat is subjected to intense heating in a vacuum for an extended duration. After the thermal vacuum bakeout test is performed, the electrical functionality of the satellite must be re-verified [23]. NASA requires that the CubeSat also have an end of mission (EOM) plan that outlines how the spacecraft will be disposed of at the end of its operational life [26]. Prior to the EOM the satellite needs to be passivated for Earth orbit or Earth reentry. The passivation of the satellite will entail the depletion of all forms of stored energy to a point where the remaining onboard energy would be insufficient to cause a breakup of the satellite. The electrical systems, specifically the batteries and the charging circuits are part of the hardware considered in this passivity analysis.

2.3 Telecommunications Subsystem

2.3.1 Interface Control Document (ICD) Requirements

As CubeSats have become more commonplace, many regulations and requirements have been placed on various facets of CubeSat development and deployment. The communications and interfacing subsystems are heavily affected by these specifications. For example, the

communications between the CubeSat and Earth must occur over a specific frequency [26]. For this reason, a frequency application for the exact frequency the spacecraft will be using must be completed and approved to obtain a license allowing communications once in orbit. As an additional requirement, CubeSats are required to have both Global Positioning System (GPS) tracking and the ability to update, in real time, the systems onboard the satellite via ground commands [27].

Some of the research into telecommunications options for this project required knowledge of Australian transmission regulations. Similar to the Federal Communications Commission (FCC) in the United States, the Australian Communications and Media Authority have a variety of licenses that require successful completion of an exam before they are issued [28]. For a standard CubeSat connected ground station, an amateur standard station license is needed for the ground station operator [29].

2.3.2 Hardware

The telecommunications subsystem hardware consists primarily of a transceiver unit to connect the on-board computer (OBC) with ground stations on Earth. This is important because the CubeSat cannot complete its mission objectives if the collected instrument data cannot be transmitted back to Earth. To allow communication between the satellite and ground, the telecommunications subsystem consists of a radio transceiver and an antenna. Typically on a CubeSat, the telecommunications subsystem transmits and receives at Very High Frequency (VHF), Ultra High Frequency (UHF), or S-Band Frequency radio ranges. The VHF band ranges from 30 to 300 MHz, while UHF ranges from 300 to 3000 MHz, and S-Band ranges from 2 to 4 GHz [30, 31].

The ability to relay data to the ground is primarily limited by three parameters: the power needed for the components, the rates of data transmission and reception, and the quality of the data being delivered. When the subsystem's components are powered on, they can draw a up to 1.5W of power, a significant amount for a CubeSat, and so coordinating the timing of radio transmissions with the rest of the CubeSat operations that consume power is essential [30]. Secondly, the transceiver and antenna have finite amounts of information they can send and receive during a certain period of time, known as data rates. Lastly, due to instrument noise, environmental effects, and software problems, information transferred may not be completely accurate. This could lead to corrupt information where the CubeSat would need to retransmit information, putting further strain on the already limited data rates. Environmental, weather related limits to data rates are unavoidable because coverage by clouds or particulates can disrupt signal transmissions at any time, and are uncontrollable due the satellite's orbit.

Figure 10 provides a block diagram of the telecommunications subsystem with all relevant components. The items in red are the telecommunications subsystem specific components. What follows is a more extensive explanation of these components.

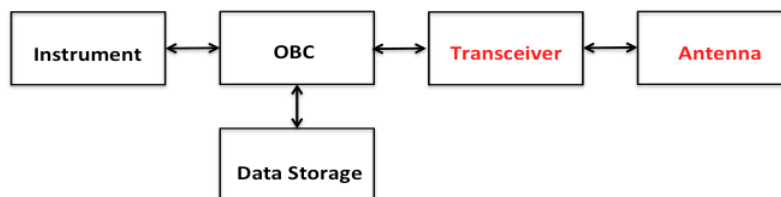


Figure 10: Telecommunications Subsystem Block Diagram

Transceiver

The transceiver is the piece of hardware that contains components used for both reception and transmission on a single board. The transceiver downlinks data from the OBC by converting

the data into a modulated RF signal suitable for transmission, then passes the data along to the antenna for physical transmission. This process also works in the opposite direction when information is being received through the antenna. A popular transceiver for CubeSats is the ISIS UHF/VHF transceiver shown in Figure 11 [32]. The transceiver can transmit or receive in both the UHF and VHF radio frequencies, and was chosen by the 2013 CubeSat Report for its flight heritage, ease of use, and robustness [1].

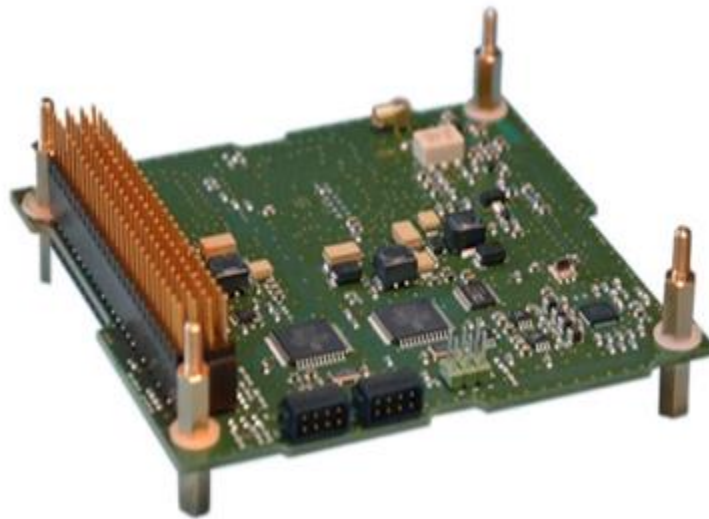


Figure 11: ISIS UHF/VHF Transceiver [32] Copyright © 2017 CubeSatShop.com

Antenna

The antenna is the component that physically sends and receives information and commands that are sent between the spacecraft and the ground stations using radio waves. CubeSat antennas must be compatible with the corresponding transceiver in terms of frequency transmission and reception (ex: UHF, VHF, S-band, etc.). Antennas can be arranged in a few configurations: monopole, dipole, or turnstile [33]. Turnstile gives the most directional ability with highest losses in signal strength, while monopole has the strongest signal but the smallest ground coverage. The dipole configuration is the simplest and most commonly used style of antenna [34].

As an example, an ISIS dipole deployable antenna compatible with the previously selected transceiver example is shown in Figure 12.

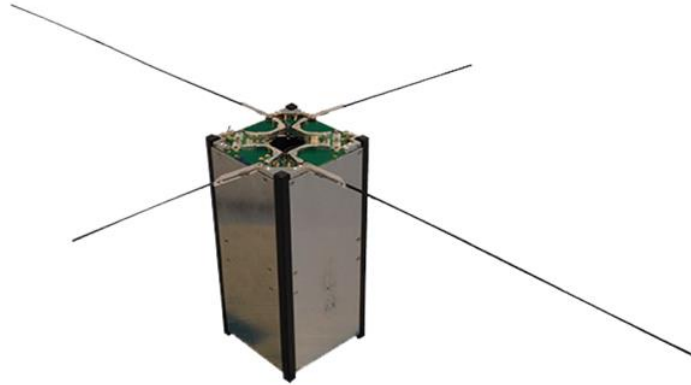


Figure 12: ISIS Dipole Deployable Antenna [35]
Copyright ©2017 Innovative Solutions in Space.

2.3.3 Ground Stations

The telecommunications subsystem would be useless without any ground terminals to send information to or receive commands from. Due to the rapid growth in the popularity of CubeSats, there are many ground stations around the world that are capable of and available for sending and receiving information. The Global Educational Network for Satellite Operators (GENSO) was a system developed by the European Space Agency (ESA) in 2007. As part of this network, ground stations around the world would be linked by common software, allowing for connected ground stations that educational satellites could use for data transmission [36]. There are three components, connected via internet, that make up the GENSO framework: the Ground Station Server (GSS), the Mission Control Client (MCC), and the Authentication Server (AUS) [36]. The three components perform duties as follows: GSS controls the ground station hardware during satellite connection, the MCC provides access to the satellite via the various GENSO stations, the

AUS authenticates that establishes links between the GSS and MCC [36]. Appendix A displays all of the ground stations in the GENSO Network as of 2012. Currently GENSO is non-operational and was not able to fully implement the system worldwide.

The two most common types of communications between space and ground are uplink and downlink. Uplink is communication in which information or commands are sent from the ground station up to the satellite, whereas downlink is when the satellite sends any kind of information (payload data, telemetry, etc.) down to the ground station for processing and manipulation [37]. Other types of communication paths include crosslink, which uses one or more satellites as relay satellites to send and receive transmissions [38]. Due to the complexity of crosslink and other more complicated methods, uplink and downlink are the methods of choice for CubeSat transmissions.

The orbital parameters of a satellite determine which stations it will be within range of it at various times during its mission. To get the most coverage for least amount of ground stations, the 2013 CubeSat MQP team picked four current ground stations for simulation purposes [1]. These stations are located at California Polytechnic State University - San Luis Obispo, University of Texas at Austin, Delft University of Technology (Netherlands), and Warsaw Institute of Technology (Poland). In addition to these four ground stations, the previous team added in a hypothetical WPI ground station for a larger downlink potential and information for a future proposal. These ground stations provided continuous coverage while the CubeSat was over North America and Europe.

In Figure 13, a ground track of a representative satellite progressing through several orbits is shown.

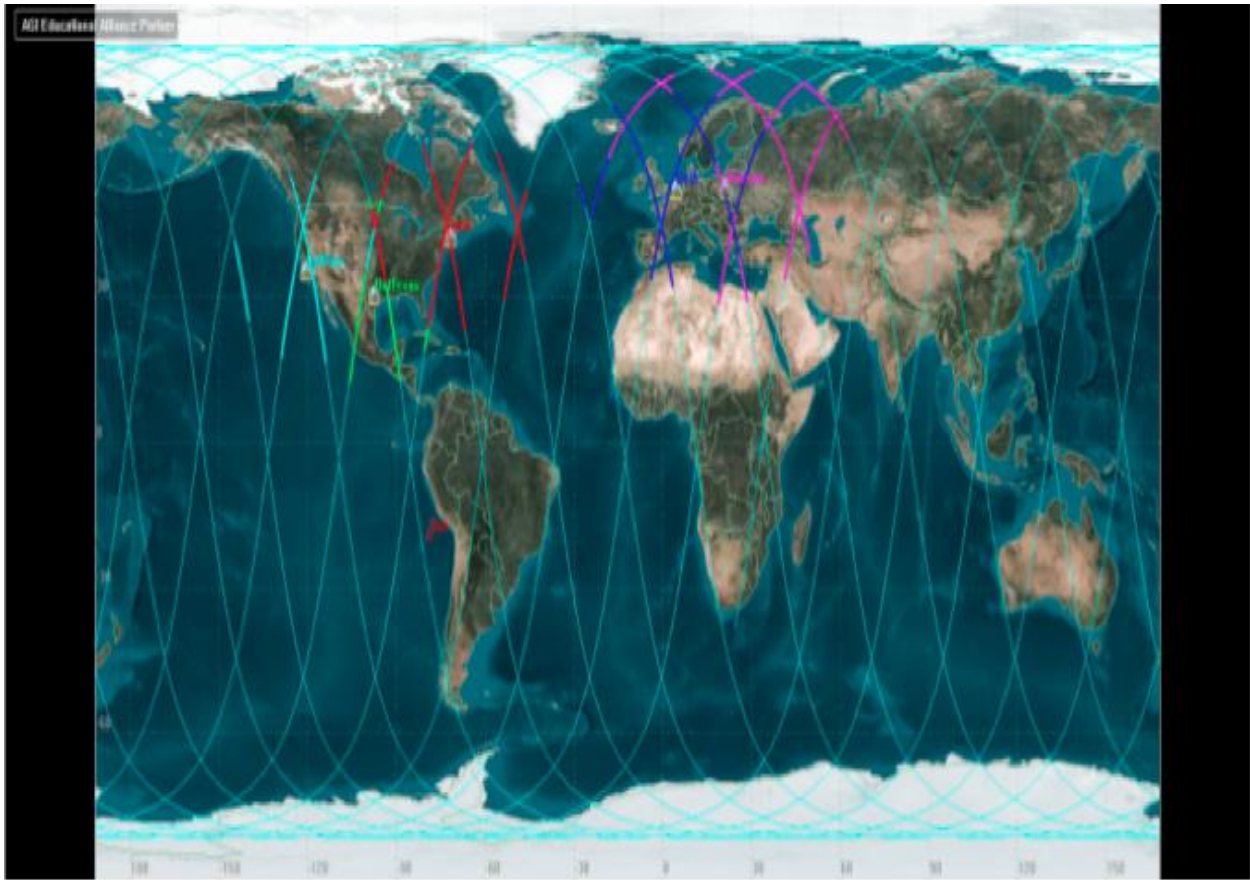


Figure 13: 2014 CubeSat Ground Coverage Map [1]

The different colored lines shown in the Figure 13 represent the satellite's location at different times that the CubeSat is downlinking to the previously listed ground stations. The particular ground stations chosen for this project and a representative ground coverage map are presented in Section 4.3.

2.4 Thermal Control Subsystem

2.4.1 Thermal Environment

The space environment presents a number of challenges for managing the temperature of a spacecraft. Most notable is the lack of significant atmosphere, forcing a body to gain or lose heat

only by radiation. In terrestrial applications, a body has two other methods of gaining or losing heat; convection and conduction. Convection is a process that takes place in fluids when a temperature gradient adjacent to a heat source is present. In natural convection, the fluid surrounding the heat source gets hot and rises allowing cold fluid to circulate to replace it, effectively removing thermal energy from the heat source. Forced convection includes the effect of a bulk, forced flow of the fluid over the heated surface. Conduction is the process of heat transfer within solids, liquids, or gases, in which atoms transfer energy between each other due to their vibrations in a lattice (in the case of solids) or through collisions with other atoms (in the case of fluids) resulting in a transfer of energy [22]. The lack of convection means the spacecraft's temperature can increase significantly when exposed to radiation. Additionally, when in shadow, the spacecraft will quickly lose heat and experience extreme cold temperatures. The wide range in environmental conditions that arise from moving between full solar illumination to complete shadow means spacecraft components can get as cold as -130°C and as hot as 100°C [22].

The key sources of radiation that must be considered when in an Earth orbit are the Sun, the Earth's reflected radiation (referred to as "albedo"), and the Earth's emitted blackbody radiation. The Sun's energy flux at earth is 1367 W/m^2 [22] and it is by far the most dominant source of heat for the spacecraft. The energy flux due to Earth's albedo is the fraction of the Sun's energy that is reflected off of the Earth [39].

$$Q = 1367 \alpha F \quad (1)$$

where α is the albedo, or reflectivity of earth, approximately 0.35 and F is the fraction of sunlit Earth in view of the spacecraft [22]. Though not as intense as the flux from the Sun, the Albedo further compounds the heat gain the spacecraft experiences when in sunlight. The Earth's blackbody radiation is the infrared radiation emitted by the earth. Though far less powerful than

the Sun's radiation at only about 231 W/m^2 , [22] it must still be accounted for in the spacecraft thermal system design. The Earth's blackbody radiation is the only major source of external energy that remains when the satellite is in eclipse, making it vital for keeping the spacecraft warm enough to operate. It is important here to note the $1/r^2$ dependence of radiation [22]. Every source of radiated energy decays with its distance, r , from the source of that radiation according to the inverse square law. This is partly why, despite its vastly colder temperature, the Earth's radiated energy contributes as much as it does to the spacecraft.

The final source that contributes to the thermal environment is the power dissipation from components of the spacecraft itself. Power dissipation is a result of the inherent inefficiencies of the components being used though most of a component's power will go to its prescribed purpose, a percentage of it will always be converted to waste heat [40]. The electronic components operating on the spacecraft generate heat that is transferred through conduction and radiation to structures inside the spacecraft. Special consideration must be taken to ensure that components that dissipate relatively large amounts of power, such as the computer, have enough contact points to allow effective conduction to surfaces where heat can be most effectively radiated into space. The inverse square law is insignificant at the distances between components. Which is why the internal surface to surface radiation within the spacecraft is so important, as the components are so close to one another radiated energy from one component will have a significant impact on the temperature of another.

2.4.2 Thermal Limits

Throughout the mission, it is crucial that the temperature of the spacecraft is maintained within a reasonable range in order to protect it and all of its internal components. Because the on-board components are designed to operate within certain temperature limits, typically at "room"

temperature, decrease in performance and significant damage can occur to them due to temperature beyond the designed range.

Each piece of equipment is characterized by two temperature ranges that it must stay within: operational temperature range and survival temperature range [22]. To perform as intended, the equipment's temperature must be maintained within the operational temperature range; the performance and efficiency of the equipment can be affected by temperatures outside of the operational temperature range [22]. At all times, the temperature of the spacecraft and all of its equipment must be maintained within the survival temperature range; significant damage and failure can be caused by temperatures outside of the survival temperature range.

Every piece of equipment is characterized by different operational and survival temperature ranges, and it is important that the temperature of each component is guaranteed to stay within its specified operational temperature range while operating and within its specified survival temperature range at all times throughout the mission.

2.4.3 Thermal Controls

During the mission, the temperature of a typical spacecraft and its equipment could likely exceed its operational or survival temperature range without the use of any thermal controls. Hence, thermal control system on a spacecraft is required to maintain desired temperature of the spacecraft and its components.

Passive Thermal Controls

Passive thermal controls are defined as those methods which do not require power to operate and transfer heat via natural processes to regulate the temperature of a spacecraft [1]. Surface finishes and radiators are common passive thermal controls applied to the spacecraft [22]. The purpose of surface finishes is to change the surface absorptivity and emissivity of surfaces on

a spacecraft to control the amount of radiation absorbed and emitted by the spacecraft. Surface absorptivity is a fraction of irradiation absorbed by a surface and is defined as a value between 0 and 1, where absorptivity of 1 represents a perfect black-body. Surface emissivity is a fraction of radiation emitted by a perfect black-body at the same temperature and is defined as a value between 0 and 1, where emissivity of 1 represents a perfect black-body. Different materials can be used as surface finishes to control the amount of radiation absorbed and emitted by the spacecraft and ultimately to maintain the temperature within an acceptable range. Figure 14 illustrates a few examples of surface finishes with corresponding values of surface absorptivity and emissivity.

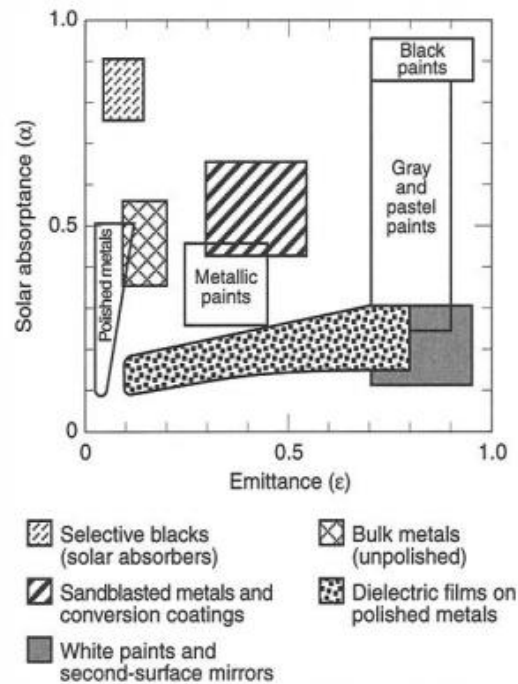


Figure 14: Surface Absorptivity and Emittance of Various Types of Materials [41]
Copyright © 2017 The Aerospace Press

Materials such as white paint, which have very high emissivity but very low absorptivity, can be used to reject solar radiation or effectively emit heat generated by the internal equipment. This is critical for a spacecraft that would otherwise experience temperatures above the specified

maximum limit due to either long exposure to the Sun or heat generated by the internal components. Materials such as black nickel/chromium, which have very high absorptivity but very low emissivity, can be used to absorb more heat from the Sun or prevent quick heat loss to the cold space for a spacecraft that would otherwise experience temperatures below the specified minimum limit due to short or no exposure to the Sun.

A *radiator* is a device that ejects heat from the spacecraft to space using specially designed panels. Radiators are panels generally made with materials that have high emissivity and low absorptivity, such as silvered or aluminized Teflon or white paint, to emit infrared (IR) radiation from the spacecraft body as much as possible while absorbing least amount of heat from the Sun [22]. The amount of heat dissipated by the radiator is governed by Stefan-Boltzmann equation:

$$Q = \varepsilon\sigma AT^4 \quad (2)$$

where Q is amount of heat dissipated from the radiator, ε is emissivity of the panel, σ is Stefan-Boltzmann constant, A is the surface area of the panel, and T is the absolute temperature of the panel [22].

The size and shape of radiators vary for different missions to meet their unique thermal requirements; large radiators are preferred for a spacecraft that generate a lot of heat, but to reduce the weight of the spacecraft, small or no radiators are preferred for a spacecraft that does not generate as much heat. Radiators can be engineered to work in several different forms, such as flat-plates mounted on the side of the spacecraft or panels that are deployed after the spacecraft is in orbit [22].

Active Thermal Control

Active thermal controls are defined as methods that require power and control to operate. Active thermal controls are more expensive and complex than passive thermal controls, but they

have the ability to control the temperature of the spacecraft more precisely [22]. Active thermal controls are typically used when analysis indicates passive thermal controls are not sufficient to keep the temperature within a desired range [4]. Examples of active thermal controls include heaters, louvers, and heat pipes.

The most common type of heater used on a spacecraft to maintain desired temperature range for components is the *patch heater* [42]. In essence, electricity is transferred through electrical resistors to generate heat. Patch heaters consist of electrical resistance elements sandwiched between two sheets of flexible electrically insulating material, such as Kapton [42]. Electricity is transferred through the electrical resistance element, and heat is generated and transferred to surfaces that are in contact through conduction. Patch heaters are generally constructed in a simple rectangular shape, but depending on their purpose, they can be created in custom shapes [42].

A *louver* is a thermal control system that modulates the radiant heat transfer of spacecraft to the space by opening or closing blades that are mounted on the system. Louver systems generally consist of five main elements: baseplate, blades, actuators, sensors, and structural elements [42]. The baseplate is a surface behind the blades, which can be either a radiator mounted on a spacecraft or an open area which directly exposes internal components to space. Sensors and actuators drive the blades to open or close when necessary. Figure 15 displays a typical louver and its mechanisms.

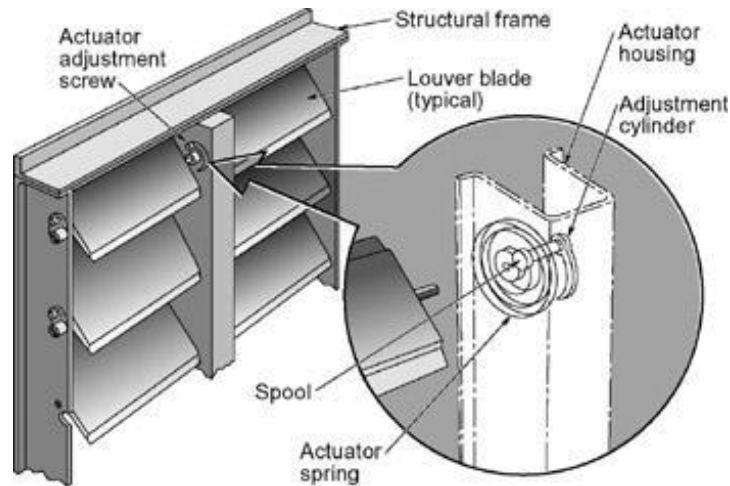


Figure 15: Schematic of Louver Assembly [42] Copyright © 2002 AIAA

When the blades are open, the base plate is exposed to cold space which allows the base plate surface to emit radiation to space by Stefan-Boltzmann equation, corrected by view factors as appropriate. When the blades are closed, the baseplate is hidden from the cold space, and radiant heat transfer does not occur.

A *heat pipe* system uses a closed two-phase liquid-flow with an evaporator and a condenser to transport heat from one location to another [42]. Heat pipes do not require power; they are considered active thermal system due moving fluids driven by capillary action within the system. Figure 16 displays schematics of a typical heat pipe system.

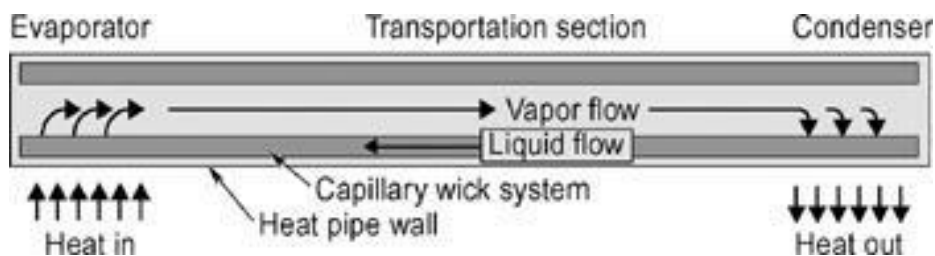


Figure 16: Schematic of Heat Pipe System [42] Copyright © 2002 AIAA

When heat is added to the evaporator, liquid in the evaporator wick vaporizes and removes some of the added heat. Vaporization depresses the meniscus in the evaporator since less liquid is present, and the difference in the curvature of meniscus causes sufficient capillary pressure to pull the liquid from the condenser wick towards the evaporator wick [42]. At the same time, the vapor flows from the evaporator to the condenser and condenses when it contacts the cooler condenser surfaces [42].

2.4.4 COMSOL Multiphysics

COMSOL Multiphysics (COMSOL) is a partial differential equation solver that uses finite element method (FEM). The software allows users to build many different types of physics-based systems including structural system, electrical system, fluid dynamics, heat transfer, and chemical system. Within each system, COMSOL has defined physics-based modules, such as AC/DC module, pipe flow module, and heat transfer module, and any physics module can be coupled together to create a multi-physics module [43].

2013 MQP group that worked on the thermal controls subsystem used COMSOL in order to create a thermal model of the CubeSat [1]. COMSOL was chosen in the previous years due to its ease of use, compatibility with existing CubeSat CAD model created using SolidWorks, and well-developed graphical user interface (GUI).

3 Methodology

3.1 Command and Data Handling Subsystem

3.1.1 System Requirements

The first step in the definition of any of a spacecraft's subsystems is to determine the operations and tasks that it needs to fulfill. For the C&DH subsystem, these requirements take the form of computational operations, commands sent to other spacecraft systems, and data storage [21]. Accordingly, these needs must be ascertained before the development of the C&DH system is commenced, such that one can make sure the system can accomplish the tasks set before it. Those in charge of developing the other subsystems on a spacecraft must thus be consulted, to learn what the OBC must command or compute for their respective systems. In addition, these subsystems might require additional information from other subsystems, and so these requirements must also be taken into account when developing the C&DH subsystem.

The following information was accordingly requested regarding each component:

1. What does the computer need to do for this sensor/system?
2. When is this sensor/system on?
3. When the system/sensor is interacting with the computer, how frequently will the computer need to perform each operation from Question 1?
4. How much data will be generated by this sensor/system?
5. How long will this data need to be stored?
6. Does the processing of this data need to be done in space?
7. How does this sensor/system connect to the computer?

Additionally, the following details regarding the particulars of each operation which a subsystem could be commanded to perform were gathered:

1. What *operations* can the subsystem be commanded to perform?
2. What *inputs* are needed to perform this operation?
3. What *outputs* are the result of this operation?
4. What *triggers* this operation to be performed?
5. When triggered, how *frequently* must this operation be performed?
6. What is the *total time* it takes for this operation to be completed?
7. Are there any other subsystems/sensors which you know *cannot* be active while your subsystem is performing this operation?
8. Similarly, is there any subsystem which *must* be concurrently operating in order to make this operation successful?

This information would prove useful in the definition of the C&DH subsystem. Once the operational requirements and means of commanding each of the C&DH system's dependents were fully understood, the C&DH system's software and hardware could be begin to be outlined.

3.1.2 Hardware & Software Definition

Software

Software development is informed by the computational needs of all the CubeSat's subsystems. Each of the subsystems which performs tasks for the satellite must be commanded to carry out such actions; additionally, each of these commands has certain input and output information which must be known by the OBC in order to initiate the correct operation. This information must be gathered from the appropriate subsystems and sensors in order to be made useful for the OBC. For example, the attitude determination and control system's (ADCS) BDOT controller, which will be used to stabilize the CubeSat upon ejection from its launch vehicle, must have as input the spacecraft's angular momentum as measured by a gyroscope and the magnetic field vector with respect to the satellite's axes. The algorithm is then invoked by the OBC, which outputs currents for the EPS to deliver to the spacecraft's magnetorquers for attitude control. In

order to intuitively streamline the understanding of each operation of this sort, block diagrams can be developed to represent each of the commands the OBC can issue, incorporating the inputs and outputs of these functions. A block diagram for a typical function is shown in Figure 17.

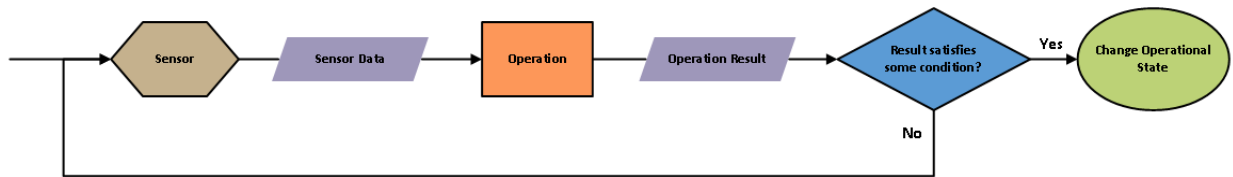


Figure 17: C&DH Block Diagram Example

In Figure 17, one can see examples of each of the elements, which are incorporated into operational sequence block diagrams. Here, the example from above is continued. A sensor such as the gyroscope produces some reading, which is used by subsystem operations such as the ADCS BDOT algorithm enacted by the OBC. This operation may result in another piece of information output for other systems to use as is the case here, or the operation may be complete in itself, without output data. Following the operation, a conditional qualifier is applied to the resultant data: if the condition is satisfied one course of actions follows, else a different one will ensue. Lastly, a certain course of events can result in a change in the spacecraft’s Operational State, a notion that will be discussed shortly. Following the detumbling example, if the resulting spacecraft angular motion is below a specified limit, the C&DH subsystem would allow the spacecraft to proceed to the next phase of its mission, otherwise it would instruct the spacecraft to carry out the same sequence of events again.

The complete operation of the spacecraft can be characterized by the interaction of many of these functions, where one operation’s results can be used in turn by others in pursuit of mission objectives. As such, these functions can be organized in larger-scale block diagrams, which

represent the whole of the spacecraft's operations throughout the span of its mission. One diagram representing the entirety of a multi-year mission would be too complicated to provide a clear understanding of the function of individual components. However, one can identify significant sub-groups of tasks that can be considered computationally independent sections of the mission operations. Each of these main groups of tasks can be considered an Operational State of the spacecraft. Continuing the earlier example, the Operational State which corresponds to the execution of the ADCS BDOT algorithm would be a Detumble operational state, which would include all necessary operations to bring the spacecraft from its initial uncontrolled spinning to a reasonable and controlled orientation. In this respect, the criteria for what is to be considered a "reasonably controlled" state must be defined, and can be incorporated into these block diagrams, determining when the OBC will allow the spacecraft to transition to another operational state.

The entirety of the operations of the CubeSat can be described by these Operational States, which can each be categorized into three main phases of mission operations: Initialization, Routine, and Deactivation. When initializing, a satellite must orient itself in its space environment and set up the spacecraft's systems to later fulfill mission requirements. The Detumble operational state discussed earlier would be incorporated into the initialization phase of the mission. Next, the routine phase of the mission ideally represents the majority of a mission's span, where it collects data from its instruments and communicates with Earth-based ground stations to relay information. Lastly, a spacecraft must safely be deactivated in order to ensure safe end-of-mission operations, consisting of turning off each of the spacecraft's subsystems. These major mission phases can be seen visualized in Figure 18, which illustrates how the satellites mission progresses from one phase to the next, and does not return to an earlier phase once complete.

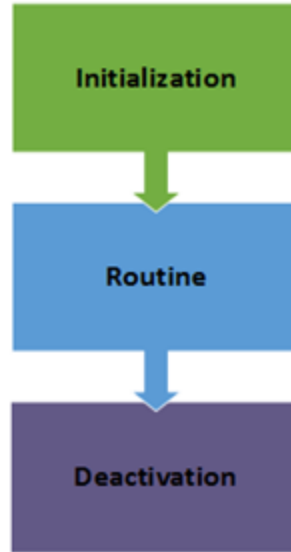


Figure 18: Mission Phases

The memory space taken up by the software which fulfills the computational requirements of the spacecraft can be estimated by using systems already implemented as examples. The textbook *Space Mission Analysis and Design, 3rd ed.* has a wealth of information to aid in producing such estimates [16]. These can be used as initial estimates for the size of the software parts of the C&DH subsystems, long before their development is actually begun [16]. This reference employs the concept of “similarity” to guide such estimates: for example, processing rate gyro data or estimating orbit propagation onboard will likely require similar computational requirements regardless of the particular spacecraft they are implemented upon.

CubeSat Functionality

A common strategy to develop and define a system is through “Model Based Systems Engineering.” Model Based Systems Engineering is a method used to clearly define functional and physical architecture using various interconnected models that incorporate system functions, operations, and components [44]. An architecture, whether functional or physical, is defined as the

total compilation of functional or physical design of a system along with their corresponding interactions. Functions that a CubeSat must perform are allocated to individual subsystems or components in an effort to ensure mission requirements are met. This is true in not only small satellites, but also in larger, more complex systems. Nevertheless, the strategy and its importance remains the same.

The universal, modular architecture of a CubeSat almost guarantees that many examples are highly comparable, making reuse of research critically important to saving time and cost. Due to this, the University of Michigan with the help of CalTech put together a fairly complete functional and physical architecture for a developed CubeSat [45]. Figure 19 shows the method by which the University of Michigan project established the CubeSat’s architecture (both functional and physical).

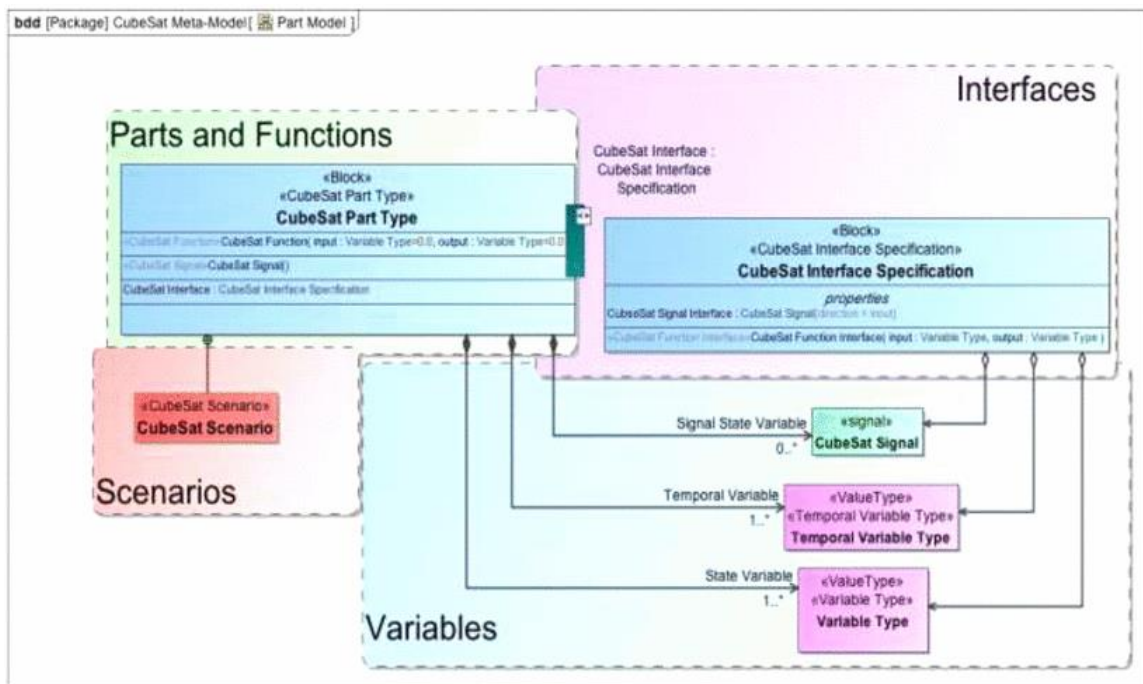


Figure 19: University of Michigan Functional Model Methodology [45] © IEEE 2012

Figure 19 shows how the CubeSat scenarios are used to define CubeSat functions and components, including the functions and components used to create interfaces between the various parts. Using this method, the University of Michigan developed a list of functions for each subsystem. These functions and their corresponding subsystems are shown in Table 2.

Table 2: List of University of Michigan Subsystem Functions [45] ©IEEE 2012

#	System Logical Component	Function (Input:DataType, Output:DataType)
1	Structures and Mechanisms	Enable Operations of Subsystems(Controls : Controls, Mechanism States : Mechanism States) Inertia Control of Position and Altitude(Forces : Force, Moments : Moment, Position : Position, Attitude : Attitude) Mass Control of Position and Altitude(Forces : Force, Moments : Moment, Position : Position, Attitude : Attitude)
2	Power Collection and Control	Regulate Energy(Solar Power : Power, Battery Electrical Power : Power) Collect Energy(Solar Power : Power, Battery Electrical Power : Power) Store Energy(Solar Power : Power, Battery Electrical Power : Power)
3	Position Determination and Control Subsystem	Determine Position(Position Reference : Position Reference Data, Energy : Energy, Information on Position : Position) Control Position(DesiredOrbit : Orbit, Energy : Energy, PositionAdjustmentForce : Force)
4	On-Board Data Handling and Command Dispatcher	Dispatch Commands(Mission Commands from Ground : Commands, Subsystem Commands : Commands)
5	Mission Data Handling	Process Data(Energy : Energy, Mission Data : Mission Data, Mission Data Processed : Mission Data) Compress Data(Energy : Energy, Mission Data : Mission Data, Mission Data Processed : Mission Data) Delete Data(Energy : Energy, Mission Data : Mission Data, Mission Data Processed : Mission Data) Filter Data(Energy : Energy, Mission Data : Mission Data, Mission Data Processed : Mission Data)
6	Mission Data Acquisition	Collect Mission Specific Data(Energy : Energy, Mission Data : Mission Data)
7	Communication	Transmit Telemetry(Flight Computer Telemetry Data : Data Rate, Flight Computer Mission Data : Data Rate, Energy : Power, Ground Station Telemetry Data : Data Rate, Ground Station Mission Data : Data Rate) Receive Operations Commands(Ground Station Data : Data Rate, Energy : Power, Flight Computer Operations Commands : Data Rate)
8	Attitude Determination and Control	Determine Attitude(Attitude Reference : Attitude, Energy : Energy, Filtered Attitude Measurements : Attitude, Sensor Measurements : Attitude Sensor) Control Attitude(Energy : Energy, Desired Attitude : Attitude, Attitude Torque : Torque)
9	Thermal Determination and Control	Detect Temperature(Thermal Reference : Thermal Data, Thermal State Data : Thermal Data) Control Temperature(Current Temperatures : Temperature, Temperature Control Commands : Commands)

Additionally, “time sequence diagrams” define the list of functions necessary to complete a system’s mission. A time sequence diagram is a figure that outlines a particular scenario where functions are being performed by physical components of a system (i.e. CubeSat subsystems) over

time, and how they interact with each other [46]. For this project, Microsoft Visio was used to create both the time sequence diagrams along with the full list of functions [47].

Following the guidelines in the University of Michigan report, the method used to develop the functions for this CubeSat was to create various system scenarios to define functions. For example, defining the common scenario of downlinking data from the spacecraft could yield a comprehensive list of necessary functions. Then, subsystem developers were consulted to ensure the correct terminology and list of functions. The final step was to compile all the functions defined into a comprehensive list.

Hardware

The hardware to be used for the C&DH subsystem must include both a processor that is capable of performing the command throughput required by the mission operations, and sufficient memory for the storage of data before it is either operated upon or relayed to Earth, and subsequently deleted. These components are described in Section 2.1.2. Additionally, one must take into consideration the different types of data interfaces used by the various spacecraft systems and sensors. If a sensor requires a certain type of interface to communicate with the OBC or other subsystems, then the OBC must support that type of interface for the system to operate, or another sensor must be found. Examples of these types of data interfaces can be found in Section 2.1.3.

The distribution of the various elements of a satellite's data structure must also be considered when selecting hardware components. This arrangement, known as the architecture of the C&DH system, can exist in various forms [16]. For example, the OBC can reside centrally with all other systems reporting to and only to it, in what is known as a Centralized Architecture, or the OBC could reside in a series configuration with all other sensors and subsystems where the same data is passed in turn to each of a satellite's systems for operation. Many commercial off-

the-shelf (COTS) OBC products available on the market employ a Bus Architecture, in which all elements of the C&DH system are accessible to each other through a central communications bus [16]. This setup is advantageous because it allows the use of other COTS products for use in other subsystems, which likely were developed with similar interfaces. Most often these OBCs were developed to support multiple variants of data interfaces, so that they can communicate with whichever other subsystems they need to. The Bus architecture is also useful because large changes in hardware or software are not required when adding a new element to the C&DH bus; as long as the new element uses the same data processing protocols, a relatively seamless integration can occur so that the OBC can have access to the new element and its capabilities like an existing ones.

The hardware selected must be able to perform its required tasks. The hardware also must be tested analytically before it is implemented into the final configuration of all subsystems, to ensure its capabilities are adequate for the anticipated operational scenarios.

3.1.3 Computing Profile Modeling

In order to assure the proper operation of the C&DH subsystem in practice, a model of the spacecraft's operations must be created. Such a model enables the simulation of each of the spacecraft's subsystems, determining if the proper selections have been made for the system's components. The C&DH subsystem can be modeled using software such as MATLAB numerical computing software to accurately simulate the spacecraft's systems and their states. At a base level, one must know when each of the satellite's subsystems and sensors will be on, which can be informed by various environmental and operational state based information. Depending on which state the spacecraft is in, some systems might be continuously operating, while other systems might be triggered on or off by situational events. This kind of model is naturally informed by one's block diagrams of the spacecraft's Operational States, which show the triggers, which cause certain

systems to turn on or off. A simple example of a system's states is shown in Figure 20. In Figure 20, the system is off until a certain event at $t = 1000s$ turns it on, then another turns it off at $t = 4000s$.

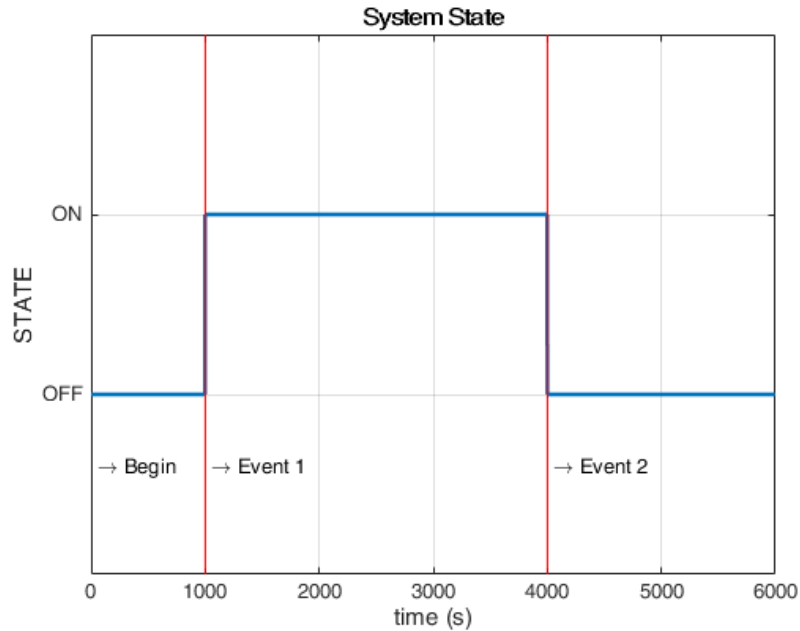


Figure 20: System State Model

Using this kind of a simulation along with other information, such as the amount of data a system will produce when it is on, one can model the operations of the spacecraft's C&DH subsystem. For the C&DH subsystem, the main capacity concerns for the system are amount of computational operations it must perform, and the memory used for data storage. Knowing when systems are on, how much and how frequently they produce data, one can create a time dependent model of the critical capacities of the system, similar to the state model. Such simulation should be divided into separate analyses for volatile and non-volatile memory usage. Sensor data is an example of information which would be stored in volatile memory, as each sensor reading would replace the previously stored reading in its place. As such, while a sensor is on, it uses a constant

amount of volatile memory. Figure 21 shows the volatile memory used by a sensor which produces 2 kB readings, with the state modeled in Figure 20.

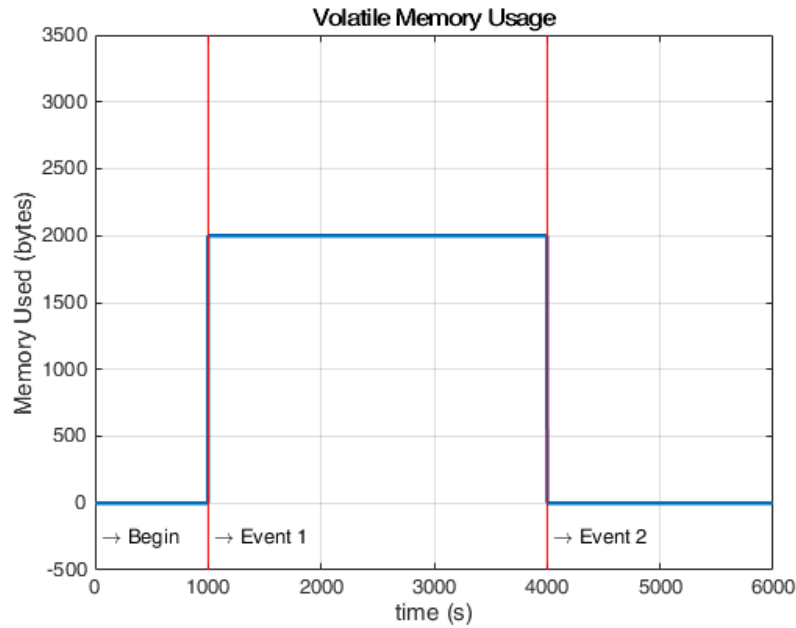


Figure 21: Volatile Memory Storage Model

Otherwise, if the data produced by a system did not replace previously stored values, data would instead accumulate over time. Such information would likely be stored in non-volatile data for protection until the data could be downlinked or deleted otherwise. For example, if the system modeled in Figure 21 was to produce 1 byte of data every second it was on, and no data was deleted from the OBC’s memory, the simulation shown in Figure 22 would result, showing the spacecraft’s nonvolatile memory usage over time.

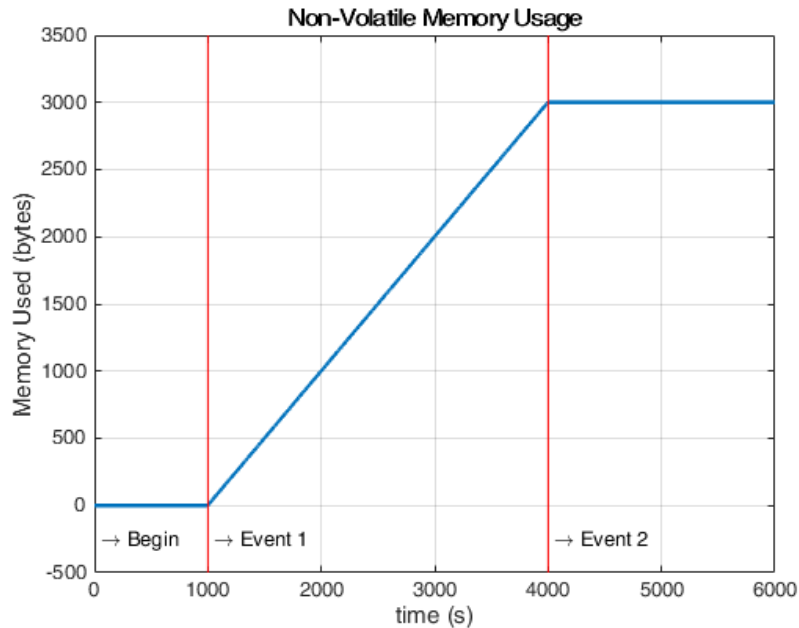


Figure 22: Non-Volatile Memory Storage Model

When all of the systems of a spacecraft are considered in this manner and the conditions for the deletion of stored data are added, a robust simulation of the memory used on board the spacecraft can be created. Since only a finite amount of storage is available on-board, if this value is surpassed at any point during the mission span, the C&DH system must be reassessed.

The definition of a spacecraft C&DH subsystem, like all others, is an iterative process. If the selected hardware is shown to be insufficient to handle the computational and data storage requirements, another piece of hardware must be sought out or compromises must be found among the developers of other subsystems. In this way, a robust and appropriately equipped C&DH subsystem can be developed to suit the satellite.

3.2 Power Subsystem

3.2.1 Power System Evaluation

The first major step in the design of a power system is determining a set of requirements for the system to meet. As a first step, the power requirements for all of the components that have been selected for this mission were compiled and from that information, the typical amount of power consumed by the CubeSat during typical operation was estimated. Next, the power output of a chosen solar array configuration was calculated using Equation 3:

$$P_{sa} = \eta_c A G_s \cos(\theta) \quad (3)$$

P_{sa}: Power generated by solar array [W]

η_c: Efficiency of solar cell

A: Area of solar cells [m²]

G_s : Solar flux in low-earth orbit (1367 W/m²)

θ: Angle of incidence between the surface normal of the solar array and the sun

As stated before, the angle of incidence of sunlight should never exceed 5 degrees, so the cosine loss term was neglected. The team then performed a solar array output simulation in STK using a CubeSat model generated by the 2013 MQP team [1]. This calculation does not, however take into account inefficiencies in the system due to the temperature of the arrays and the electrical interfaces between the array and the power users. As such, the total power transferred to the CubeSat's batteries will be less than this figure would suggest.

The effects of the thermal environment on the power output of the solar panels must also be accounted for. Solar panel efficiencies are often reported for a temperature of 301 K, but the CubeSat will be subjected to a wide range of temperatures. Equation 4 describes the effect of the solar cell temperature on the cell's efficiency.

$$\eta_{c2} = \beta(T_1 - T_2) + \eta_{c1} \quad (4)$$

η_{c2} : Efficiency of solar cell at temperature T_2

β : Temperature coefficient, dependent on cell material [K^{-1}]

T_1 : Reference temperature (typically 301 K) [K]

T_2 : Temperature of interest [K]

η_{c1} : Efficiency of solar cell at reference temperature T_1

Using Equation 4, and data for the temperature of the solar arrays over time, a robust estimate of the power generated by the solar arrays can be created.

Another major constraint on the power system that was identified was the total current load on the battery. The maximum current that can be supplied by a battery without risking damage to it is proportional to its total capacity and is listed within the battery documentation. When the final power profile is created, this maximum current must be taken into account.

3.2.2 Power Component Selection

The 2012 MQP group identified a number of Clyde Space components as ideal selections for the mission including battery, EPS and PDM boards, and solar panels [4]. Many of these components were no longer available for purchase, but Clyde Space components were still prioritized to supply all of the power system components due to their extensive flight heritage [4].

For this mission, the Clyde Space 25-02452 3UA EPS was chosen to serve as the main EPS board [23]. The selection of the main EPS board is of vital importance as the overall power system architecture will depend upon the specific component. For instance, in both the 2012 and 2013 MQP mission studies, the task of conditioning and distributing power to the CubeSat was delegated to a specific PDM board (Clyde Space model number CN-SWT-0035-CS) [1,4]. However, on the newer Clyde Space EPS that was selected for this work, these capabilities are handled on the same board that manages the incoming solar panel power [23]. Once the EPS is

chosen, a battery board can be selected that meets all specific mission requirements and easily integrates with the EPS. Clyde Space offers CubeSat batteries in a wide range of capacities that are designed to interface with their EPS components. The final, important step in the selection of power system components is the selection of the solar array configuration. The solar arrays must provide adequate power to all of the CubeSat’s power users while also not interfering with the CubeSat’s primary instrument payload. Additionally, the array configuration must be compact enough to fit inside the P-POD deployer before deployment and must not adversely impact the thermal profile of the CubeSat.

3.2.3 Power System Distribution

Most CubeSat electrical boards are designed to be vertically integrated using the 104 pin PC-104 connector bus, which is comprised of two adjacent 52 pin connectors known as Header 1 (H1) and Header 2 (H2) respectively. For example, to refer to a specific pin, the designation typically takes the form of H1:23 to denote pin 23 on Header 1 [48]. A diagram of the EPS, with labeled solar array (SA) connectors and the main headers is shown in Figure 23.

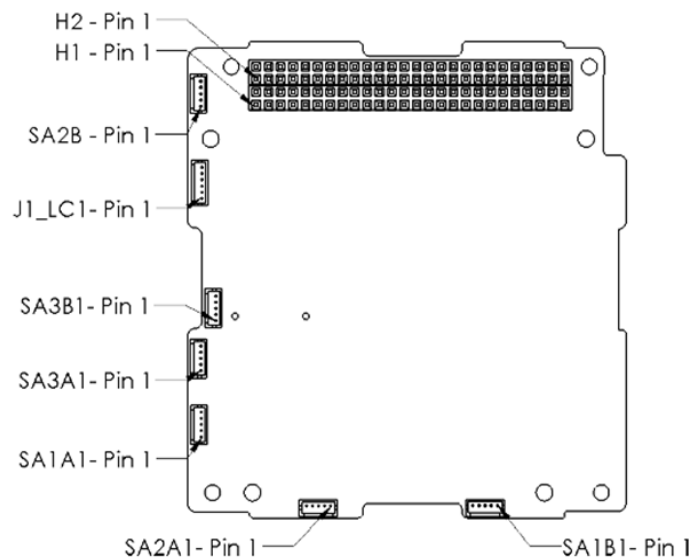


Figure 23: Clyde Space 25-02452 3U EPS [23]. Copyright © 2016 Clyde Space Ltd.

The PC-104 bus easily connects all electrical boards in a compact, vertical “circuit stack.” A possible circuit stack configuration for this mission would be, beginning from the top and stacked as follows: a VHF/UHF transceiver, the OBC board, the battery board, the EPS board, and optionally other boards if needed.

Power generated by the solar panels is routed to three of the six total solar array (SA) connectors on the EPS. These SAs are paired into two channels, labeled A and B. Each of the three SA pairs is connected to their own individual battery charge regulator (BCR) located on the EPS board. These BCRs serve to control the voltage and current outputs of their connected solar arrays, using the maximum power point tracking (MPPT) algorithm, which attempts to maximize the solar array efficiency by maintaining each array at its individual maximum power point. Figure 24 shows the wire connections between the solar arrays, the SA connectors, and their respective BCR.

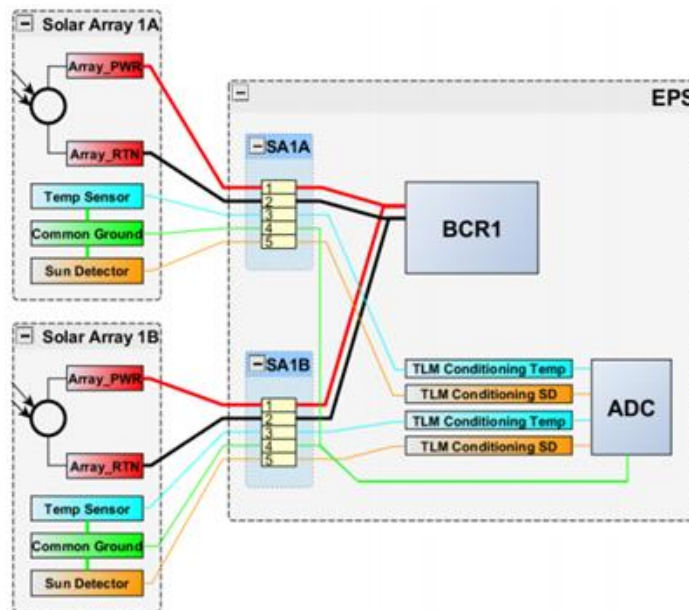


Figure 24: Example Solar Array Configuration SA1-3 [23] Copyright © 2016 Clyde Space Ltd.

The chosen EPS board contains two Buck BCRs and one SEPIC BCR [23]. The Buck BCRs allow the EPS to interface to strings of four to eight solar cells in series and can deliver up

to 90% of the array's power. It is named for its utilization of a Buck power converter, which is a type of DC-DC power converter which steps down voltage from input to output. The SEPIC BCR on the other hand, allows the EPS to interface to arrays of two triple junction cells in series, while delivering up to 80% of the array's power. Triple junction cells are specialized solar cells made from multiple materials in order to capture a larger range of the electromagnetic spectrum and thus produce more power per cell than single-junction cells [57].

These BCR's charge the battery and have two distinct modes of operation: maximum power point tracking (MPPT) mode and end of charge (EoC) mode. MPPT is used when the battery voltage falls below a preset voltage and employs a constant current charge method, operating at the maximum power point for the connected solar panel. Once the battery voltage reaches the EoC voltage, EoC mode is enabled, which employs a constant voltage, tapering current to charge the battery until it is at full capacity. In EoC mode, the solar array operation point is moved away from the maximum power point and the BCR draws only the required power, leaving the excess dissipated in the arrays as heat.

The BCRs also supply power to four power conditioning modules (PCMs) located on the EPS board. Three of these PCMs convert power into separate 3.3 Volt, 5 Volt, and 12 Volt power outputs with a deviation of $\pm 1\%$ peak to peak. The fourth PCM provides a direct voltage connection to the battery, supplying the current battery voltage (typically 7.6 Volts). All four of these outputs are routed to the main CubeSat bus as well as a series of power distribution modules (PDMs) also located on the main EPS board. An overview of the EPS, including the PCMs and PDMs is shown in Figure 25.

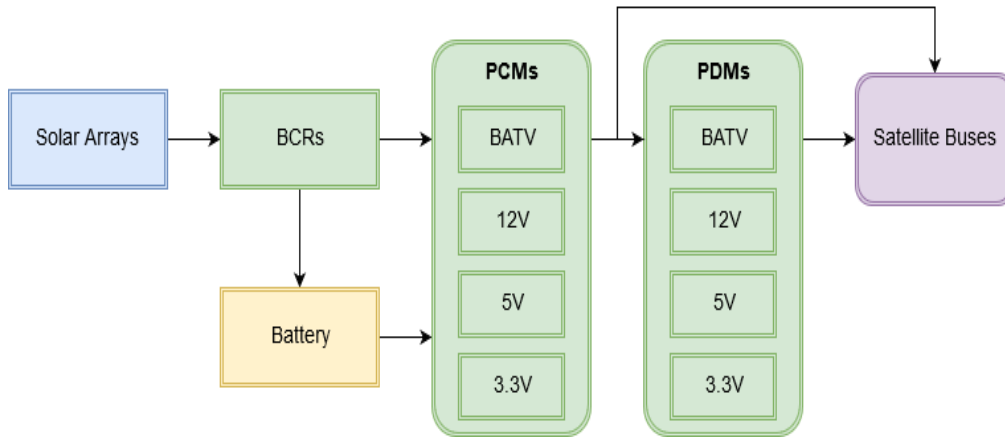


Figure 25: EPS Board Power Flow

The PDMs provide additional power outputs to the main CubeSat bus and contain ten MOSFET switches, which can be individually commanded on and off to control the power state of individual components. Of these ten switches, switches 1-2 output at a maximum voltage of 12 Volts, switches 3-4 at a maximum of 8.3 Volts, since they connect directly to the battery, switches 5-7 at a maximum of 5 Volts, and switches 8-10 at a maximum of 3.3 Volts. Each switch can also support a maximum current of 1 Amperes before it triggers its PDM's latching current limiter (LCL), which provides overcurrent protection to the PDM by switching it off after a certain interval of excessive current draw. A full list of the pin locations of each PCM and PDM are located in Appendix E. In addition, the power return for each switch must go to the ground pins H2:29, H2:30, or H2:32 on the CubeSat bus. These ground pins shall also carry current.

The boards that populate the circuit stack, including the OBC, receive power through the direct PCM connections on the CubeSat bus header and are not powered on through a PDM switch. Once the pull pin is removed and the deployment switches are no longer actuated, the boards in the stack receive uninterrupted power.

3.2.4 Telemetry Communication

Each solar array includes an integrated temperature and sun sensor. Information from the sensors along with the voltage and current from each solar panel as measured by the BCRs is relayed to the EPS, which can be queried by the OBC to report such information. The OBC can also query the EPS for other telemetry data such as the output current and voltage of each individual PDM switch, PCM, and BCR [23].

Additionally, the OBC can command each individual PDM on and off. Each PDM can be commanded on indefinitely or for a specified length of time after which it will automatically switch off. The status of each PDM can also be retrieved and the OBC may set an initial switch configuration, which will take effect upon power up of the CubeSat.

Control of the EPS by the OBC is done using an Inter-Integrated Circuit (I²C) network, which consists of a two-line system between multiple boards, using two pins on the CubeSat bus; a clock line and a data line. Each board in the stack contains an I²C node, which can communicate with the master I²C node on the OBC. More information about the I²C data interface can be found in Section 2.1.3.

3.2.5 Power Profile Modeling

To insure that the power subsystem fulfills the CubeSat's power requirements, a model of the spacecraft power subsystem was created. Such a simulation could be of a very similar form to that used to model the C&DH subsystem, with a few major differences. In such a simulation, the most important figures to model as a function of time would be the total charge of the battery, the total power draw of the entire CubeSat, solar array power production, and the total current draw. After hardware is selected, this simulation will be used to evaluate if that hardware meets the mission requirements and to establish a feasible operational sequence for the mission. Should the

selected hardware prove insufficient to meet the simulation requirements, either the simulation requirements will be changed to meet the capabilities of the selected hardware or new hardware will be selected.

3.3 Telecommunications Subsystem

3.3.1 Ground Station Network Analysis

The main objective for the telecommunications subsystem, is to have clearly defined ground station access time on a regular basis and the corresponding data budget profiles. The primary method in mapping the CubeSat's ground station network along with its corresponding data budgets were calculated using Systems Tool Kit or STK. STK is a software simulation tool that allows for detailed definition of satellite properties, ground station properties, and their interaction [49]. Most notably, STK provided the amount of time the CubeSat was available for data transfer with a ground station after all losses were taken into account. The following sections detail how STK can be used in this way.

As part of the STK analysis, several assumptions were made about the Ground Station Network accessible to the CubeSat. The major assumption was that the CubeSat could tap into the GENSO Ground Stations around the world. The most previous MQP completed in 2013 performed studies to choose five stations that would provide suitable coverage [1]. These stations consist of Cal Poly, University of Texas, WPI, Delft University, and Warsaw Institute of Technology. These ground stations were included in the STK simulation along with the CubeSat to calculate when and for how long the CubeSat could access each in a typical orbit. The orbital parameters from the 2013 MQP are slightly different from the current work [1]. The orbital parameters for this study were as follows: a 24-hour period, inclination of 98.44° , a circular orbit with an altitude of 700

km, and a right ascension of the ascending node (RAAN) of 142.252° were used to create a satellite in the program [1]. A ground track from this particular STK scenario is shown in Figure 26.

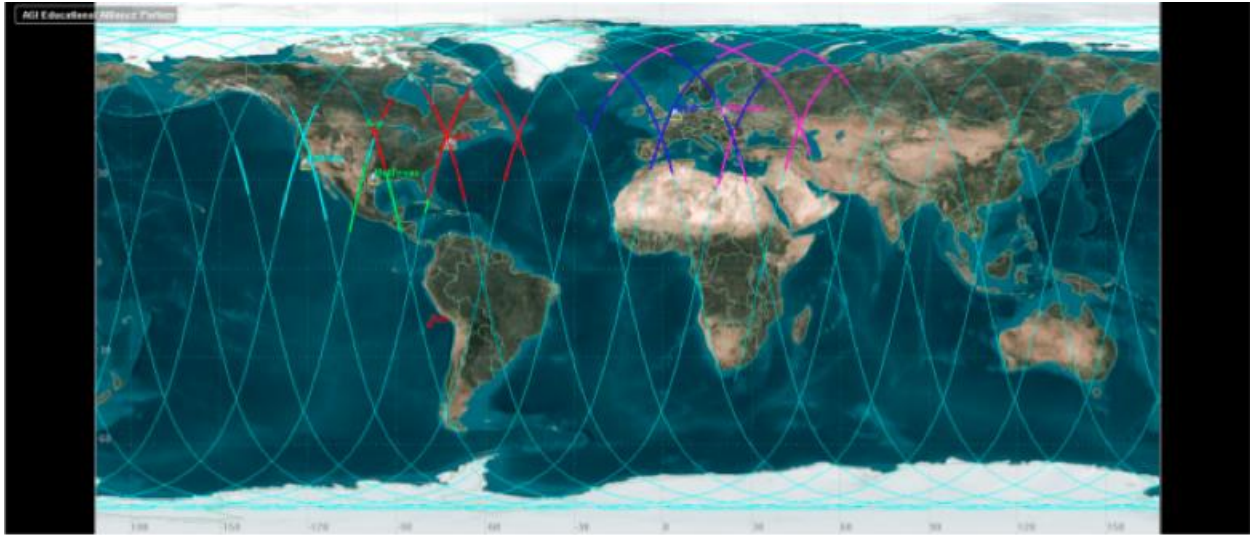


Figure 26: STK Ground Station Ground Track

To verify the 2013 MQP's baselined ground station network, research was conducted by the CubeSat team into the operational ability of GENSO [1]. The 2013 MQP planned to use the GENSO ground stations to communicate to and from the CubeSat, as described in Section 2.3 [1]. However, online research along with correspondence with professors at the California Polytechnic State University, it was determined that the GENSO network was no longer operational and different stations needed to be chosen as the ground stations for the present study.

The new set of chosen ground stations consist of two stations: University of California - Los Angeles in Los Angeles, CA and Warsaw Institute of Technology in Warsaw, Poland. These locations were considered to be available for usage of the team's CubeSat. Secondly, it was determined that an addition of a mobile ground station (MGS) at WPI in Worcester, MA would be feasible and very valuable.

Mobile Ground Station (MGS)

A mobile ground station (MGS) is a station that is small enough to be deployed with relative ease while incurring a small cost to build. At its most fundamental level, a mobile ground station needs communications devices (transceiver and antenna), a computer with CubeSat auto-tracking software, a physical base to support and house these components, and the various wires and connectors that connect the pieces together.

Two objectives for this project with respect to the MGS were to first, identify a design that was could be realized and second, obtain enough information so that an accurate cost estimation could be made. A mobile ground station built at the University of Hawaii at Manoa was identified that became a model for this project's MGS design [50]. A picture of the completed ground station at the University of Hawaii can be seen in Figure 27.



Figure 27: Built University of Hawai'i at Manoa Mobile Ground Station [50]

The design of the structure is relatively simple. A wooden base was designed to house the antenna via a telescoping piece, extending the antenna into the air. An azimuth and elevation rotor were attached to the antenna to allow for movement in any direction, to track the satellite's position and be in position for incoming/outgoing communications. This physical hardware was then attached to a laptop with satellite tracking software that auto-tracks the satellite's position.

The most complete research paper found that had a detailed MGS design and costing information described the MGS built at the University of Hawaii (Manoa) in 2007 [50]. This study was therefore used to cost the MGS option for this project. Since the study is approximately ten years old, some of the components have been discontinued, in this case, comparable but newer technologies were used. The complete description of the proposed MGS, including a component and price list, is provided in Section 4.3.

Once the available set of Ground Stations were established, calculations of the daily access time and data budgets for the CubeSat could be conducted.

Ground Stations - Access Time

Access time from the CubeSat to the trio of ground stations was calculated using STK. A detailed explanation on how access time is calculated in STK is provided in Section 3.3.3. Access time is defined as time available for the CubeSat to downlink data, constrained by the limits of both the CubeSat's communication system and the target ground station.

3.3.2 Second Mobile Ground Station Case Study

Purpose and Criteria

Due to amount of payload data created and the lack of access time (thus available data downlink), a case study to determine the best location for a second mobile ground station was conducted.

The criteria used to select the second mobile ground station's location were that 1) the location had to be a WPI Global Project Programs location so that the location has an affiliation with WPI along with students yearly attending the sites, 2) the ground station collects data outside of the baseline data collection zones so that the total quantity of data that can be downloaded increases, and 3) that the location is a recurring project center so that WPI students frequent the location multiple times a year. Based on these criteria, Asunción, Paraguay, Bangkok, Thailand, Cape Town, South Africa, and Melbourne, Australia were selected as potential sites for the case study.

Station Selection

The four stations were entered into an STK simulation to analyze the added data and access time for the WPI CubeSat. Figure 28 shows a world map generated in STK showing the four candidate stations.



Figure 28: Second MGS Case Study STK Scenario

3.3.3 STK Analysis

Scenario Definition

A scenario in STK is the single file that houses all of the satellite, ground station, and hardware information needed to fully define the system.

To define the scenario, the CubeSat's orbital parameters are entered into the CubeSat's definition along with the ground stations that are defined as *Facilities* in the software. The longitude, latitude, and altitude of the ground stations were inputted to create each of the *Facilities*. The hardware associated with both the ground stations and the satellite are also defined, identified by the name of the corresponding objects such as *Receiver*, *Transmitter*, and *Antenna*. The assumed specifications for each piece of hardware are listed in Table 3. These assumptions allowed calculation of access time and data budget information for the assumed, baseline case.

Limits and Constraints

The satellite's orbital parameters are described as followed: an inclination of 98.44° , an altitude of 600 km, and RAAN of 142.252° .

The satellite is assumed to have a transmitter operating in the UHF band with the characteristics found in Table 3 [32].

Table 3: Transmitter Attributes

Frequency	435.5	MHz
Power	0	dBW (1 Watt)
Data Rate	9.6	Kb/s
Modulation	BPSK	
Pointing Loss	-1	dB

The CubeSat also has an assumed antenna that is designed for the UHF band with the characteristics outlined in Table 4 [35].

Table 4: Antenna Attributes

Length	.55	m
Length/Wave Length	.799	
Efficiency	.55	
Refraction Model	ITU-R P.834-4	
Range Limit	3000	km

For every one of the ground stations, the hardware incorporated a medium complexity receiver model with the characteristics described in Table 5 [1]. The medium complexity of the model just defined the amount of attributes that can be assigned to the hardware.

Table 5: Ground Station Attributes

Gain	32.8	dB
Line loss	4	dB
LNA (Low noise amplifier)	1.2	dB
Refraction Model	ITU-R P.834-4	
Min Elevation angle	5	degrees
Doppler Shift	+/-25	KHz

This information can be used to model the various pieces of communications hardware for the CubeSat system in STK to construct the uplink and downlink profiles, along with the link budget.

Link Budget

An important concept in satellite communications is the link budget. The link budget fully defines all of the gains and losses experienced by a signal travelling from a transmitter to a receiver [51]. The link budget is given by Equation 5.

$$\text{Received Power(dB)} = \text{Transmitted Power(dB)} + \text{Gains(dB)} - \text{Losses(dB)} \quad (5)$$

Using this equation, it is possible to calculate the dB margin, or the amount of allowable data loss.

STK has the ability to calculate the link budget with its related parameters such as effective isotropically radiated power (EIRP), received isotropic power (RIP) and bit error rate (BER). If all of the hardware limits and constraints are incorporated into the STK model, a scenario analysis can be generated to gather the signal information. Figure 29 displays the Link Budget report's information over a representative time period with a sample ground station.

Time (UTC)	EIRP (dBW)	Recv. Frequency (GHz)	Recv. Iso. Power (W)	Flux Density (dBW/m ²)	g/T (dB/K)	C/No (dB*Hz)	Bandwidth (kHz)	C/N (dB)	Eb/No (dB)	BER
1 Jan 2019 00:09:29.602	21.000	0.435010	6.885616034230e-014	-117.395102	6.000000	135.778567	19.200	92.3456	91.9559	1.000000e-030
1 Jan 2019 00:10:29.000	21.000	0.435010	1.001214862445e-013	-115.769257	6.000000	137.404412	19.200	94.5714	93.5817	1.000000e-030
1 Jan 2019 00:11:29.000	21.000	0.435009	1.567621247677e-013	-113.822119	6.000000	139.351550	19.200	96.5185	95.5288	1.000000e-030
1 Jan 2019 00:12:29.000	21.000	0.435008	2.657292528917e-013	-111.530137	6.000000	141.643533	19.200	98.8105	97.8208	1.000000e-030
1 Jan 2019 00:13:29.000	21.000	0.435006	4.647655818515e-013	-109.102191	6.000000	144.071478	19.200	101.2385	100.2488	1.000000e-030
1 Jan 2019 00:14:29.000	21.000	0.435001	6.446466722788e-013	-107.681313	6.000000	145.492356	19.200	102.6593	101.6696	1.000000e-030
1 Jan 2019 00:14:34.524	21.000	0.435000	6.464448724023e-013	-107.669215	6.000000	145.504454	19.200	102.6714	101.6817	1.000000e-030

Figure 29: Sample Link Budget Report

The columns in this report are the Time in which the signal was received, the EIRP in dB, the Received Frequency in Hz, the Received Power in W, the Flux Density of the signal in dB/m², a pre-defined value of g/T (the antenna's gain-to-noise temperature) in dB/K, the original carrier to noise ratio, C/N₀ in dB, the Bandwidth measured in Hz, the final carrier to noise ratio C/N

measured in dB, the energy per bit to noise power spectral density ratio, E_b/N_0 , measured in dB, and finally the pre-defined bit error rate (BER). Understanding the link budget for each access period is imperative while analyzing the amount of data being sent by the CubeSat because the smaller the amount of link budget margin, the smaller the amount of data that can be transferred during access times.

Access Time

To calculate the *Access Time* of a CubeSat in relation to the *Ground Stations* for a particular scenario, a scenario analysis must be executed in STK. The *Access* report describes the exact *Start Time* and *Stop Time* in which the access occurred, the duration of the access, and the names of the two objects that experienced the access (i.e. Cubesat-to-Receiver2). A screenshot of sample access time results from the report can be seen in Figure 30.

For the *Access Time* report, the previously described orbital elements, objects, and their corresponding specific attributes were entered into the scenario definition. First, the Ground Stations are defined as *Facilities* with their exact Latitude, Longitude, and altitude. Second, a *Receiver* and *Transmitter* are assigned to each facility with their assumed hardware's information described earlier in Section 3.3.3. Next, the CubeSat's *Antenna* and *Transmitter* need to be defined using the characteristics of the hardware described earlier in this section. Once all of these parameters are entered, the user can select the objects to run the *Access Time* report. This reports out information about the access of the CubeSat to each selected ground station. In this same report, the link budget for each access time can also be determined.

AGI Educational Alliance Partner				26 Jan 2017 14:46:55
Satellite-CubeSat-To-Facility-Melbourne, Facility-UCLA, Facility-Warsaw, Facility-WPI: Access Summary Report				
CubeSat-To-Melbourne				
	Access	Start Time (UTCG)	Stop Time (UTCG)	Duration (sec)
	1	1 Jan 2019 02:36:24.331	1 Jan 2019 02:39:58.924	214.593
	2	1 Jan 2019 04:06:29.745	1 Jan 2019 04:18:55.533	745.787
	3	1 Jan 2019 05:42:57.507	1 Jan 2019 05:54:07.079	669.571
	4	1 Jan 2019 15:54:27.722	1 Jan 2019 16:02:27.158	479.435
	5	1 Jan 2019 17:28:16.325	1 Jan 2019 17:41:09.095	772.771
	6	1 Jan 2019 19:05:16.725	1 Jan 2019 19:14:09.140	532.415
	Min Duration	1 1 Jan 2019 02:36:24.331	1 Jan 2019 02:39:58.924	214.593
	Max Duration	5 1 Jan 2019 17:28:16.325	1 Jan 2019 17:41:09.095	772.771
	Mean Duration			569.095
	Total Duration			3414.573
CubeSat-To-UCLA				
	Access	Start Time (UTCG)	Stop Time (UTCG)	Duration (sec)
	1	1 Jan 2019 00:33:08.876	1 Jan 2019 00:41:37.271	508.395
	2	1 Jan 2019 08:15:17.104	1 Jan 2019 08:16:45.051	87.947
	3	1 Jan 2019 09:44:20.162	1 Jan 2019 09:56:47.497	747.335
	4	1 Jan 2019 11:21:00.249	1 Jan 2019 11:31:46.554	646.305
	5	1 Jan 2019 21:33:50.496	1 Jan 2019 21:42:41.099	530.603
	6	1 Jan 2019 23:07:55.489	1 Jan 2019 23:20:44.561	769.072
	Min Duration	2 1 Jan 2019 08:15:17.104	1 Jan 2019 08:16:45.051	87.947
	Max Duration	6 1 Jan 2019 23:07:55.489	1 Jan 2019 23:20:44.561	769.072
	Mean Duration			548.276
	Total Duration			3289.656
CubeSat-To-Warsaw				
	Access	Start Time (UTCG)	Stop Time (UTCG)	Duration (sec)
	1	1 Jan 2019 00:08:16.968	1 Jan 2019 00:20:57.677	760.709
	2	1 Jan 2019 01:44:44.779	1 Jan 2019 01:56:30.528	705.749
	3	1 Jan 2019 11:48:36.524	1 Jan 2019 11:55:31.424	414.900
	4	1 Jan 2019 13:22:41.170	1 Jan 2019 13:35:15.286	754.115
	5	1 Jan 2019 14:58:32.999	1 Jan 2019 15:10:38.444	725.445
	6	1 Jan 2019 16:35:19.748	1 Jan 2019 16:42:42.576	442.827
	7	1 Jan 2019 22:46:37.119	1 Jan 2019 22:56:38.102	600.984

Figure 30: STK Access Time Report

Daily Data Transfer

Even more important than calculating the access time is quantifying the amount of data that can be transferred between ground stations and the spacecraft during its mission span. From calculations presented in the 2013 MQP report [1], the average data rate from the spacecraft to the ground assumed for the STK analysis was 1101 byte/s. Using the access time calculated earlier and multiplying it by the data rate, the downlink and uplink budgets can be determined. Depending on the time of year and orientation of the satellite's orbit in relation to the ground stations, the

overall uplink and downlink budgets can vary. A graph of a sample annual downlink and uplink access time can be seen in Figure 31.

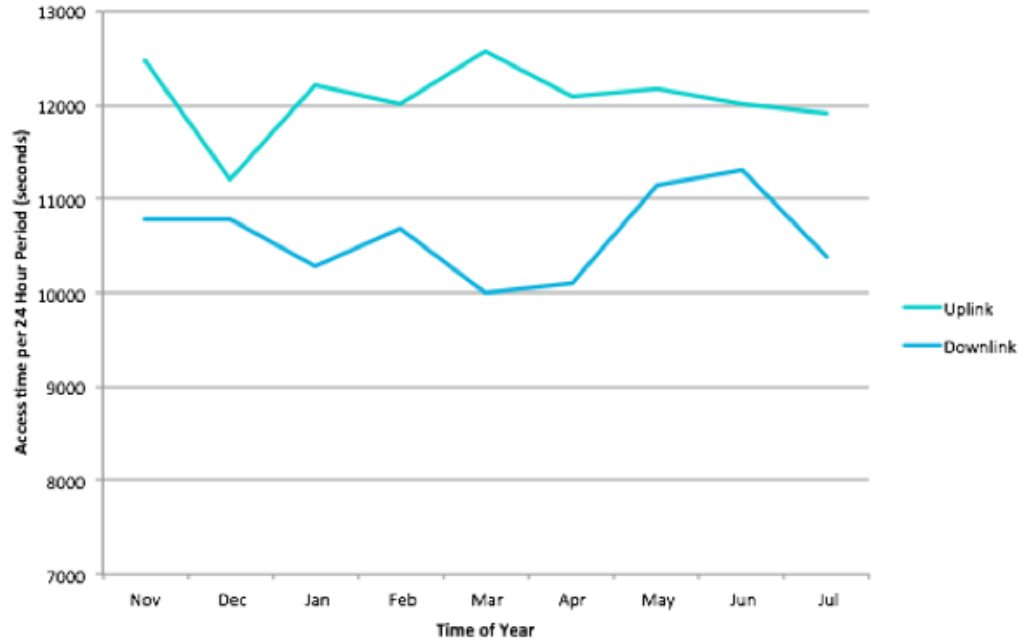


Figure 31: Access Time vs. Time of Year.

Due to CubeSat’s precessing orbit, the CubeSat will have a variable amount of time over each ground station and in turn, the amount of data transferred will vary throughout the year. This information is incredibly valuable so the mission operators know exactly how much data can be sent to and from the CubeSat throughout the year.

3.4 Thermal Controls Subsystem

3.4.1 STK Analysis

Systems Tool Kit (STK) was used to model the orbit of the CubeSat to gather thermal characteristics of CubeSat for some representative orbits. In the following discussion, specific

terms used for parameters in STK are italicized. The CubeSat was modeled in STK as a *Satellite* using orbital parameters given in Table 6.

Table 6: Orbital Parameters of CubeSat [7]

Start Date	0:00:00 January 1, 2019
Altitude	600 km
Inclination	98.44°
RAAN	142.252°
Argument of Perigee	0°

The attitude of the CubeSat was assumed to be in *Sun Alignment with Nadir Constraint*, which aligns the CubeSat body x-axis with the spacecraft-sun vector and rotates the body coordinate system so that the nadir vector always has no component in the y-axis and positive component in the z-axis of the CubeSat body coordinates. Because the attitude determination and control subsystem does not specify the orientation of CubeSat body y-axis and z-axis, this attitude was chosen because it meets the mission requirement that the x-axis must be pointed towards the Sun and simplifies the COMSOL simulation performed, which is described in section 3.4.3 [9]. Figures 32 shows the orientation of CubeSat body coordinate system, and Figure 33 display the *Sun Alignment with Nadir Constraint* orientation of the CubeSat.

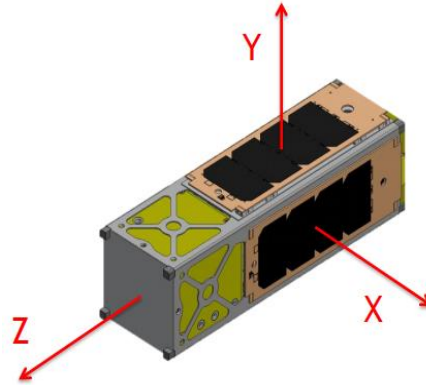


Figure 32: CubeSat Body Coordinate System Using the RHR [1] Copyright © 2013 WPI

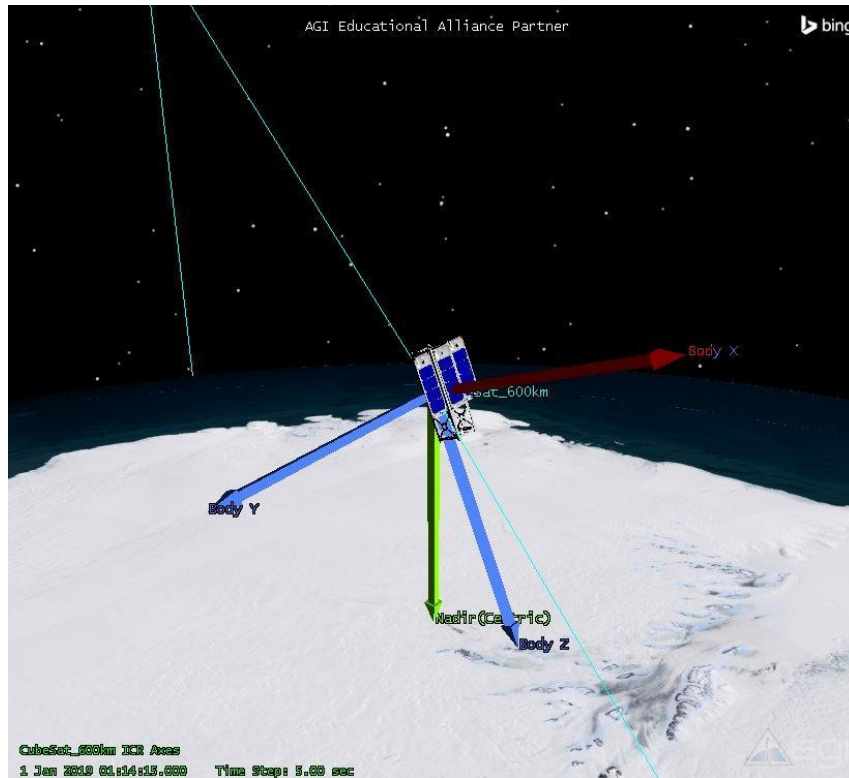


Figure 33: Illustration of *Sun Alignment with Nadir Constraint* Orientation

STK was primarily used to determine when and for how long the CubeSat is expected to be exposed to the Sun and to extract the coordinates of the nadir vector of CubeSat with respect to the CubeSat body coordinate system. From STK, three built-in reports were generated as Comma

Separated Values files (.csv) using Microsoft Excel for five representative orbits from the beginning of the mission: *Solar Intensity* report, *Beta Angle* report, and *Nadir Vector* report.

The *Solar Intensity* report consists of the time since the beginning of mission in seconds and the intensity of sunlight the CubeSat experiences as a percentage of full illumination. An intensity of 0% indicates that CubeSat is shaded from the Sun, and conversely an intensity of 100% indicates that CubeSat is fully illuminated by the Sun. Intensities between 0% and 100% indicate that CubeSat is in penumbra phase. *Solar Intensity* is used to calculate the amount of heat flux experienced by CubeSat throughout its orbit in COMSOL simulation described in section 3.4.3.

The *Beta Angle* report consists of the time since the beginning of mission in seconds and the value of beta angle, which is the angle between the spacecraft orbital plane and spacecraft-sun vector. Beta angle was used to calculate the value of view factor used in equation 1 from Section 2.4.1 to calculate albedo.

The *Nadir Vector* report consists of the time since the beginning of mission in seconds and x, y, and z components of unit nadir vector with respect to the CubeSat body coordinate system. The report was used to determine the CubeSat surfaces that experiences both Earth's blackbody radiation and albedo in COMSOL simulation in Section 3.4.3.

3.4.2 CubeSat CAD Model

External Model

As part of the team's thermal analysis, it was necessary to construct a simplified model of the CubeSat that could be used with in COMSOL. The vendors of the components of the spacecraft provided CAD models of their parts, which could be used to create a preliminary model of the complete system. However, the level of detail in these models is unnecessary for conducting the

thermal analysis as the amount of unknowns, such as power consumption by individual components within a circuit board, mean that such a level of precision would be meaningless. In addition, the large amount of detail in the vendor provided models would create complex geometry, which COMSOL could not properly mesh to solve its heat transfer equations. Highly detailed circuit boards, hinges, and other components needed to be simplified to the minimum level of detail relevant to thermal analysis. Mass, general surface area, and conduction paths between parts of the CubeSat were of particular importance when simplifying the model, as these are important variables in the heat transfer equations as described in Section 3.4.4. Another driving factor behind simplifying the model is that of computation time when the model is imported into COMSOL and analyzed.

While using COMSOL to evaluate heat transfer in the spacecraft the user must define which surfaces experience different forms of heat transfer. In order to get accurate results, all surfaces of the spacecraft must be defined in COMSOL as both radiating energy based on their temperature and receiving radiated energy from other faces of the spacecraft. As the number of surfaces in the spacecraft increases, the number of computations COMSOL must perform increases dramatically, causing the time it takes for the program to complete its simulation to accordingly increase. Previous MQPs had also encountered the problem of requiring simplification, and had created a simplified model of the CubeSat themselves, however there were several problems with that model [1]. Firstly, the hinges on the 2013 simplified model, as seen in Figure 34, did not accurately capture what the actual hinges were shaped like. Due to the complexity of the accurate hinges and their importance in conducting heat between the solar panels and the CubeSat body, integrating and simplifying the correct hinges was of utmost priority.

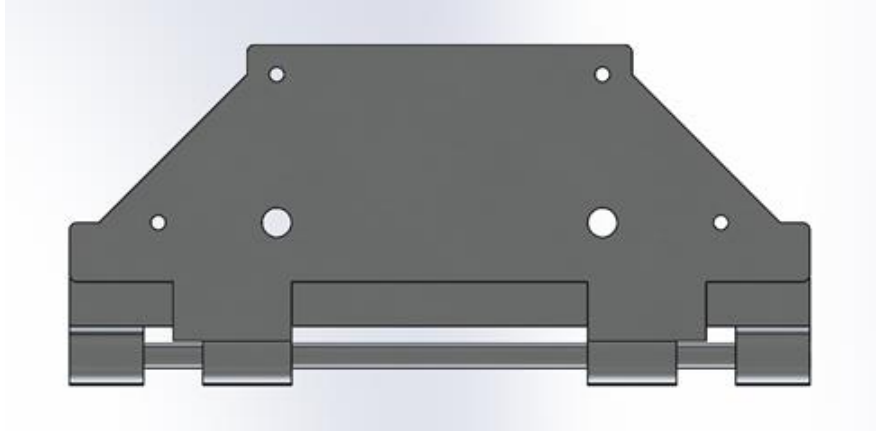


Figure 34: 2013 MQP CubeSat Solar Panel Hinge [1] Copyright © 2013 WPI

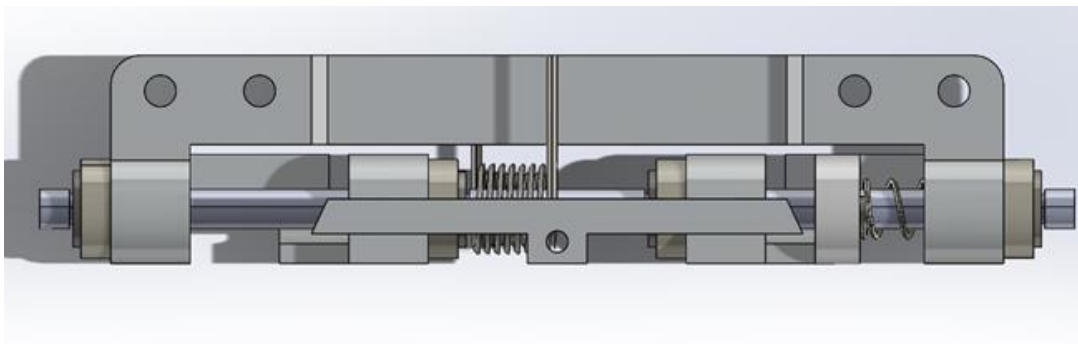


Figure 35: Clyde Space Hinge for Mounting Solar Panels to CubeSat Body [7]
Copyright © 2016 Clyde Space Ltd.

Once the simplified hinges were included in the model, the next step in the simulation process was to examine the high fidelity model of the actual part thoroughly, and proceeding to remove all parts that were not useful to the analysis. The team defined these non-essential parts as components, which had small surface area and/or small mass, generally meaning they could neither absorb from nor emit large amounts of energy to their surrounding parts. Some parts, despite meeting necessary requirements, were too complicated in form to be easily used in COMSOL. These parts had to be recreated using simpler geometry and substituted into the model. Screw holes were simplified to be purely cylindrical instead of being countersunk and threaded.

While simplifying the hinges, springs were removed due to their many curves and small amount of mass, making them both difficult to use in COMSOL and not very thermally relevant. Most of the washers and spacers were removed and the central rod thickened to compensate for lost mass and to maintain contact with the mounting components of the hinge. By removing these surfaces the simulation was simplified to a level manageable by COMSOL. Figure 36 displays the simplified solar panel hinge model.

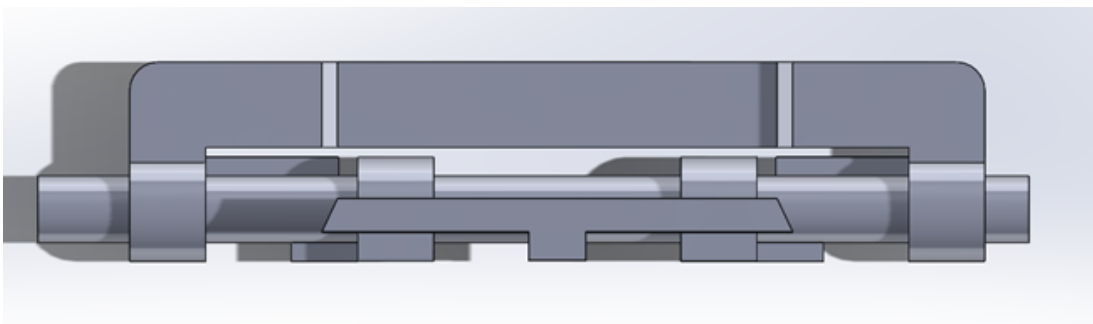


Figure 36: Simplified Hinge for Mounting CubeSat to Body

The CubeSat solar panels were simplified as well. Again, it was necessary to remove a number of holes to reduce the number of surfaces for COMSOL to process, and merging the two layers of the actual solar panel (i.e. the substrate and the cells) into one layer for simplicity. Figure 37 displays the simplified solar panel model.

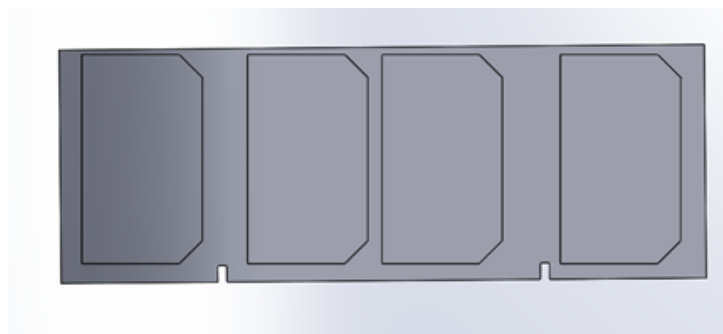


Figure 37: MQP Simplified Solar Panel and Cells

The frame of the CubeSat was based on the Pumpkin MISC 3 3U 715-00553 and few changes were needed to simplify it, owing to its simple sheet metal design [7]. A number of screw holes were removed and the model was integrated into the CubeSat assembly. The final product of the external structure simplification can be seen in Figure 38.

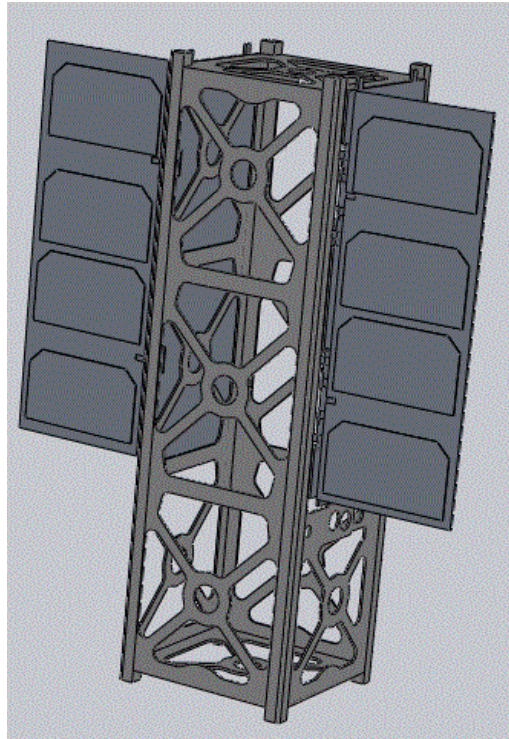


Figure 38: MQP Simplified External Structure

Internal Model

The thermal model created by the 2013 MQP Team provided a good starting point for the external structure of the CubeSat, but had no internal components [1]. The model created by the 2014 MQP included some modeling of the internal heat sources of the CubeSat that served as the starting point for this portion of the project [56]. For this project, mounting pegs were added to connect the vertical computer board stack mount to the frame, and expanded the model to include all five layers of the circuit stack.

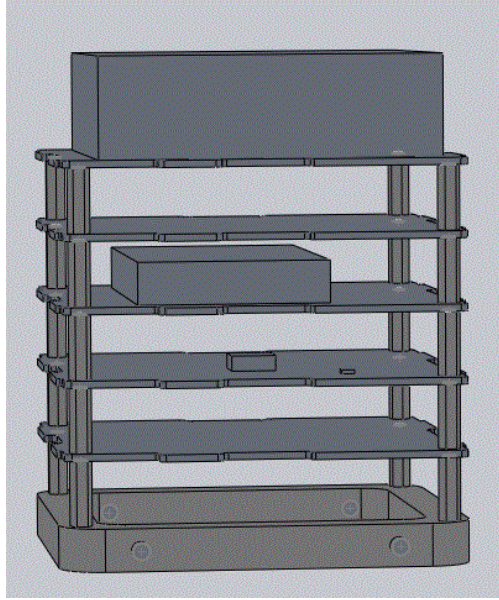


Figure 39: Simplified Circuit Stack with Heat Dissipating Components

The largest change the team made to the internal structure was to add multiple heat sources on the circuit boards to represent the electronic components that dissipate heat. The team worked with the power subsystem team to get a list of the primary power users, and accordingly the primary heat producers. From there, a test arrangement of component placements was created in order to produce simple heat sources in the approximate correct locations for more accurate thermal analysis.

A further refinement to the thermal modeling of a CubeSat was the merging of its internal and external components. This allows for a vastly more accurate idea of the temperatures seen by the components the thermal control subsystem seeks to protect.

3.4.3 COMSOL Multiphysics

COMSOL was chosen again to complete the project this year to be consistent with and build upon the works done by the 2013 and 2014 MQP groups [1, 56]. For this project, *Heat Transfer in Solids with Surface to Surface Radiation* interface under *Heat Transfer* module was

selected. This interface contains the same physics as *Heat Transfer in Solids*, but it allows users to include the physics defined in *Surface to Surface Radiation* interface, which involves physics regarding radiant heat transfer among surfaces. All equations that govern the physics within the interface can be found in *Heat Transfer Module User's Guide* [43].

Global Definitions

In COMSOL, multiple constants that are used throughout the simulation, including those described in Section 2.4.1, were defined as *global parameters*, which allows the user to access the values easily by their corresponding variable name. Table 7 illustrates the parameters defined as *global parameters*.

Table 7: Defined Global Parameters

Parameter	Variable Name	Value [Units]
Solar constant	S	1367 [W/m ²]
Earth IR flux at 600 km orbit	B	193 [W/m ²]
Albedo constant	A	0.35
View factor	F	0.6
Temperature of deep space	Tspace	2.7 [K]
Component waste heat factor	N	0.1

Earth IR Flux at 600 km orbit, in units of $\frac{W}{m^2}$, was determined using the inverse square law

$$B = 231 \frac{R_e^2}{(R_e + h)^2} \quad (6)$$

where R_e is the radius of the Earth and h is the altitude of the spacecraft, in units of km.

The view factor, a portion of the Earth in the CubeSat’s field of view, was determined using a graph as illustrated in Figure 40.

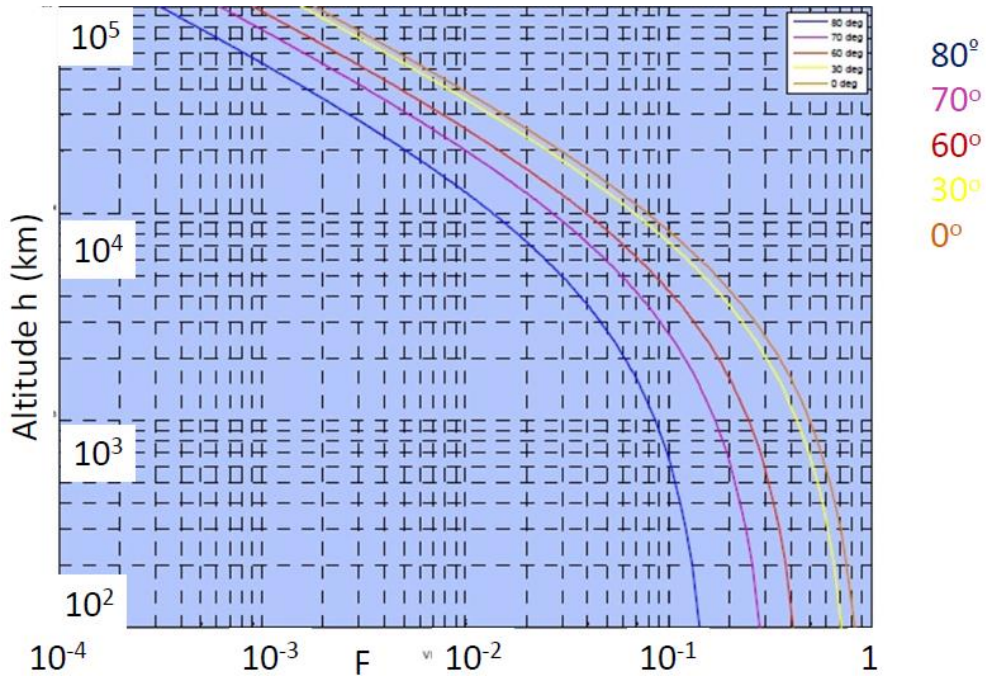


Figure 40: View Factor as a Function of β and Altitude [52]

where β is the beta angle, which was extracted from STK analysis and has a value of 32° , and h is the altitude of the spacecraft.

Before importing the *Solar Intensity* report and *Nadir Vector* report, they were modified for ease of use in COMSOL. For the *Solar Intensity* report, the intensity values, expressed as a percentage, were divided by 100 to normalize the intensity value to range from 0 to 1. For the *Nadir Vector* report, the report was divided into three separate .csv files to have the first file consist of only the positive x-component of the nadir vector, the second file consist of only the negative x-component of the nadir vector, and the third file consist of only the z-component of the nadir vector. The files were named *posx*, *negx*, and *z*, respectively. The separation of the *Nadir Vector*

file was necessary in order to use the values defining a boundary condition which is described in the **Boundary Condition** sub-section. Then the *Solar Intensity* report, *posx* file, *negx* file, *z* file, and *Access Time* report, described in Section 3.3.3, were imported as *Interpolation* functions, which is one of the built-in COMSOL functions that is defined by an imported file containing the values of the function in discrete points [76]. So, each file was imported as a function of time with discrete values, such as solar intensity, at each time value. When the *Interpolation* function is called within COMSOL, it returns the discrete value corresponding to specific time. If the value at that specific time is not defined in the imported file, the value is calculated using linear interpolation based on the values that are given in the imported file. For each *Interpolation* function, a function name and the position in file must be defined. A function name is the name the user can use to access the values, and the position in file is the column number that contains the discrete values after the spatial coordinates, such as time [76]. Table 8 shows the variable name and the position in for the imported files.

Table 8: Variable Name and Position in File for Each Report

File Name	Description	Variable	Position in File
<i>Solar Intensity</i>	Solar intensity	SI	1
<i>posx</i>	Positive x-component of Nadir Vector	posx	1
<i>negx</i>	Negative x-component of Nadir Vector	negx	1
<i>z</i>	z-component of Nadir Vector	z	1
<i>Access Time</i>	Data Transmission time	AT	1

Geometry

By default, an add-on called *LiveLink™ for Solidworks*, which allows the users to easily

import any CAD models created in SolidWorks to COMSOL, is provided within COMSOL. To prevent any issues regarding different software versions, the finalized CubeSat CAD model was saved as a parasolid format (.x_t) before importing. Figure 41 illustrates the front view of the CubeSat, and Figure 42 illustrates the rear view of the CubeSat in COMSOL GUI.

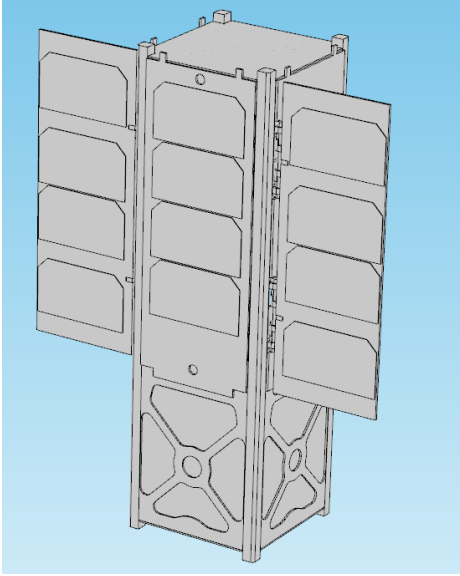


Figure 41: Front View of CubeSat in COMSOL

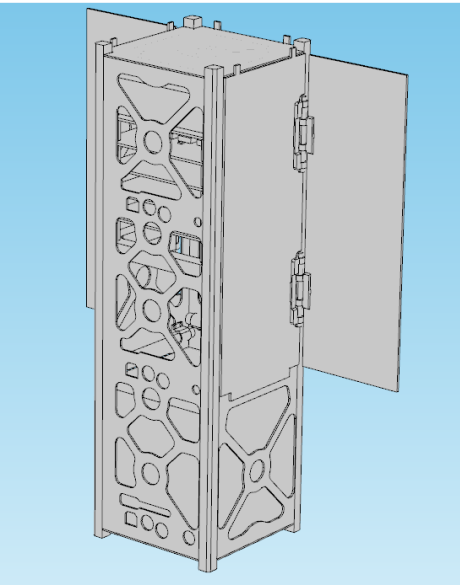


Figure 42: Rear View of CubeSat in COMSOL

To finalize the geometry in COMSOL, the *Form Assembly* option was chosen due to increased complexity in CAD geometry rather than *Form Union*, which is the option 2013 MQP groups have used [1]. In *Form Union*, two connected boundaries from different domains are considered united, and COMSOL recreates a single shared boundary for both domains. On the other hand in *Form Assembly*, two connected boundaries from different domains are considered separate, and COMSOL does not recognize that the boundaries are connected. To define the contact between the boundaries, *Identity Pair* definition must be created for corresponding boundaries. Within *Form Assembly*, COMSOL can automatically generate *Identity Pair* definitions under *global definitions* for the boundaries in contact with other boundaries, but due to complex geometry of the imported CubeSat CAD model, *Identity Pair* definitions were created manually.

Materials

COMSOL has its own built-in material library with material properties predefined. Materials from the built-in library that best represent each component of the CubeSat were chosen and applied correspondingly. Table 9 lists the materials chosen from the library for each component.

Table 9: Materials Chosen for CubeSat Thermal Model

Component	Material
External Frame	Al 5052-H32 [Ref. 298K] ¹
Stack Mount and Standoffs	Al 5052-H32 [Ref. 298K] ¹
Printed Circuit Boards	FR4
Solar Panel Hinges	Al 5052-H32 [Ref. 298K] ¹
Solar Panels	Al 5052-H32 [Ref. 298K] ¹

Solar Cells	GaAs [solid, <100> axis] ²
Magnetorquers	Copper

¹ Material Properties are referenced at 298 K (room temperature)

² Refers to the piezoelectric effect [79]

The material library does not always have all the values of properties required to compute the solutions; some values of some properties needs to be manually specified by the user. Table 10 illustrates material properties that were manually defined.

Table 10: Manually Defined Material Properties

Material	Heat Capacity (J/kg-K)	Thermal Conductivity (W/m-K)	Density (g/cm ³)	Surface Emissivity	Surface Absorptivity
Aluminum 5052-H32	900 ^[53]	138 ^[54]	2.68 ^[54]	0.115 ^[55]	0.23 ^[55]
FR4	-	-	-	0.9 ^[56]	0.49 ^[55]
GaAs	-	-	-	0.85 ^[57]	0.92 ^[57]

Boundary Conditions

A *Heat Flux* boundary condition was used to model the external radiation from the environment. As described in Section 2.4.1, there are three sources of radiation that incident upon the exterior surfaces of the CubeSat: radiation from the Sun, Earth's blackbody radiation, and albedo. All three sources were modeled as *Heat Flux* with *general inward heat flux* option, which adds q_0 , a user defined heat flux, to the total flux across the selected boundaries [77].

For the radiation from the Sun,

$$q_0 = \alpha S SI(t) \quad (7)$$

where $SI(t)$ is the solar intensity as a function of time, α is the solar absorptivity of the material, and S is the solar constant. An assumption that the attitude control system of the CubeSat works perfectly was made, which makes the positive x-axis of CubeSat body axis to point towards the Sun at all times. Therefore, *Heat flux* boundary condition was only applied to the sun-facing surfaces normal to the x-axis.

For the Earth's blackbody radiation and albedo, multiple sets of boundary conditions were defined to corresponding faces of the CubeSat that absorbed the radiation. The *Nadir Vector* report generated from STK was used to determine the surfaces at which the Earth emitted radiation is absorbed. The positive x-component of the nadir vector indicates that the front surfaces (i.e. the Sun-facing surfaces normal to the x-axis) absorbs Earth emitted radiation. The negative x-component of nadir vector indicates that the rear surfaces (i.e. anti-Sun-facing surfaces normal to the x-axis) absorbs Earth emitted radiation. The positive z-component of nadir vector indicates that the bottom surfaces (i.e. Earth-facing surfaces normal to the z-axis) absorbs Earth emitted radiation. *Heat Flux* boundary condition was applied to different surfaces using *general inward heat flux* option with q_0 defined as listed in Table 11. Because of the assumed attitude of the CubeSat in STK, the z-component of nadir vector cannot be a negative value. Hence, *Heat Flux* boundary condition excludes the top surfaces and was only created and applied to the bottom surfaces of the spacecraft.

Table 11: Defined q_0 for Each Surface

	Earth IR	Albedo
Front Surfaces	$q_0 = B \varepsilon \text{ pos}x(t)$	$q_0 = S A F \alpha \text{ pos}x(t) SI(t)$
Rear Surfaces	$q_0 = B \varepsilon \text{ neg}x(t)$	$q_0 = S A F \alpha \text{ neg}x(t) SI(t)$
Bottom Surfaces	$q_0 = B \varepsilon z(t)$	$q_0 = S A F \alpha z(t) SI(t)$

To model the heat dissipated by the internal components, a *Heat Source* boundary condition was used with *Overall heat transfer rate* setting, which defines volumetric heat dissipated Q , with units of $\frac{W}{m^3}$, as

$$Q = \frac{P_{tot}}{V} \quad (8)$$

where P_{tot} is the total amount of power dissipated by the component, and V is the volume of the component. Due to time constraint and the level of sophistication of the project, not all electrical components were included in the simulation. Table 12 provides the component, the peak power, and the quiescent power each component draws.

Table 12: Power Usage of Selected Components

Component	Peak Power (W)	Quiescent Power (W)
OBC	1	0.165
GPS	0.8	-
Magnetorquers (3)	0.825	0

Gyroscope (3)	0.04	0.03
Magnetometer	0.00033	0
Transceiver (Transmitter)	4.32	0
Sphinx-NG	8	1
EPS	0.2	0.2
Battery (Heater)	0.6	0.1

Due to the time constraint of the project, a very rough assumption that the components have 90% efficiency and 10% of the drawn power is dissipated as waste heat was made. In theory, this is not completely accurate because each component has its own defined value of efficiency, and every electrical component within the boards dissipates a different amount of heat. For the purpose of this project, the amount of heat dissipated by each component is characterized as

$$P_{dissipated} = NP_{used} \quad (9)$$

Since the amount of exact power drawn by components was not available at the time when the team conducted the simulation, rough assumptions of power consumption were made

For the Sphinx-NG, GPS, magnetorquers, gyroscope, magnetometer, and fine sun sensor, each component was assumed to consume maximum power during full solar illumination and quiescent power during the umbra phase. Therefore, each component has P_{tot} defined as shown in Table 13 where N is defined as a waste heat factor.

Table 13: P_{tot} of Components

Component	P_{tot} (W)
Sphinx-NG	$N[(8 - 1)SI(t) + 1]$
Magnetorquers (3)	$2.475NSI(t)$
Gyroscope (3)	$3\{N[(0.04 - 0.03)SI(t)] + 0.03\}$
Magnetometer	$0.00033NSI(t)$

For the OBC, GPS, and EPS each component was assumed always active and consume maximum power at all times. Table 14 provides P_{tot} for OBC and EPS.

Table 14: P_{tot} of OBC and EPS

Component	P_{tot} (W)
OBC	N
EPS	$0.2N$
GPS	$0.8N$

For the heater integrated into the battery, the component was assumed to consume peak power when the heater is on and quiescent power when the heater is off. The heater turns on when the temperature of the battery drops below 0°C and turns off when the temperature is above 5°C [58]. To model the heater *Events* module was created to monitor the temperature of the battery and to turn on/off the heater accordingly. A variable called *HeaterState* was created to indicate the state of the heater; 0 indicates that the heater is off, and 1 indicates that the heater is on. Figure 43

describes the operation of the heater.

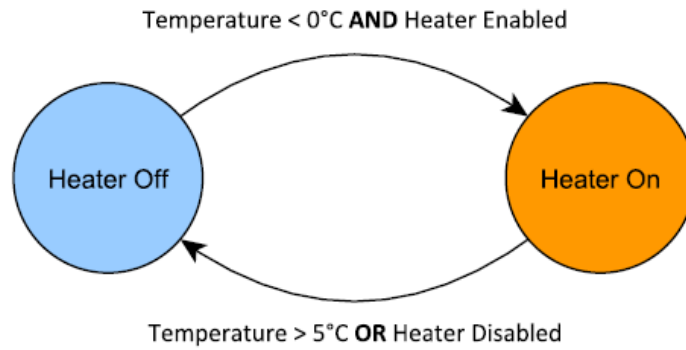


Figure 43: Operation of the Heater [58] © 2016 Clyde Space Ltd.

Therefore, the P_{tot} dissipated by the battery heater is described as following:

$$P_{tot} = N[HeaterState(0.6 - 0.1) + 0.1] \quad (10)$$

For the transceiver, it was assumed to use peak power during transmission and quiescent power while on standby. Therefore, P_{tot} dissipated by the transceiver is described as following:

$$P_{tot} = 4.32NAT(t) \quad (11)$$

A *Diffuse Surface* boundary condition was applied to simulate the surface-to-surface radiation inside of the CubeSat. In theory, the radiation emitted by the internal components, such as the circuit boards, magnetorquers, and Sphinx-NG, is absorbed by all of the surfaces inside of the CubeSat surrounding the components. While the boundary condition must be applied to all the surfaces inside the structure, simplifications had to be made because when COMSOL solves for the surface-to-surface radiation, it calculates the view factor, the amount of surface area visible by another surface area, of all finite elements of specified boundaries for all other individual finite element of specified boundaries. As a result, the computer may not be able to handle the calculation

due to memory shortage if too many boundaries are specified or if the mesh is too fine and contains too many finite elements. Therefore, the boundary condition was only applied to only the top surface of Sphinx-NG, top and bottom surfaces of all circuit boards, top and bottom faces of the vertical stack mount, and inside surfaces of CubeSat surrounding the components to reduce the simulation run time. Figure 44 displays the boundaries to which *Diffuse Surface* with surface-to-surface setting was applied.

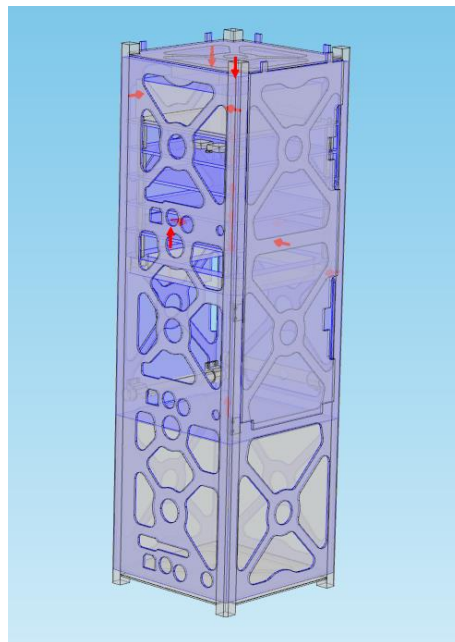


Figure 44: Boundaries Selected for Surface-to-Surface Radiation

Again, a *Diffuse Surface* boundary condition was applied to the outside surfaces of the CubeSat to simulate radiant heat transfer from the body into the cold space. In the boundary condition settings, surface-to-surface radiation was not included, and the ambient temperature was defined as

$$T_{amb} = T_{space} \quad (12)$$

where T_{space} is the temperature of the deep space defined under *global definitions*.

A *Thermal Contact Pair* boundary condition was used to define *Identity Pairs* that are in pressured contact due to mounted screws or bolts. *Thermal Contact Pair* defines specified *Identity Pairs* to be in thermal contact as a solid, which incorporates thermal contact conductance. A *Thermal Contact Pair* boundary condition was applied to surfaces between standoffs and circuit boards, surfaces between vertical stack mount and the frame, surfaces between hinges and external frame, and surfaces between hinges and aluminum panels. In the boundary condition, user input settings were defined as shown in Table 15.

Table 15: Thermal Contact Pair Settings [5]

Description	Setting
Constriction Conductance	Cooper-Mikic-Yovanovich correlation ^[78]
Gap Conductance (Hg)	$Hg = 0 \left[\frac{W}{m^2 K} \right]$
Radiative Conductance	Gray-diffuse parallel surfaces
Surface Roughness (avg. height of asperities)	$\Sigma_{asp} = 1 \text{ } [\mu\text{m}]$
Surface Roughness (avg. slope of asperities)	$M_{asp} = 0.4 \left[\frac{\mu\text{m}}{\mu\text{m}} \right]$
Contact Pressure (P)	$P = 200 \text{ } [\text{kPa}]$
Microhardness	$H_c = 3 \text{ } [\text{GPa}]$
Friction Heat	$Q_{fric} = 0 \left[\frac{W}{m^2} \right]$

A *Continuity Pair* boundary condition was used to define *Identity Pairs* to form continuity. *Continuity Pair* allows COMSOL to treat the defined *Identity Pairs* to be in union, much like the *Form Union* from the *Geometry* settings. For example, given two rectangles with one side of rectangles touching, *Identity Pair* can be defined for the boundaries on the touching side to

consider them as a pair and *Continuity Pair* can be defined for that *Identity Pair* to allow COMSOL to treat two rectangles as one geometry. The *Continuity Pair* condition was applied to remaining boundary pairs after *Thermal Contact Pair* boundary condition have been defined, such as boundary pair between the bolts and vertical stack mount, between the hinge and the pin, and between the payload Sphinx-NG and the frame.

3.4.4 Iterative Thermal Analysis and Design

Once both the external thermal environment and the internal components are characterized, multiple COMSOL simulations were conducted as an iterative process to meet the operational and survival temperature requirements of all components. Figure 45 illustrates the idea of iterative thermal analysis and design process taken in order to finalize the design of thermal control system.

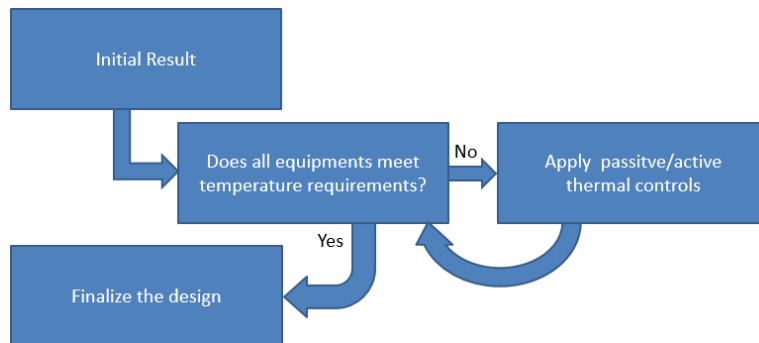


Figure 45: Iterative Process of Thermal Analysis and Design

Starting from the initial result of the COMSOL simulation, the temperature of the each component was analyzed to make sure that it was within the specified temperature ranges. If the result indicated that the temperatures of some components exceed the specified limit, all possible passive thermal controls were applied first before considering and applying active thermal controls. For passive thermal controls, mainly surface finishes and radiators, specific value of

surface emissivity of the corresponding surfaces would be assumed in the finite element model. For active thermal controls, mainly heaters, louvers, or heat pipes, generation and integration of simplified model of corresponding system in the finite element model would be required. The process repeated until all components met the temperature requirements, and the corresponding design of the thermal control system was finalized.

4 Results

4.1 Command & Data Handling Subsystem

4.1.1 System Requirements

After consulting the designers of various other subsystems regarding the operations which were required of the C&DH subsystem, information was tabulated. The full table of subsystem and sensor data processing needs can be found in Appendix C, and the table of command operations can be found in Appendix D.

Where information was unknown by the leaders of certain subsystems, *Space Mission Analysis and Design, 3rd ed.* was consulted to provide typical information regarding the sizing of a satellite C&DH subsystem [16]. The sensor and subsystem computing needs were input into a spreadsheet to estimate how much memory the supporting software for those functions might require. The methods described in Ref. 15 enabled the use of “similarity” in the generation of such estimates, using previously created C&DH subsystems as examples for how much this system could operate. An uncertainty factor of 2 was used to overestimate the size of the C&DH system’s needs, so that as software needs likely would grow throughout the development of the satellite, the C&DH system could still handle such growth. Ultimately, it was estimated that the computer would require 12.25 MIPS of throughput. Additionally, an estimate of 0.92 MB of storage necessary for software storage was needed in support of these functions. The spreadsheet used to perform the calculations can be found in Appendix E.

4.1.2 Hardware & Software Definition

Software

From the information collected regarding the spacecraft systems' functionality, supplemented by requirements imposed by government agencies and the P-POD deployment device, and the specific scientific mission requirements assumed for this study, Operational State diagrams could be derived. Ultimately, five distinct Operational States of the CubeSat were found to exist independently of one another, as outlined in Figure 46.

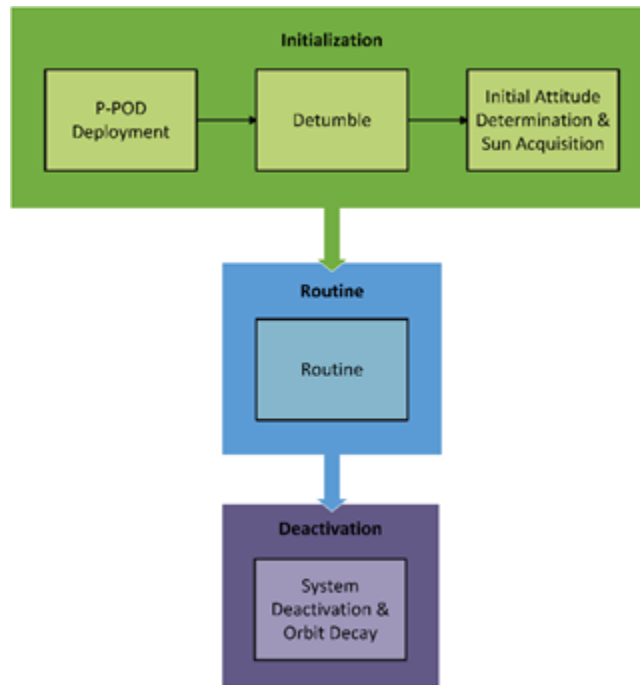


Figure 46: SphinX-NG Mission Operational States

Throughout the course of the mission, the CubeSat will adhere to the sequence of operations described in Figure 46, and as previously stated in Section 3.1.2, should perform these operations out of sequence only in the event that an anomaly requires it to do so. Such a scenario could occur if while in Routine, an anomaly occurred such that the spacecraft began to spin at a

problematic rate, and accordingly the mission directors commanded it to revert to the Detumble state to correct the situation, proceeding through Initial Sun Acquisition on its route back to Routine.

Once this global understanding of the entire spacecraft's operations was established, a more detailed study could be completed to define the particular details of precisely how each Operational State is achieved through the C&DH subsystem's commands. A block diagram was produced to represent each of the six Operational State's operational sequences. Firstly came the sequence to represent the P-POD Deployment Operational State, as shown in Figure 47.

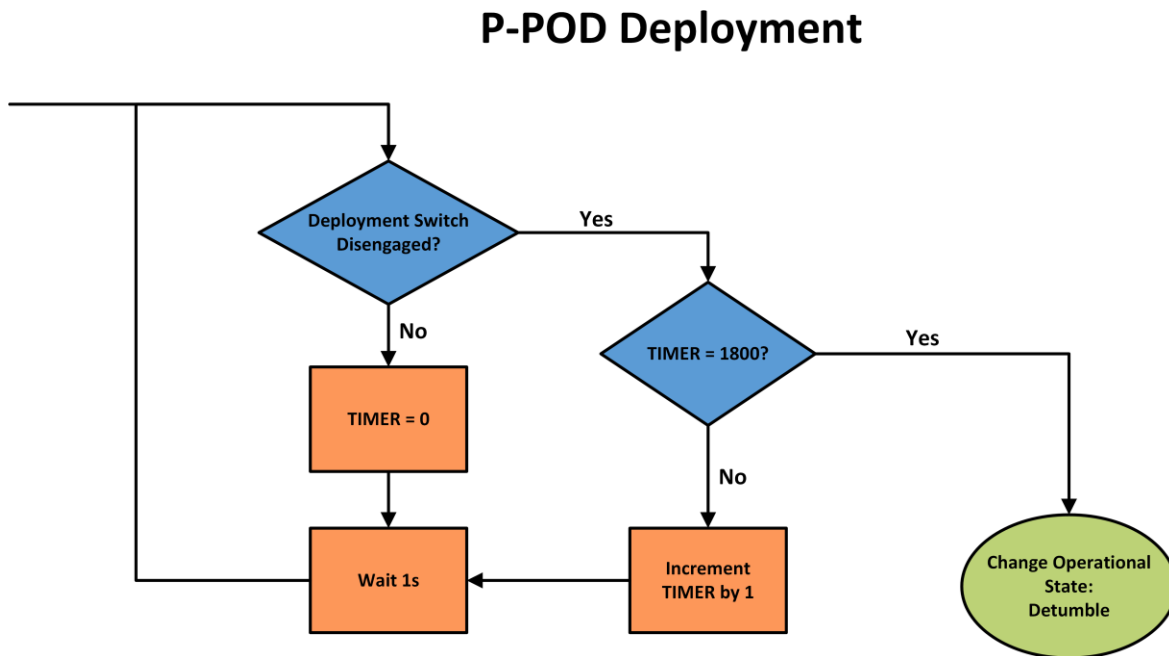


Figure 47: P-POD Deployment Operational State

Following ejection from the Poly-Picosatellite Orbital Deployer (P-POD), the deployment switch described in Section 2.1.3 will be activated since it will no longer be held depressed by the P-POD. Following this activation, a timer will commence for 30 minutes before allowing the

spacecraft to begin subsequent operations. If the deployment switch were to be pressed back down during this time (potentially indicating that the CubeSat had been jarred in its deployer, causing the switch to briefly disengage and then reengage), the timer would be reset to insure that the CubeSat does not attempt to begin its operations while still inside the P-POD. Once the deployment switch has safely remained disengaged for 30 minutes, the C&DH subsystem will allow the CubeSat to progress in its operations. Next, the spacecraft will transition to the Detumble Operational State, which is outlined in Figure 48. During Detumble, the ADCS BDOT control algorithm is used to reduce the rotational motion of the spacecraft until it is at an acceptably low value [9]. To carry out this algorithm, the OBC gathers angular velocity information from the gyroscope and magnetic field information from the magnetometer, and instructs the EPS to adjust the current supplied to the magnetorquers following the results of the BDOT controller. Once the spacecraft is at a stable state (defined as when all angular velocity vector elements are less than 0.1 rad/s), the solar panels and antennae are deployed, and the spacecraft is rechecked to eliminate any disturbances in angular motion which their deployment might have caused. Once this deployment has occurred and the spacecraft is in a controlled state, the OBC will allow the craft to proceed to the next state. This following Operational State, Initial Attitude Determination and Sun Acquisition, is outlined in Figure 49.

Detumble

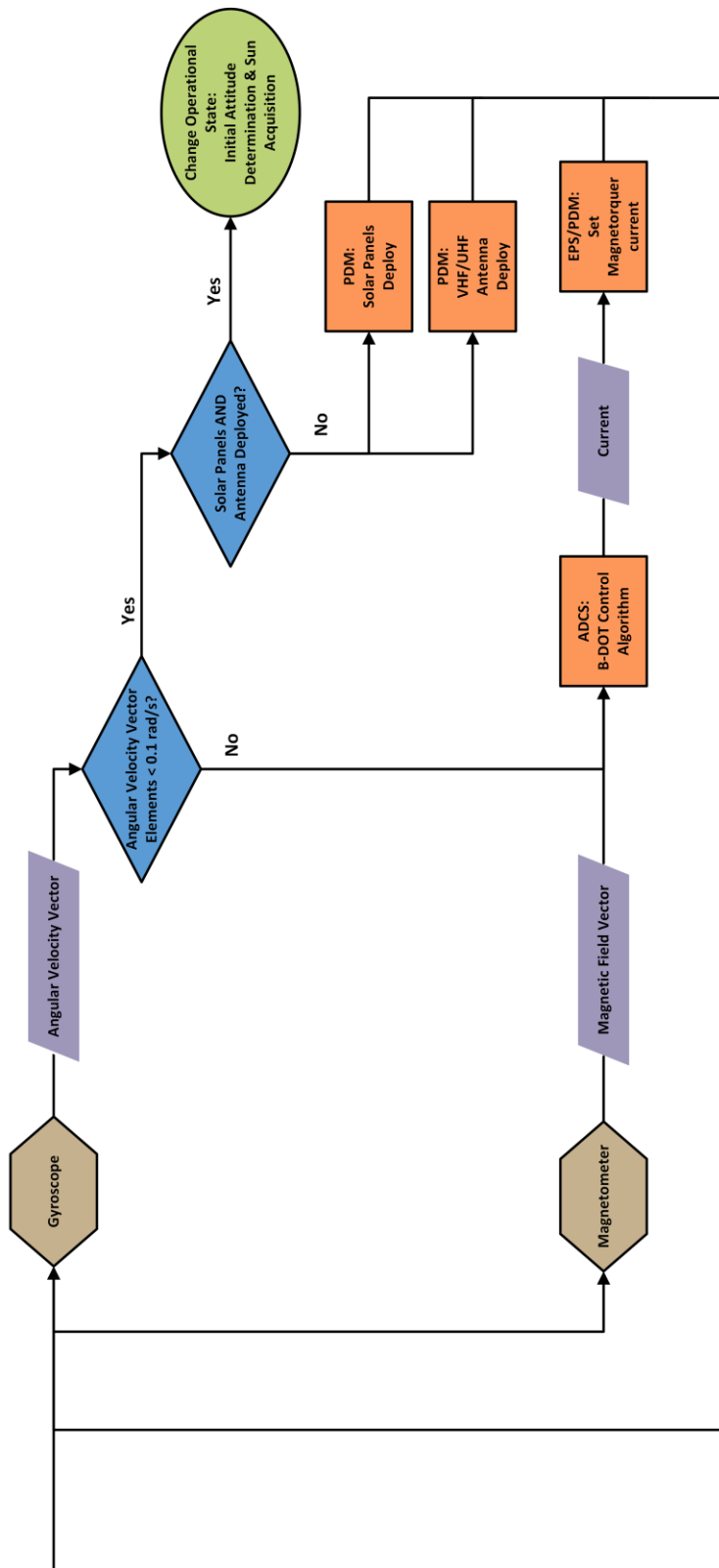


Figure 48: Detumble Operational State

Initial Attitude Determination & Sun Acquisition

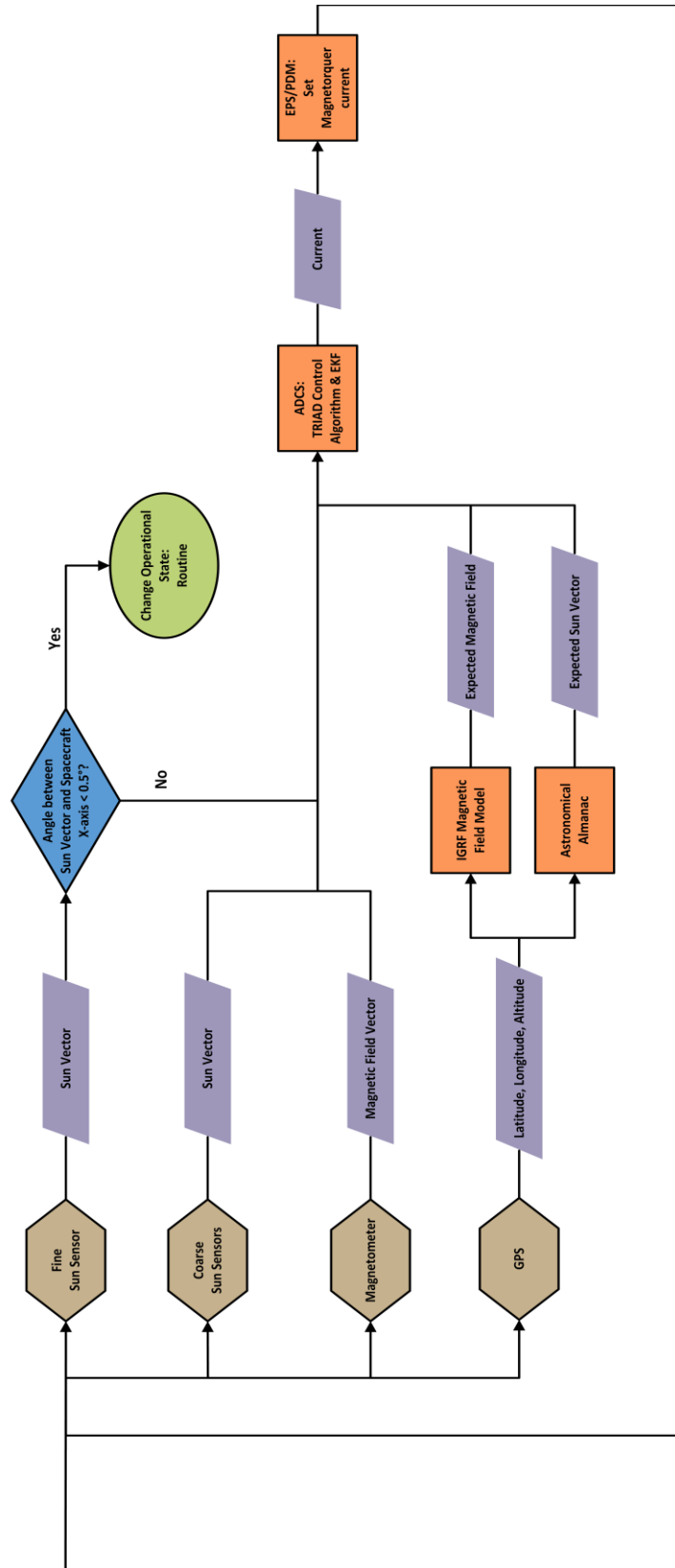


Figure 49: Initial Attitude Determination and Sun Acquisition Operational State

During the Initial Attitude Determination and Sun Acquisition state, the ADCS control algorithm used throughout the majority of the mission is introduced: the TRIAD algorithm [9]. This algorithm takes as input sun vectors from the spacecraft's sun sensors, the magnetic field vector from the magnetometer, and GPS coordinate information. The OBC uses the GPS data to generate expected values for the sun and magnetic field vectors from databases associating the CubeSat's position in orbit to these models. Via the TRIAD algorithm and an Extended Kalman Filter, the OBC then commands the EPS to adjust the current levels supplied to the magnetorquers to correct the difference between measured (by the magnetometer and sun sensor) and desired (calculated using GPS data) values for the sun and magnetic field vectors. Once the spacecraft has sufficiently aligned its x-axis – and thus the payload instrument and solar panels – within 0.5° of the sun vector, the OBC transitions the spacecraft into the Routine phase of its mission. The Routine Operational State is shown in Figure 50.

The spacecraft will spend the majority of its lifespan in the Routine Operational State, which is where all mission critical scientific data collection and communication with Earth-based ground stations will occur. While in Routine, the TRIAD attitude control algorithm is enacted when the spacecraft is on the sunward side of the Earth [9]. Furthermore, if the spacecraft is over a Ground Station, all scientific data collection is halted and communication with Earth via the radio transceiver is prioritized. This serves to ensure that the large amounts of data created by the payload and other systems can be downlinked and replaced in the spacecraft's memory as soon as possible. Additionally with this setup, any time-critical uplinked commands can be received and addressed as soon as possible by the C&DH subsystem. If the spacecraft is not over a Ground Station, the SphinX-NG instrument is turned on to collect scientific data. As long as no command is received to deactivate the system, the spacecraft will continue Routine operations indefinitely.

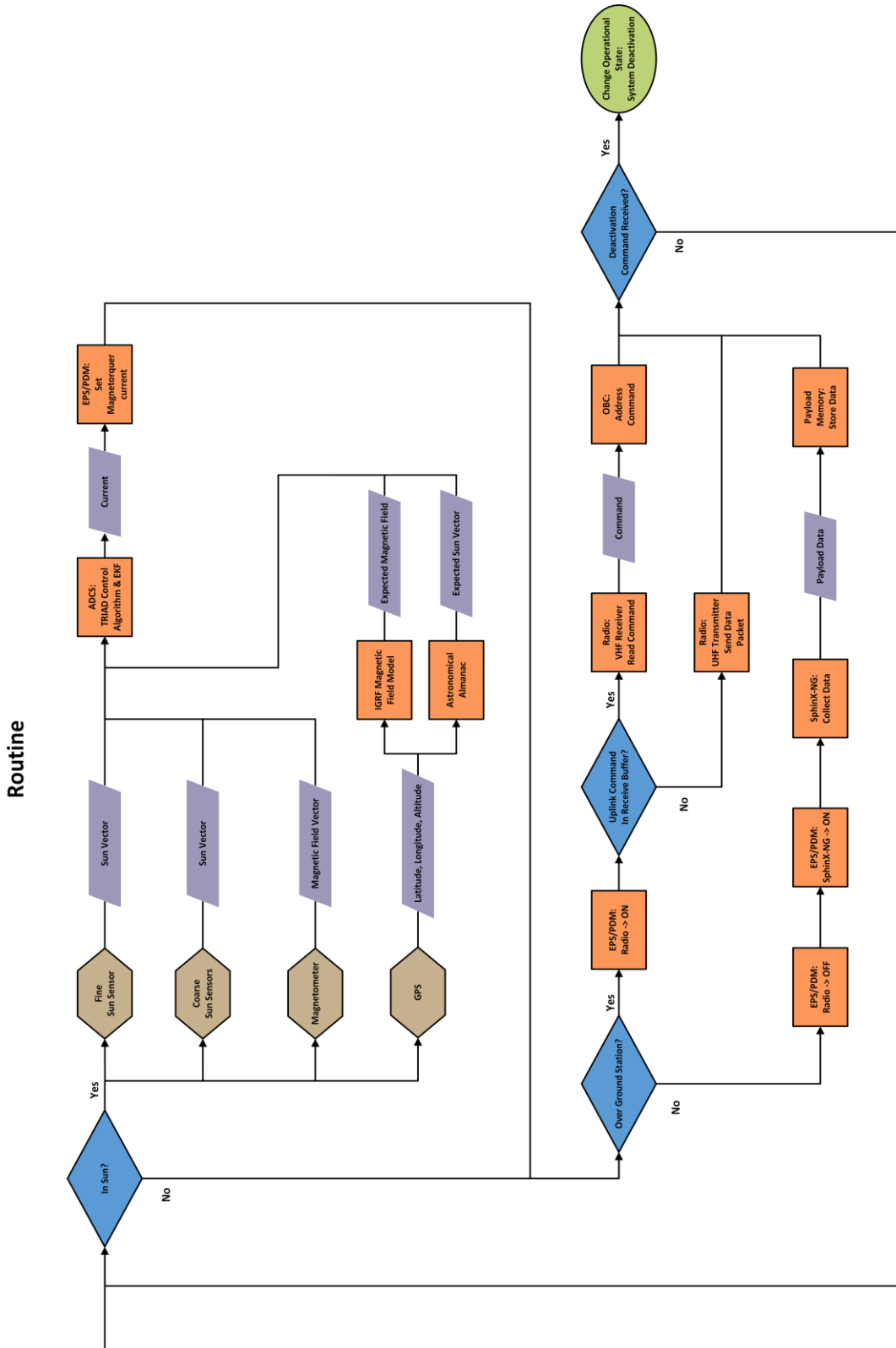


Figure 50: Routine Operational State

System Deactivation & Orbit Decay

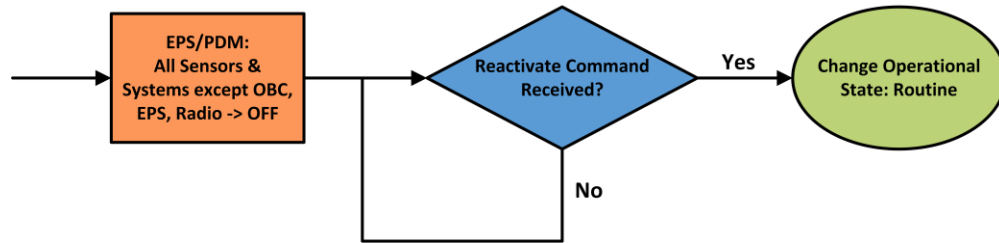


Figure 51: System Deactivation & Orbit Decay Operational State

The System Deactivation state consists of the OBC commanding each of the sensors and subsystems on board the CubeSat to turn off, preparing each for eventual reentry and breakup in Earth’s atmosphere. The spacecraft will remain in this Operational State unless a command is received to reactivate it. Typically however, CubeSats do not often survive until a time when they can be commanded to deactivate, due to an environmental anomaly or critical component failure. Nevertheless, this Operational State should be envisioned so that it could be enacted if a mission timeline was carried out ideally.

CubeSat Functionality

Multiple time sequence diagrams were created to ensure a comprehensive understanding of system functions. The two diagrams created were “Request Telemetry” and “Request Payload Data,” since these two are two of the most common operations performed by the spacecraft. Figure 52 and 53 display the “Request Payload Data” and “Request Telemetry” diagrams, respectively.

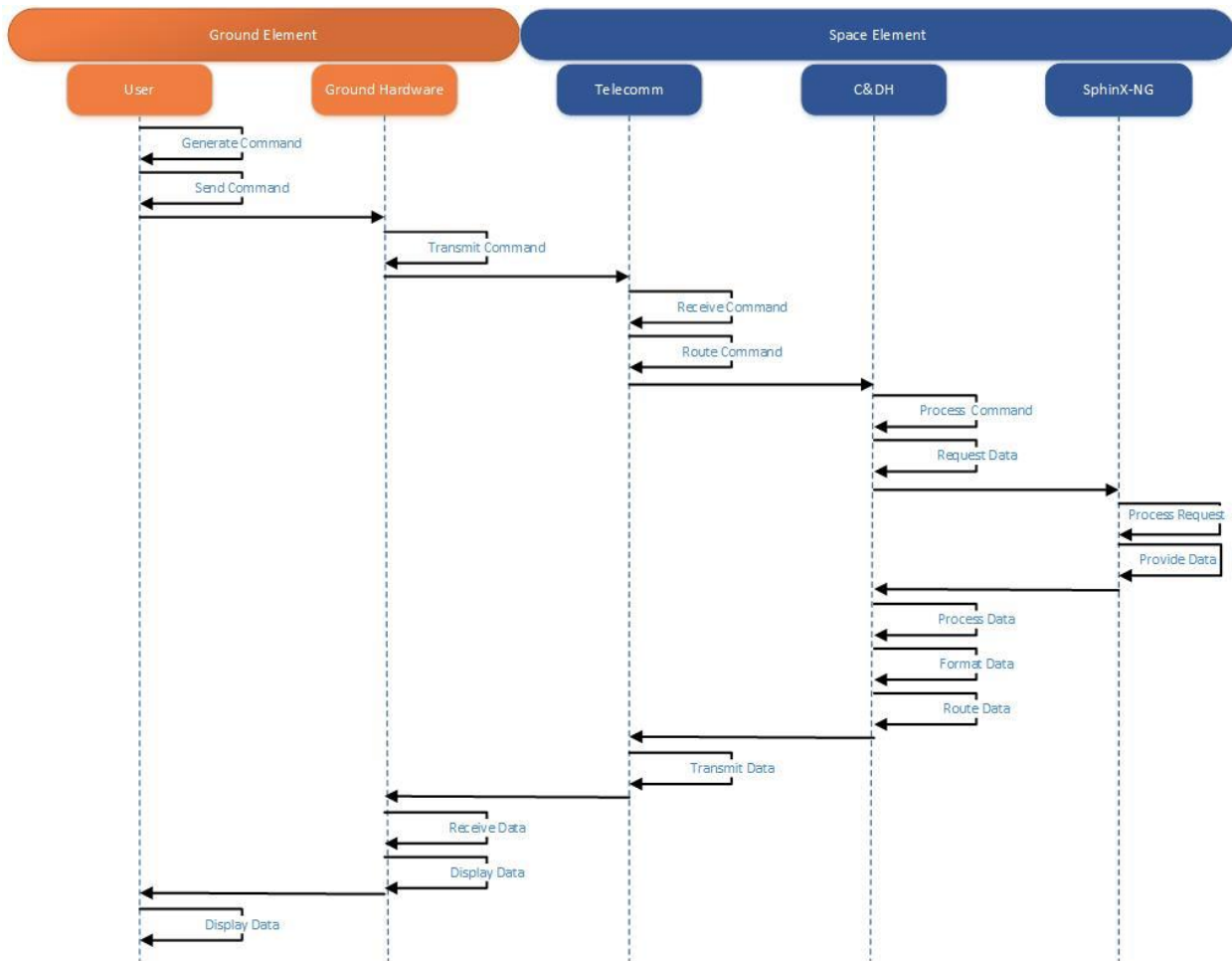


Figure 52: Request Payload Data Diagram

The diagrams display functions by the recursive loops that are acted onto each physical subsystem (lines that loop onto the dotted timeline). The lines connecting different subsystems are the communications between subsystems and passing of data. To use this chart, one would begin in the upper left where a ground operator (user) sends a command to the CubeSat. The command is verified and routed to the proper subsystem (ACDS) via the C&DH subsystem. Once the data is provided, it is routed via the C&DH subsystem then back down to the ground operator.

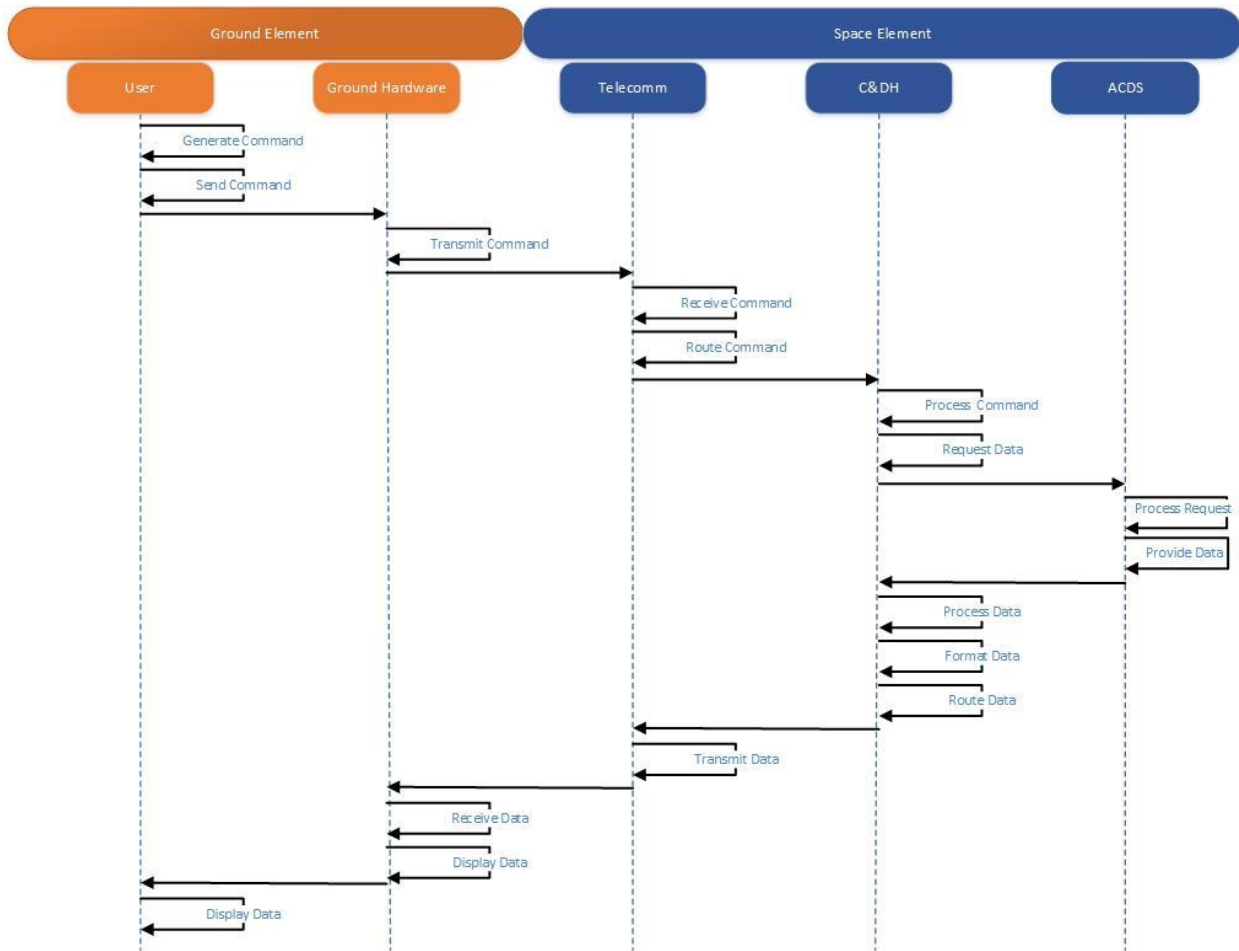


Figure 53: Request Telemetry Diagram

The diagrams from these functions were then compiled to create the full list of necessary functions for the CubeSat while cross-checking with the University of Michigan project. This finalized list can be found in Figure 54.

Having compiled the full list of functions, the final step was to verify with the subsystem teams regarding such available functionality. From there, the work of the functional architecture would be used to identify any gaps previously missed in the physical architecture. At its current level of development, the functional architecture hasn't been used to find gaps in the architecture,

however, when the functions are broken down further into the component level, missing functionality will become more apparent.

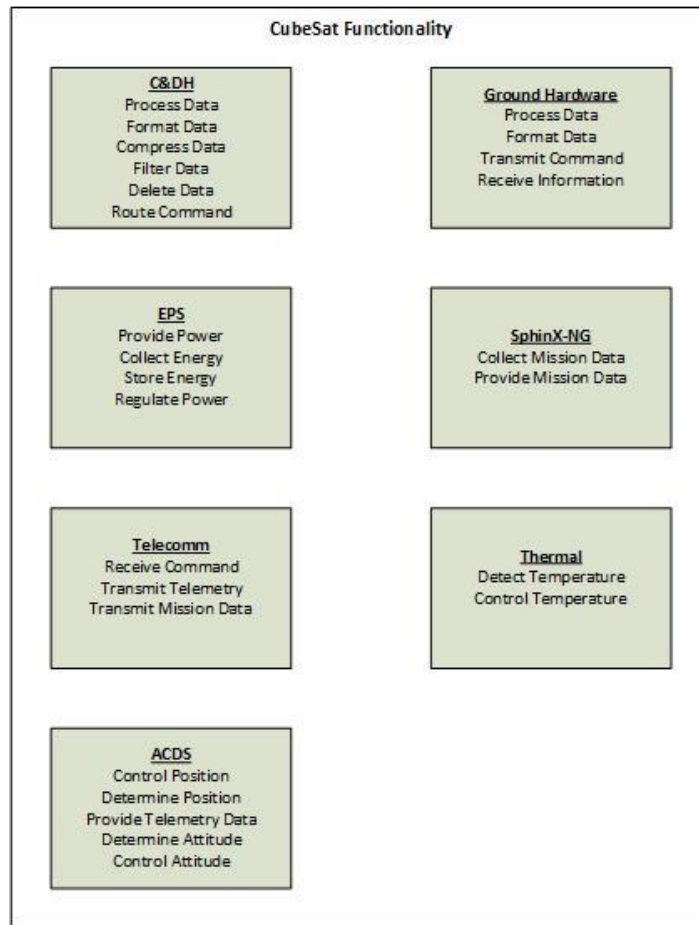


Figure 54: Total Function List [45]

Hardware

Data interfaces among the various elements that are part of the network that is the C&DH subsystem were analyzed to ensure compatibility. Figure 55 is a block diagram that shows these data interfaces between the OBC and the other subsystems and sensors that must transfer data.

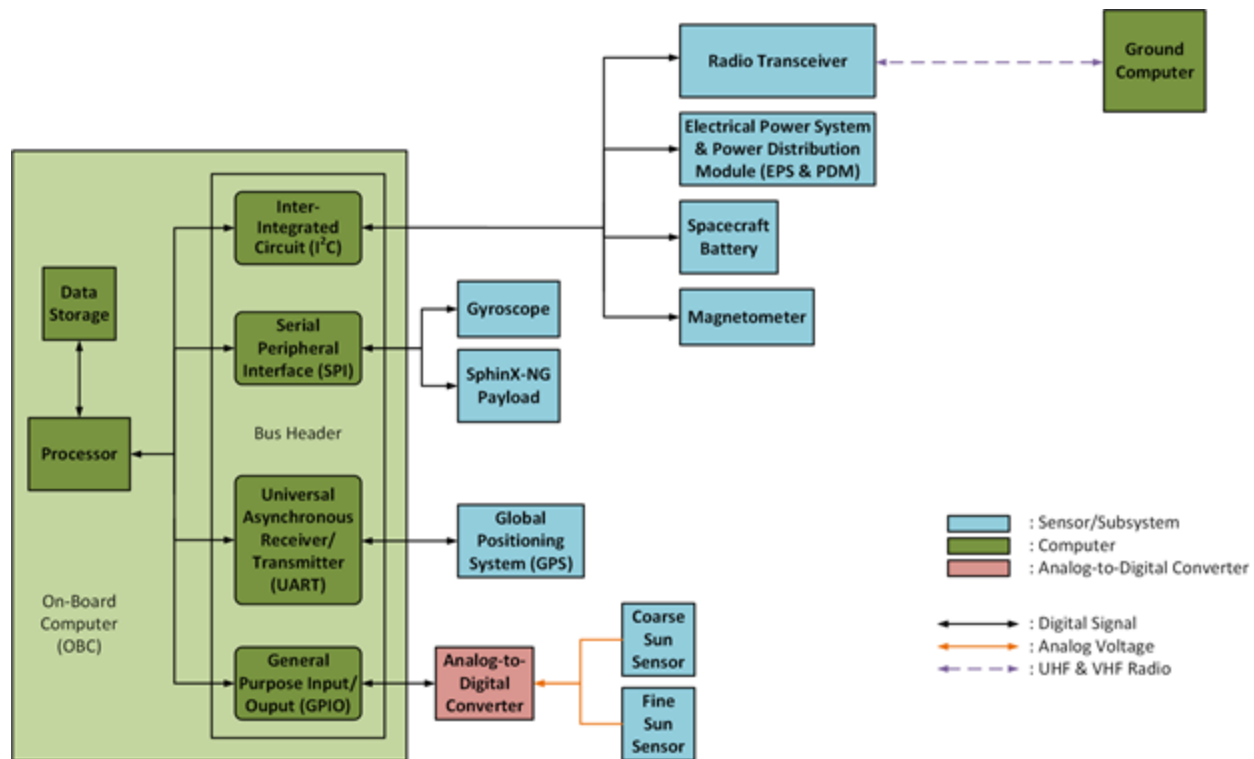


Figure 55: Command and Data Handling Subsystem Block Diagram

The other computer boards which are part of the “stack” mentioned in Section 2.1.3 use the same physical 104 pin header as described in Section 3.2.3 to interface; each of these boards and the magnetometer use the I²C protocol to communicate with each other and the OBC. Additionally, the SPI interface is used to connect the gyroscope and SphinX-NG payload to the OBC, and the UART interface is used to communicate with the GPS receiver. The spacecraft’s fine and coarse sun sensors produce analog signals that must be converted for use by the computer. Accordingly, the signals produced by the sun sensors must be conditioned by an analog-to-digital converter before they can be used in the remainder of the C&DH subsystem. Each of these protocols is supported by the baseline Clyde Space Nanosatellite On-Board Computer, and thus feasible interfaces can be made between the OBC and each of its C&DH dependents successfully.

The data storage element of the C&DH subsystem must be handled by the OBC and the payload instrument, both of which have memory capacity. Table 16 outlines the baseline C&DH subsystem’s memory, according to the baseline Clyde Space Nanosatellite OBC and SphinX-NG payload’s data sheets.

Table 16: C&DH Subsystem Memory Capacity

Memory Type and Location	Available Memory
OBC MRAM	8 MB [14]
OBC Flash	4 GB [14]
SphinX-NG Flash	128 or 256 GB [13]

When performing simulations, these values represent the maximum capacity available for data storage on board, and thus must not be exceeded. Additionally, as per the system requirements established in Section 4.1.1, the Clyde Space Nanosatellite OBC can capably handle the estimated 12.5 MIPS of throughput required, as it supports processing speeds of up to 62.5 MIPS. The Clyde Space OBC incorporates 8 MB of magnetoresistive random access memory (MRAM) available for code storage and execution, and accordingly the 0.92 MB of anticipated software will be held there [14].

4.1.3 Computing Profile Modeling

The first step in creating a model timeline of a spacecraft’s operations is to determine exactly when each of its components operates. This can be accomplished by using the Operational State diagrams to see which sensors and subsystems are necessary for each state. Table 17 shows

the components that were present in the Operational State diagrams, which must also be included in the modeling of the C&DH subsystem.

Table 17: C&DH Subsystem Components

Component Type	Component Name
Subsystem	On-Board Computer (OBC)
	Electrical Power System (EPS)
	Radio Transceiver
	SphinX-NG Payload
Sensor	Magnetorquers
	Gyroscope
	Magnetometer
	Global Positioning System (GPS)
	Coarse Sun Sensors
	Fine Sun Sensor

During the Initialization Phase of the mission, all sensors and systems are on throughout each operational state, but during the Routine Operational State, conditional factors must be taken into account when considering which systems produce data at which times. In order to inform when these conditional situations occur, time-indexed vectors of sun exposure and ground station exposure were collected from the team leaders for the thermal control and telecommunications

subsystems, respectively. These vectors were coordinated to both begin at 1/1/2019 0:00:00, and were produced via analysis in STK. The resulting vectors are plotted in Figure 56.

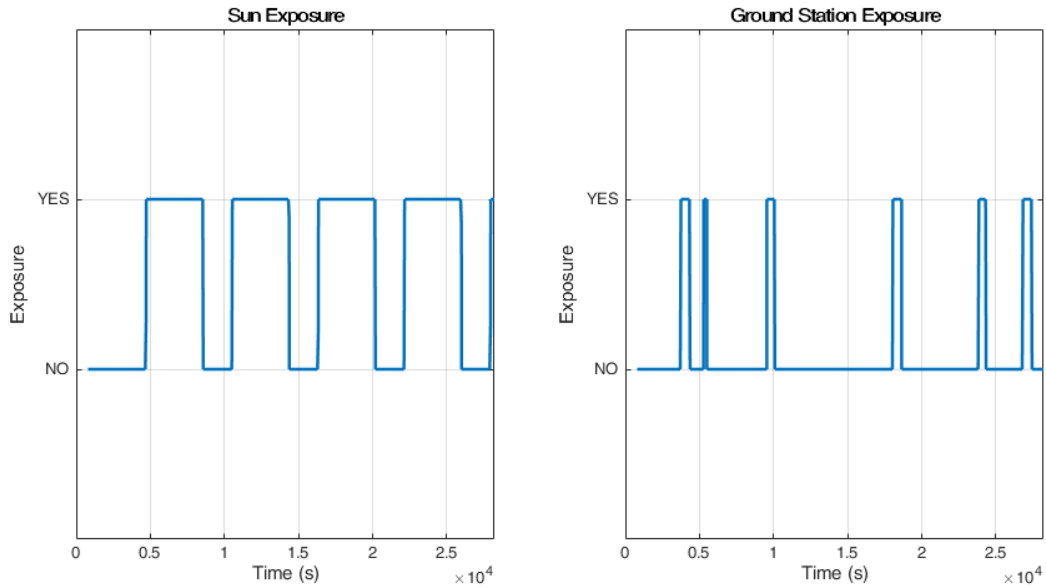


Figure 56: Sun and Ground Station Exposure

Using the information that determines whether a component is on or off, accompanied by an estimate of the time each of the Initialization states will take and several typical orbits during Routine, one can create a timeline of subsystem states. Table 18 shows the time estimates that were made for each Operational State’s span.

Table 18: Operational State Estimated Time Spans

Operational State	Estimated Time Span (s)
P-POD Deployment	1,800
Detumble	1,200

Initial Attitude Determination and Sun Acquisition	180
Routine	25,000

A span of 1,800 s (or 30 minutes) was used to model P-POD Deployment due to the P-POD requirement of a 30-minute delay following ejection from the launch vehicle. The ADC subsystem leaders provided a high estimate of the time Detumble would take, and additionally estimated that the spacecraft would take at most 180 s to turn 180°, the maximum angle the spacecraft would have to turn to fully align with the sun [9]. The timespan for Routine was limited by the length of the Sun Exposure vector, which allowed for about 4.5 orbits to be modeled in this simulation.

Using these time spans, the information from the Operational State diagrams, and the Exposure Vectors, a model of subsystem and sensor states was created, and is shown in Figure 57. An important distinction to make is that these plots represent when the systems are “on,” as defined by the condition that they are interacting as part of the C&DH subsystem, in particular. In other words, a certain board may be receiving power at all times, but will be indicated in these state plots as being “off,” since it is not producing or using any data at the time and thus does not affect the status of the C&DH subsystem.

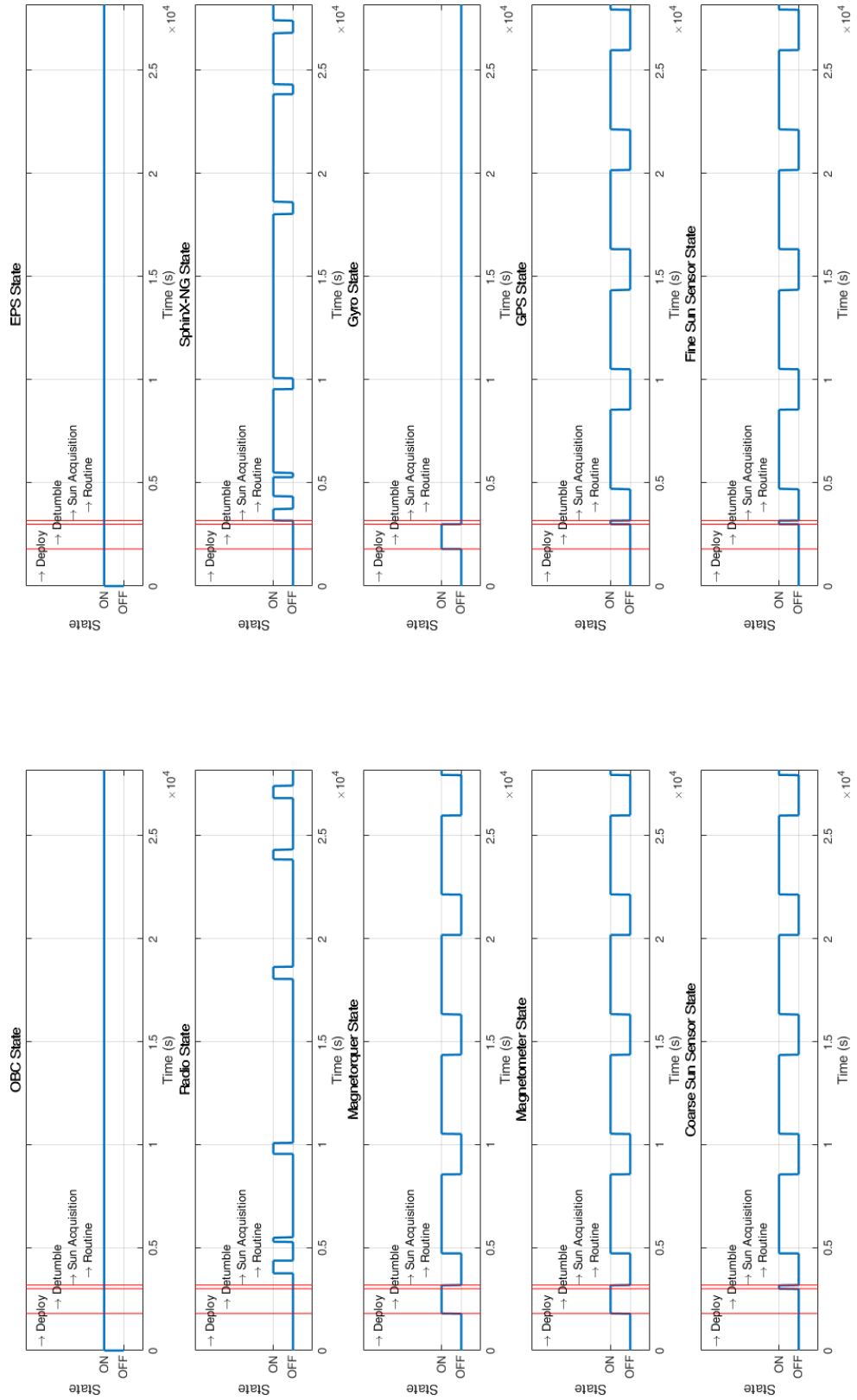


Figure 57: Subsystem and Sensor States

These plots can be used to perform additional simulations of the data produced by each component. Such analysis was split into two analyses: one for data usage in volatile storage, and another for data accumulation in non-volatile storage. Sensor data is included in volatile storage due to its short-term usefulness for OBC calculations, while payload data and health statistics collected from computer boards are stored in non-volatile memory to prevent erasure in a fault. The data used for sensor data and calculation remains constant while a sensor's data is being collected, because each time a new data point is created, it replaces the previously stored value, instead of creating a new one. Health and payload data accumulate over time however, since the previously stored information is not written over each time a new piece of data is introduced. The Clyde Space Nanosatellite OBC is unique in that it does not incorporate conventional "volatile" storage, but instead incorporates magnetoresistive random access memory (MRAM), as noted in Section 4.1.2. While this storage is actually non-volatile in the sense that the data it stores would not be deleted if the OBC were turned off, it still serves the same functions that conventional volatile storage would. Thus, in these analyses, volatile calculations and sensor data storage will be simulated as stored in MRAM storage.

Unfortunately, it was out of the scope of this particular project to identify the precise amounts of data produced by each sensor and subsystem, so when information was unavailable, estimates were made.

Firstly, the MRAM storage was simulated. Table 19 shows the data used as input for the MRAM simulation; when on, these components are presumed to use the amount of memory indicated.

Table 19: MRAM User Information

Memory User	Memory Used	Number Present
Magnetorquers	30 kB*	3
Gyroscope	100 kB*	1
Magnetometer	100 kB*	1
Global Positioning System (GPS)	200 kB*	1
Coarse Sun Sensors	20 kB*	5
Fine Sun Sensor	30 kB*	1

Note: Values denoted by a (*) represent estimated values.

A maximum of 7.92 MB of storage was available, accounting for the 0.92 MB of software storage as estimated in Section 4.1.1. Each sensor's MRAM data use is plotted in Figure 58. Subsequently, the sum of all such data was plotted to ensure that it did not exceed the maximum MRAM available, as seen in Figure 59.

In this simulation, the Clyde Space Nanosatellite OBC could capably handle the sensor operations it would be tasked to perform in support of the mission.

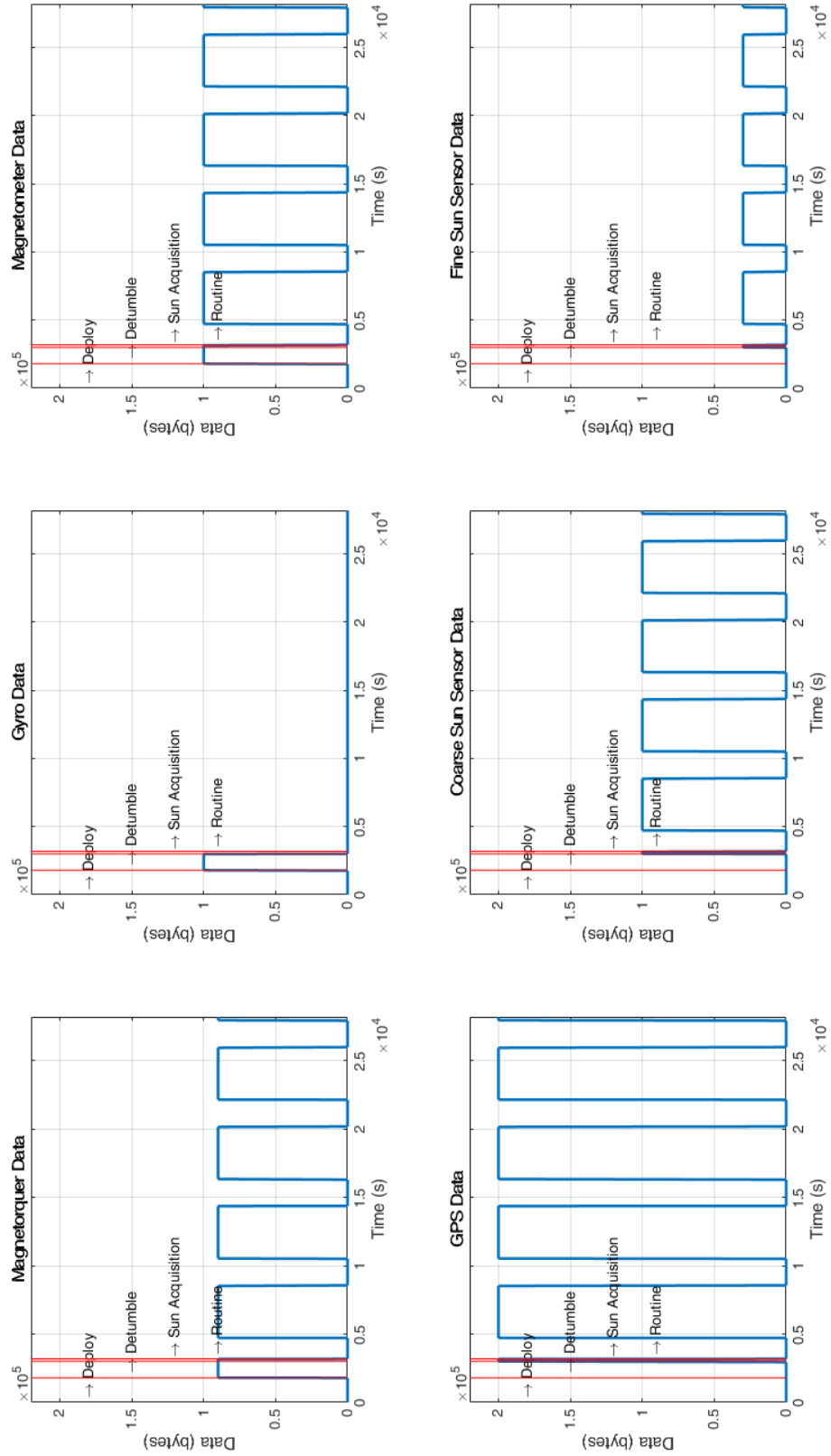


Figure 58: Simulation of Individual Users of MRAM

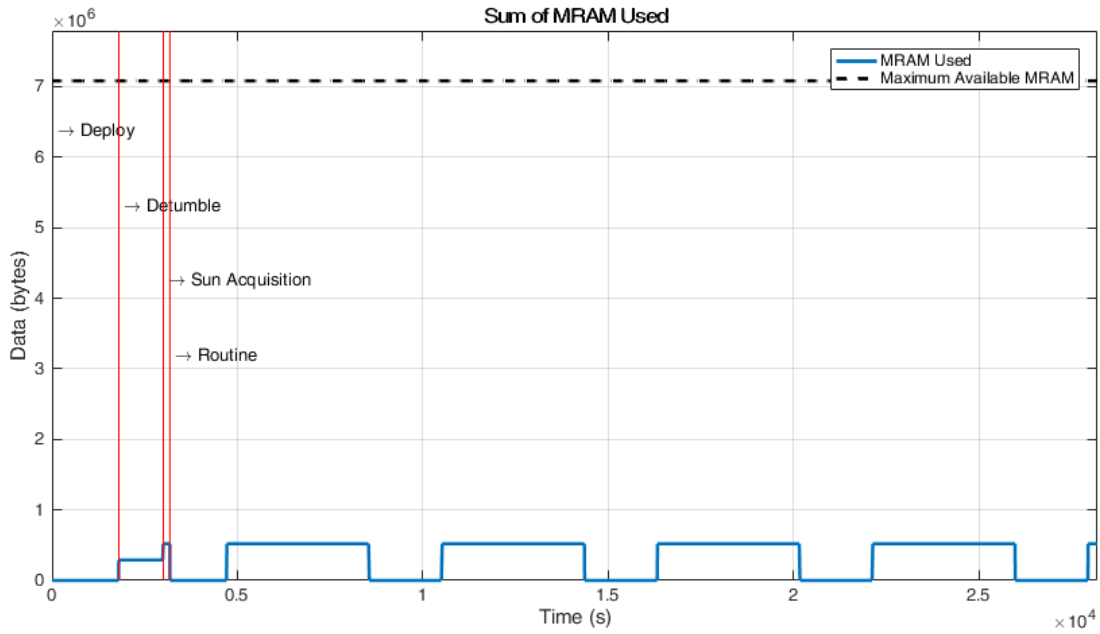


Figure 59: Simulation of Sum of All Users of MRAM

Next, the spacecraft health and payload data, which accumulates over time was simulated. This data was considered to be stored in the OBC’s flash memory. Table 20 shows the data used as input for the flash memory simulation.

Table 20: Non-Volatile Data Producer Information

Data Producer	Data Produced
On-Board Computer (OBC)	0.2 kB/s*
Electrical Power System (EPS)	0.05 kB/s*
Radio Transceiver	50 B/s* (Uplink) 1171.30 B/s (Downlink)

SphinX-NG Payload	6828.70 B/s
-------------------	-------------

Note: Values denoted by a (*) represent estimated values.

This data was used to simulate the flash memory, which was used over time. The results of the calculation for each individual flash memory user's data use is plotted in Figure 60.

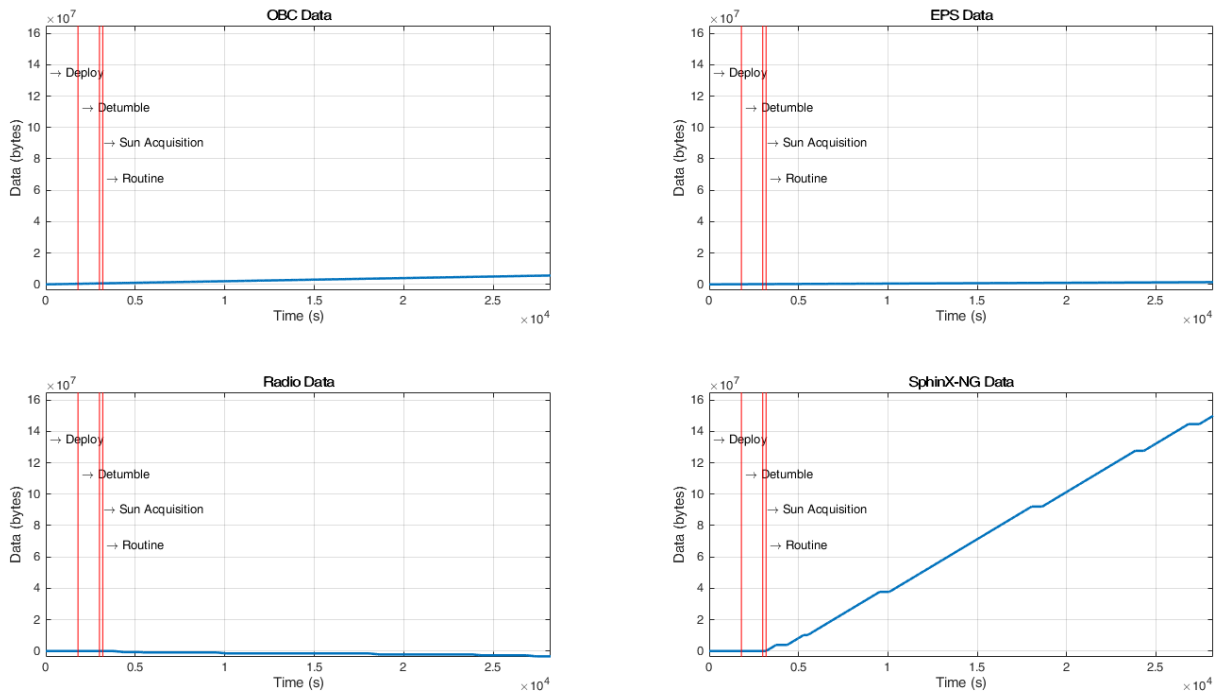


Figure 60: Simulation of Individual Users of Flash Memory

The sum of all flash-memory-stored data used was subsequently plotted in Figure 61.

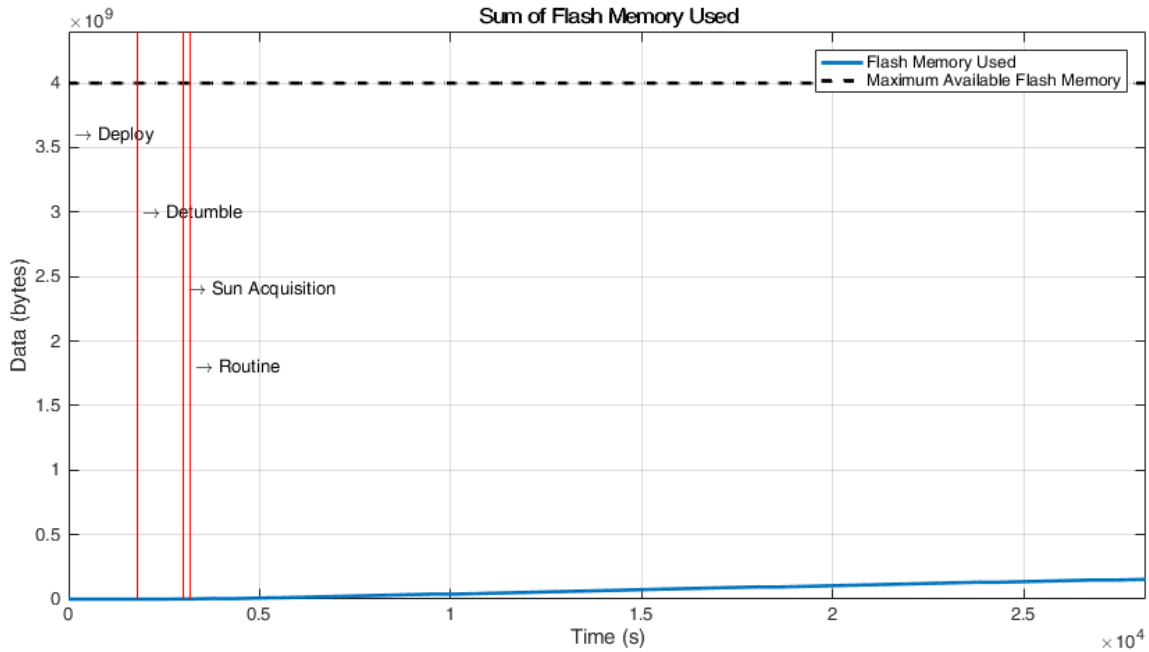


Figure 61: Simulation of Sum of All Users of MRAM

According to this simulation, the Clyde Space Nanosatellite OBC can handle the demands of the mission, at least for the duration of about 4.5 orbits. However, it is of concern that there is an upward trend in the data accumulating in flash memory. To estimate the time it would take for the OBC flash memory to become saturated (at 8MB), Microsoft Excel was used to plot the data of Figure 61 and approximate a linear trend line. The resulting equation for flash memory accumulation was

$$DA = 1579.7t - 77507 \quad (13)$$

where DA is data accumulated in Bytes, and t is time in seconds. The R^2 value for this approximation was 0.9931, indicating it was quite a good approximation. At this rate, the flash memory would become full after 58.6 days, or about 670 orbits at the CubeSat’s 600 km circular orbit [7]. At this point, the 256 GB of flash memory of the SphinX-NG would still be available, but the excesses of data accumulating would still need to be downlinked to Earth at some point in

order for the data collected to have any use. Thus, the operations of the spacecraft may need to be rethought, should similar trends arise when more information about these subsystems eventually arises in the future.

Once adjusted, this analysis should be repeated after any changes are made to the C&DH system or its requirements, improving the accuracy of the simulations as more information regarding the data and memory usage of each subsystem becomes known.

4.2 Power Subsystem

4.2.1 Final Hardware Configuration

The specific hardware components that define the power system were selected early on in the development of this mission. As further analysis was performed, these selections were updated to match the mission requirements.

To serve as the main EPS, the team identified a 3rd Generation 3U EPS from Clyde Space as the ideal choice for this CubeSat's mission [23]. It has extensive flight heritage and interfaces easily with much of the other hardware that was selected for our mission. This EPS also includes built-in maximum power point tracking (MPPT) capabilities as well as overcurrent and battery under-voltage protection. However, unlike the configuration that the 2013 MQP group [1] selected where the EPS and PDM were isolated to separate boards, this EPS integrates the PDM onto the same board, saving size and weight, and reducing the complexity of wiring for the CubeSat. An image of the EPS board is shown below in Figure 62.

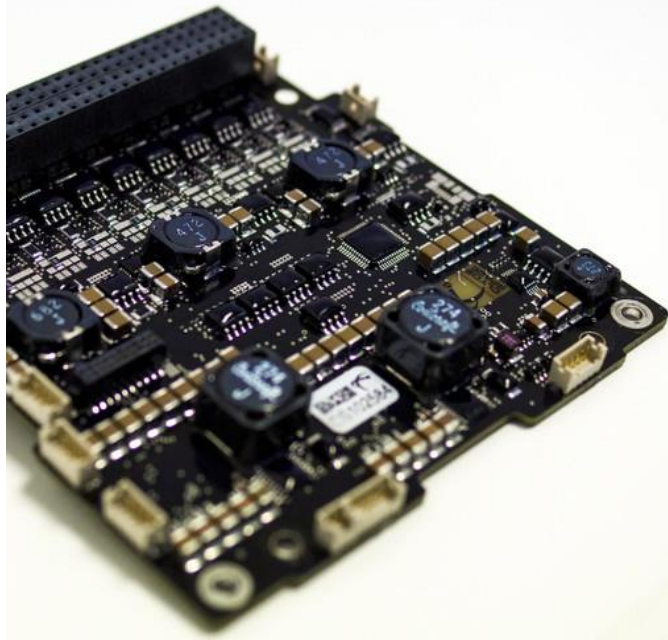


Figure 62: Clyde Space 3U EPS [23] Copyright © 2016 Clyde Space Ltd.

For this mission the team initially chose a Clyde Space 30 W-hr lithium-polymer standalone battery. Later it was determined that this battery would not be able to supply a sufficient current to power both the instrument and the CubeSat's base functions at the same time. This determination is described in Section 4.2.3. As such, a 40 W-hr Clyde Space battery was identified which could meet this demand. Based on analysis of power usage over four orbits, it was determined that this 40 W-hr capacity will more than meet the energy requirements and a Clyde Space product would ensure compatibility with the chosen EPS and other computer boards. The Clyde Space battery is shown in Figure 63.

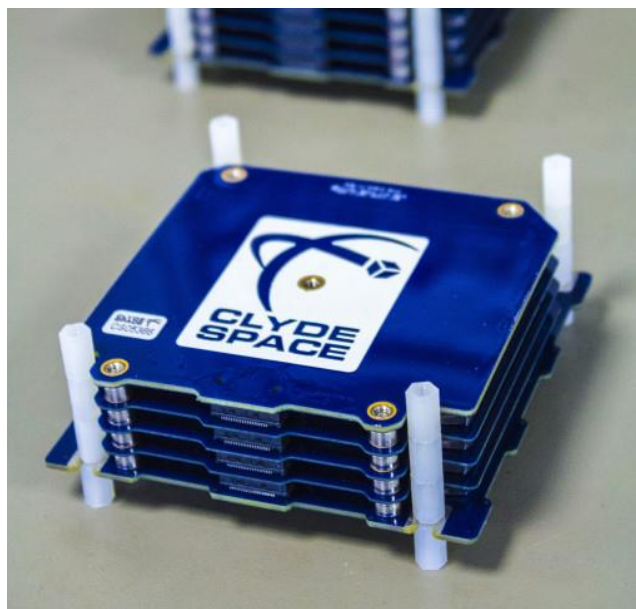


Figure 63: Clyde Space 40 W-hr CubeSat Battery [59] Copyright © 2016 Clyde Space Ltd.

For the CubeSat's solar arrays, a set of panels manufactured by Clyde Space that meet the mission requirements were identified. They consisted of a pair of single-deployable 2U panels and a single body-mounted 2U panel. These panels each utilize 4 Spectrolab UTJ triple-junction solar cells which advertise a 28.3% efficiency at 28 °C [57]. The deployable panels utilize Clyde Space's Thermal Knife Driver technology to deploy to a 90° angle from their initial stowed configuration [60]. These panels are all flight-proven hardware designed to easily interface with the Clyde Space EPS that was chosen for this mission.

Once these components were selected, a finalized power budget was created for this mission. It includes the average power consumption values of every power-drawing component on the CubeSat as well as each one's voltage and current requirements. This final budget is outlined in Table 21.

Table 21: CubeSat Power Budget

Group	Component	Manufacturer	Part no.	Peak Power (W)	Nominal Power (W)	Quiescent Power (W)	Current (mA)	Voltage (V)
C&DH	OBC	Clyde Space	01-02928	1.0	0.35	0.165	150	Batt
ADC	Coarse Sun Sensor	Space Micro	CSS-01	0	0	0	3.5	-
	Fine Sun Sensor	New Space Systems	NSS-CSS	0.05	0.05	0	10	5
	Gyroscope	Analog Devices	ADXRS453	0.04	0.03	0.03	8	5
	Magnetic Torquer (3)	ZARM Technik AG	MT0.5-1	0.825	0.3	0	165	5
	GPS	Surrey Satellite Technology	SGR-05U	0.8	0.8	0	160	5
	Magnetometer	Honeywell	HMC5883L	<0.01	<0.01	0	0.1	3.3
Payload	Instrument		Sphinx-NG	8.00	8.00	1.00	1600	5
Power	EPS	Clyde Space	CS 25-02452	0.2	0.2	0.2	24	Batt
	Battery	Clyde Space	CS 01-02686	-	-	-	2400	7.6
	Center Solar Panels	Clyde Space	CS 25-02871	-	-	-	-	-
	Side Solar Panels	Clyde Space	CS 01-02880	-	-	-	-	-
Telecomm	Transceiver	ISIS	TRXUV VHF/UHF	4.8	3.3	0.4	600	Batt

The final hardware choices and their estimated cost are listed in Table 22. The current price for the solar panels is bespoke so the cost estimates from the 2013 MQP were used [1].

Table 22: Power Hardware Cost

Component	Part Number	Cost (each)	Number	Cost (total)	Ref.
EPS	CS 25-02452	\$4,900	1	\$4,900	[23]
Battery	CS 01-02686	\$4,300	1	\$4,300	[59]
Center Solar Panels	CS 25-02871	\$4,000	1	\$4,000	[1]
Side Solar Panels	CS 01-02880	\$4,150	2	\$8,300	[1]
Total				\$21,500	

4.2.2 Final Wiring Results

The circuit stack will connect the EPS board, battery board, OBC, and transceiver together, using a PC-104 connector bus, allowing for the easy transfer of power and data throughout the CubeSat. In addition to the major stack components, the Sphinx-NG instrument, magnetorquers, and individual sensors must be connected to the main header. The solar arrays will be connected directly to the SA connectors located on the EPS.

The team determined that the simplest solution for connecting and mounting the smaller components was to integrate them into a discrete circuit board containing a PC-104 connector that will slot directly into the circuit stack, hereafter referred to as the “unifying board”. This unifying board will contain connection points for gyroscope, magnetometer, coarse sun sensors, and magnetorquers, as well as serial ports for the GPS and fine sun sensor. The team identified the Pumpkin CubeSatKit Protoboard as the ideal circuit board backbone for the unifying board due to its versatility and flight heritage [61]. The Pumpkin Protoboard is shown in Figure 64.

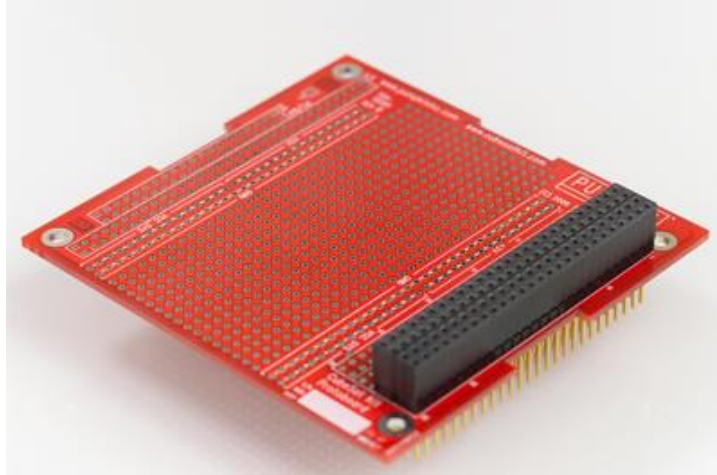


Figure 12: Pumpkin CubeSatKit Protoboard [61] Copyright © 2007 Pumpkin Inc.

The power connections of each of the components connected to the unifying board will be routed to the pin location corresponding to one of the EPS's PDM outputs. This will allow the OBC to switch individual components on and off using the EPS's integrated PDM switches. The specific pin assignments are detailed in Appendix E. The pin layouts and connectors for each individual component can be found in Appendix F. The exact power interface for the Sphinx-NG is not known at this time and should be determined by future work.

Special attention must be paid to the power connections for the magnetorquers. The torque that they produce is directly proportional to the current flow through them so this current flow must be finely controlled to allow for any type of fine control over the CubeSat attitude. Such control is easily achievable using pulse width modulation (PWM) to adjust the effective current through the torquers. PWM functions by rapidly switching the voltage source on and off, inducing an effective current proportional to the ratio of on versus off time, known as the duty cycle [62]. In addition to the PWM control circuitry, additional circuitry must be implemented to switch the flow of current to each torquer and allow for current to flow in both directions through them. This additional control circuitry will also be implemented on the unifying board. The exact design of

this control circuitry and the unifying board layout is outside the scope of this project and should be the focus of future work.

4.2.3 Power Profile Results

The analysis of the selected power hardware was performed using a modified version of the MATLAB simulation, which was developed to analyze the C&DH subsystem. The constant and accumulating data profiles were adapted to represent constant power draw and total power usage, respectively. The major inputs to the program consisted of the power draw of each individual component, the power states of each individual component, the total capacity and maximum DoD of the battery, the maximum current supplied by the battery, and the solar array power production. The sun and ground station exposure vectors shown in Figure 56 were also used for this simulation. These inputs were used to calculate the total power draw, current draw, and battery charge from initial deployment through four full orbits.

For this simulation, the power states were defined as when each individual component was drawing power. The two major components of note in this regard are the radio and the Sphinx-NG as these two components account for the majority of the CubeSat's power usage. Their operational states are shown in Figure 65.

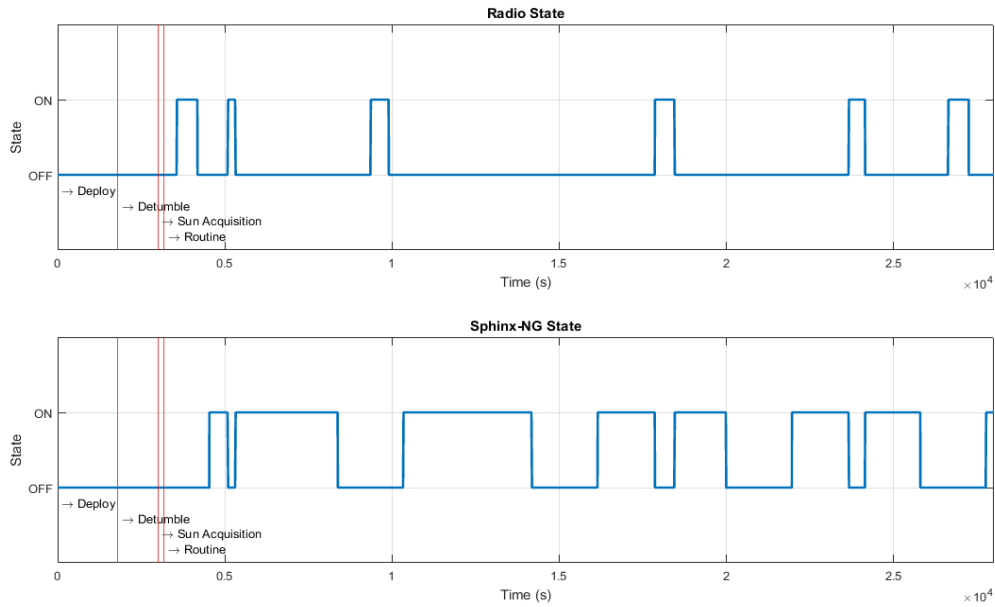


Figure 65: Radio & Sphinx-NG Power States

Current

The first step in evaluating the selected hardware was to analyze the total current draw over time. For the 30 W-hr battery that was initially selected, the maximum current it can supply is 1800 mA. This was determined to be insufficient to support both the instrument and the remainder of the CubeSat’s basic functions as shown in Figure 66. Due to this, the 40 W-hr battery was chosen as a replacement and then shown to be able to supply sufficient current as shown in Figure 67.

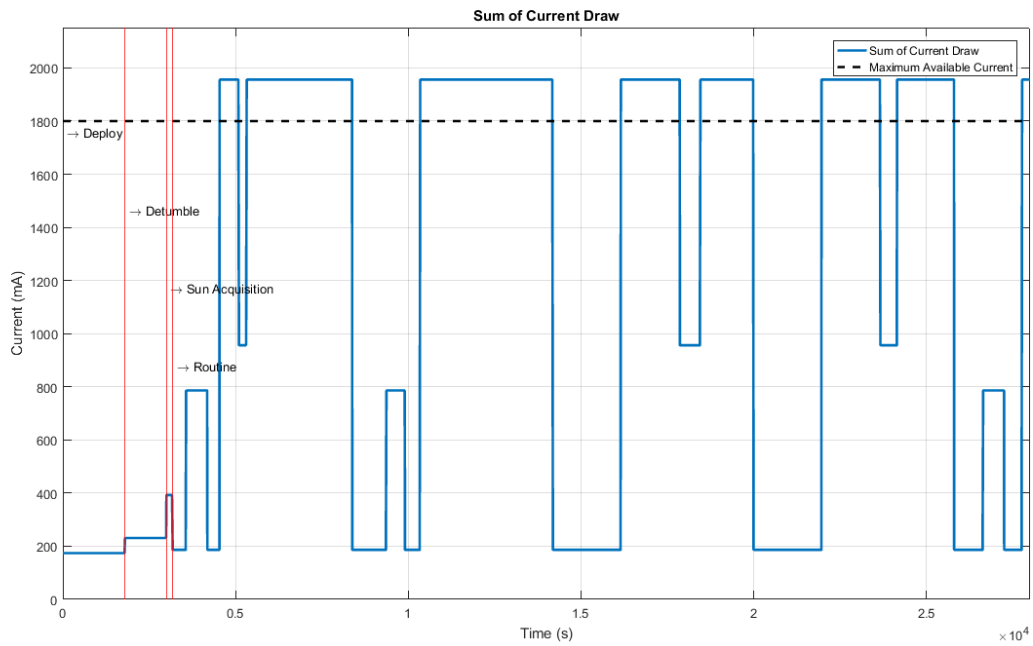


Figure 66: Sum of Total Current Draw (30 W-hr)

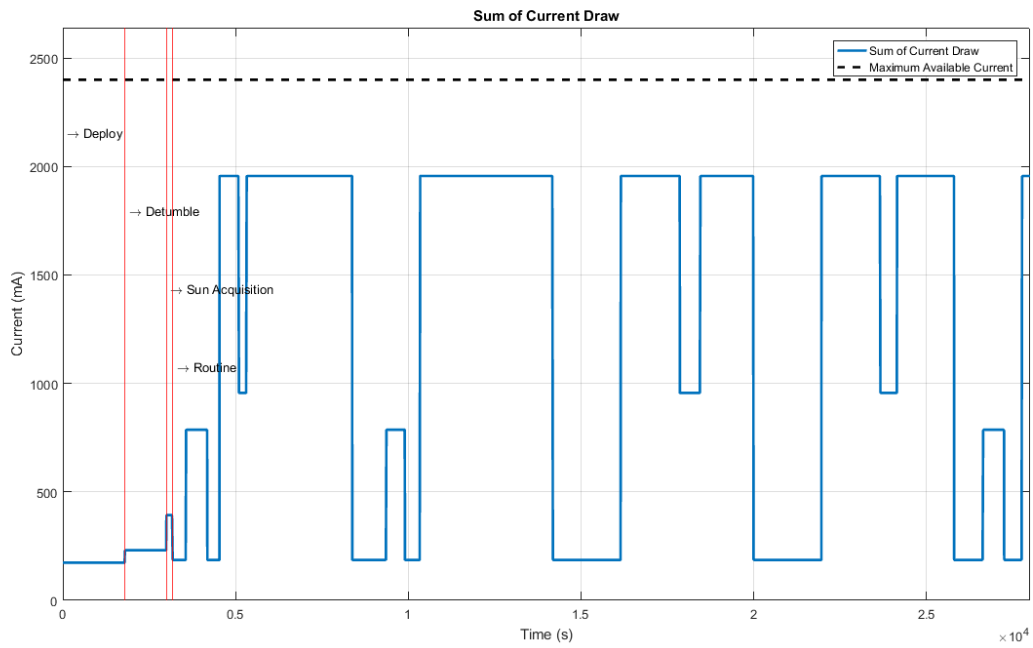


Figure 67: Sum of Total Current Draw (40 W-hr)

Solar Array Power Production

To begin evaluating the power production of the solar arrays, the Equation 3.1 was used to determine a baseline power production level for the selected solar panel area. The selected solar panels each consist of four Spectrolab-UTJ triple junction cells with an efficiency rating of 28.3% and cell area of 26.62 cm² [57]. Across all three solar panels this translates to a total cell area of 319.4 cm². Due to the strict Sun-facing requirements of this mission, the cosine losses mentioned in Section 3.2.1 due to the Sun angle of incidence were neglected. As such, the total power production of the solar arrays was calculated to be 12.36 W. This number is further reduced due to assumed inefficiencies in the array construction and the EPS BCRs, both of which are assumed to be 90% efficient [22, 23]. These inefficiency assumptions were made based on the EPS documentation and Ref 20. The resultant power output of 10.01 W more accurately represents the power transferred to the battery.

Thermal effects on the power output must then be taken into account using Equation 3.2. This 10.01 W result represents the power output at 301 K, at which point the cell efficiency equals 28.3% and the β value for the Spectrolab UTJ cells is 0.000204 K⁻¹. Thermal data generated using COMSOL was implemented to determine the power production over the course of four orbits. The solar panel temperature data is shown in Figure 67 and the solar panel power production is shown in Figure 68. The panels range in temperature from 270 K to nearly 380 K over the course of a single sunlight period, with the total power production decreasing from 10.1 W to 9.5 W as seen in Figures 68 and 69.

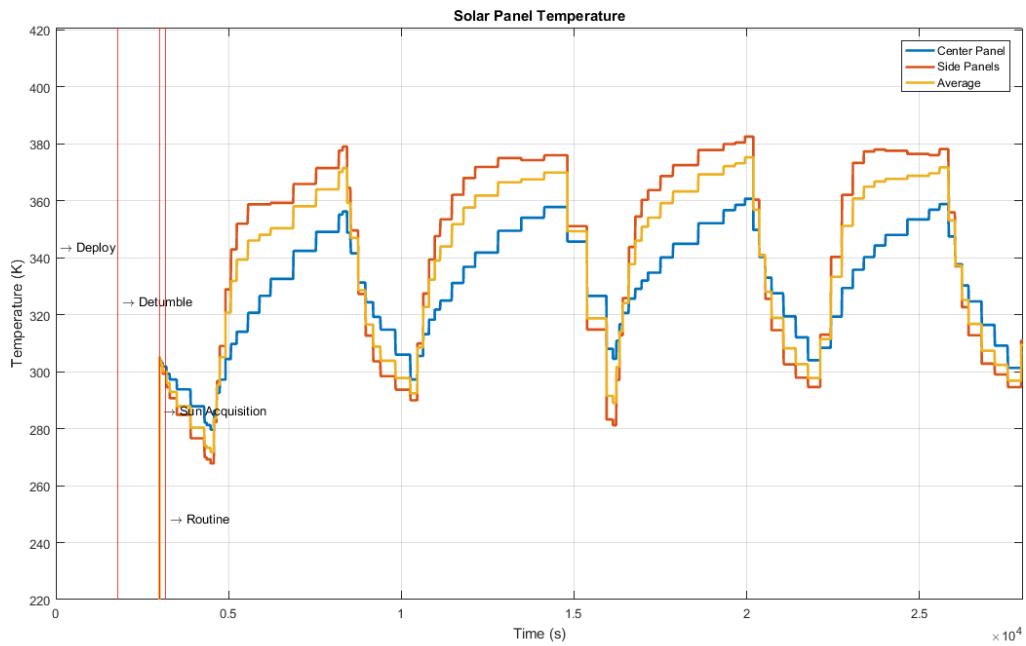


Figure 68: Solar Panel Temperature

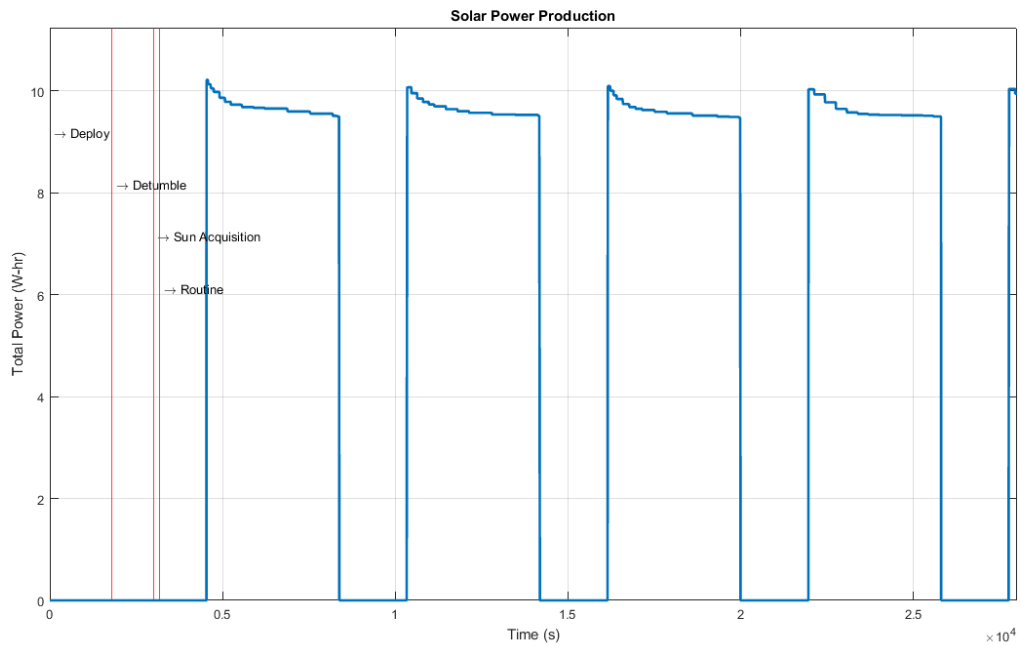


Figure 69: Solar Panel Power Production

Power Consumption

The total power consumption of the CubeSat is of great importance for the further evaluation of the power subsystem. This analysis was performed by first identifying a constant power usage for each component, and multiplying that amount by the component's power state (i.e. 1 for on, or 0 for off), then finding the resultant sum of all power profiles. The power consumption levels assumed for each component are listed in Table 23. These assumptions are based off of the peak power draw of each component. These consumption figures also take into account the efficiency of the power bus that is supplying them with power, to better represent the total power each one is drawing from the battery.

Table 23: Simulation Individual Component Power Consumption

Component	Consumption (W)
OBC	1.053
EPS	0.202
Transceiver	4.848
Sphinx-NG	8.602
Magnetorquers (detumble)	0.245
Magnetorquers (routine)	0.061
Gyroscope	0.043
Magnetometer	0.00033
GPS	0.860
Fine Sun Sensor	0.054

The total power consumption over time is shown in Figure 70.

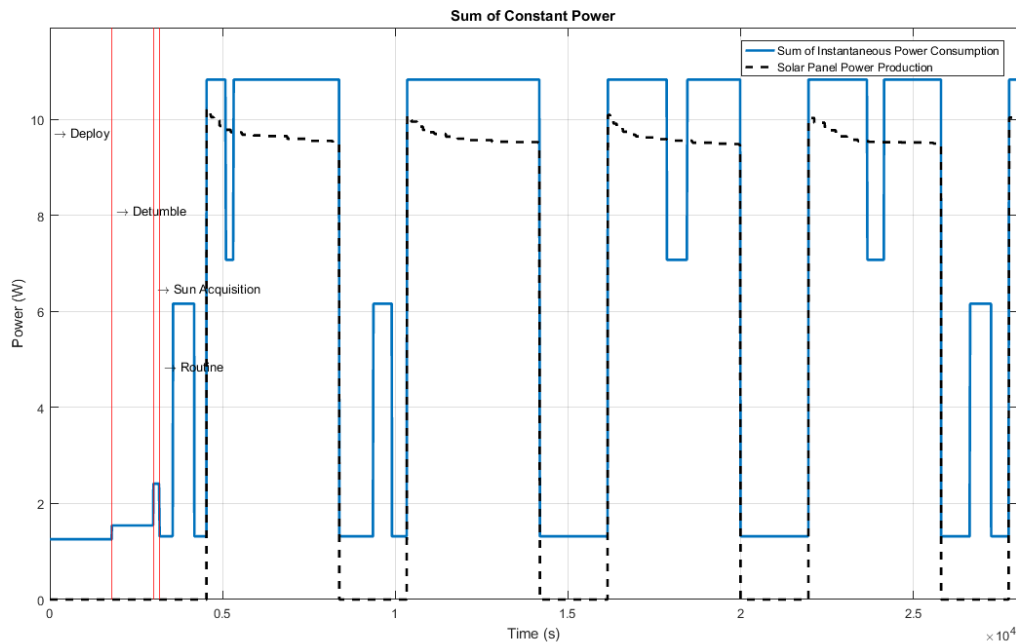


Figure 70: Sum of Constant Power Consumption

Upon initial inspection, it is seen that the power consumption is nearly always greater than the power production. This suggests that the current hardware configuration cannot support the current power profile.

Battery Charge

The final major step in evaluating the power subsystem performance is in the determination of the battery charge over time. The MATLAB simulation accomplishes this by taking the total power consumption and summing it over a specific time span. It then subtracts this amount from the current battery charge before adding the power production over the same period, keeping this total at or below the battery's capacity. This analysis was performed for the previously identified 40 W-hr battery capacity, power consumption, and power production, the results of which are shown in Figure 71.

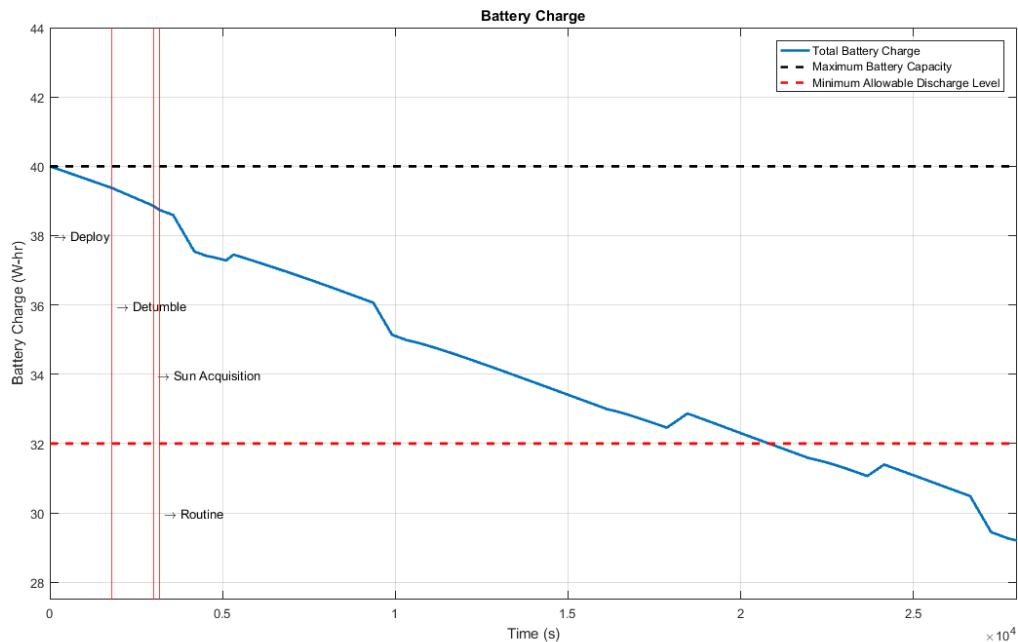


Figure 71: Battery Charge vs. Time

From this analysis, it can be seen that the current hardware configuration is not compatible with the current instrument state vector, as the battery charge falls below the maximum depth of discharge after only six hours. As the hardware configuration is near the limits of its capabilities, the instrument’s power state was alternately modeled such that the Sphinx-NG was only turned on every other orbit as shown in Figure 72. The analysis of battery charge was then repeated using this new state vector, the results of which are shown in Figure 73. It can be seen from this further analysis that this new state vector would allow for sustained operation well within the capabilities of the selected power hardware.

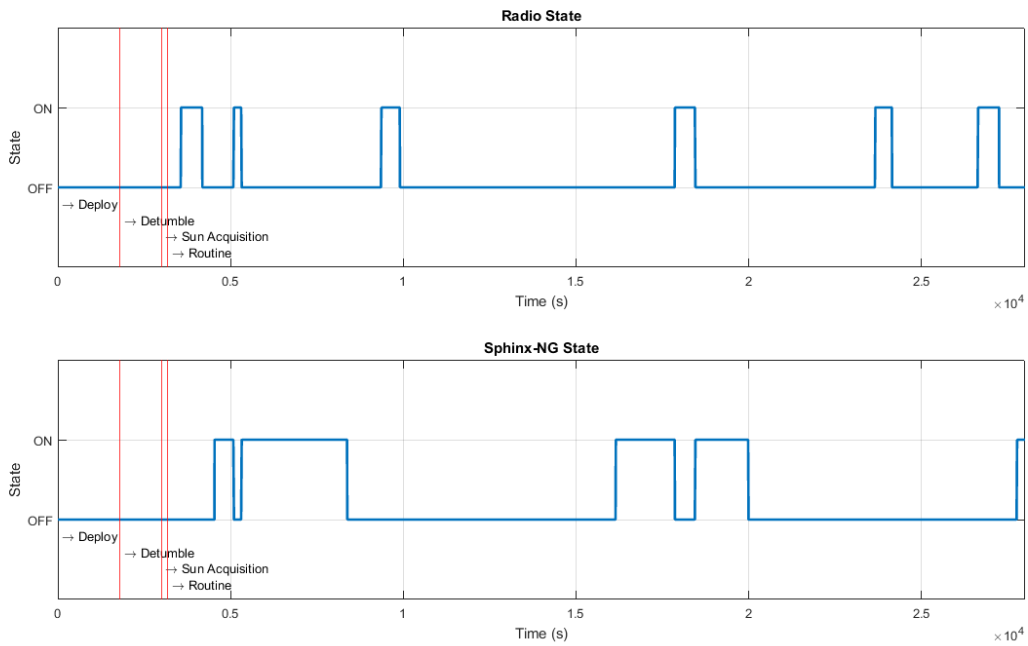


Figure 72: Altered Radio & Sphinx-NG State Vectors

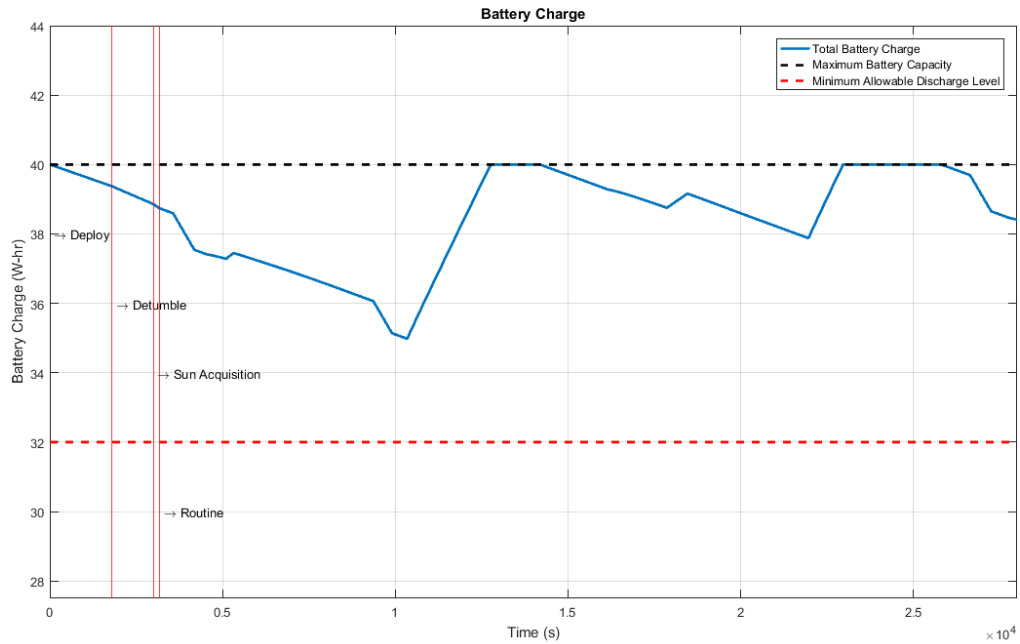


Figure 73: Battery Charge (Altered Sphinx-NG State Vector)

4.3 Telecommunications Subsystem

4.3.1 Mission Modeling and Timelines

Using the Ground Stations available by GENSO, preliminary data budgets for both downlink and uplink were established. STK analysis was used to generate an estimate of the annual access time per ground station, as shown in Figure 74.

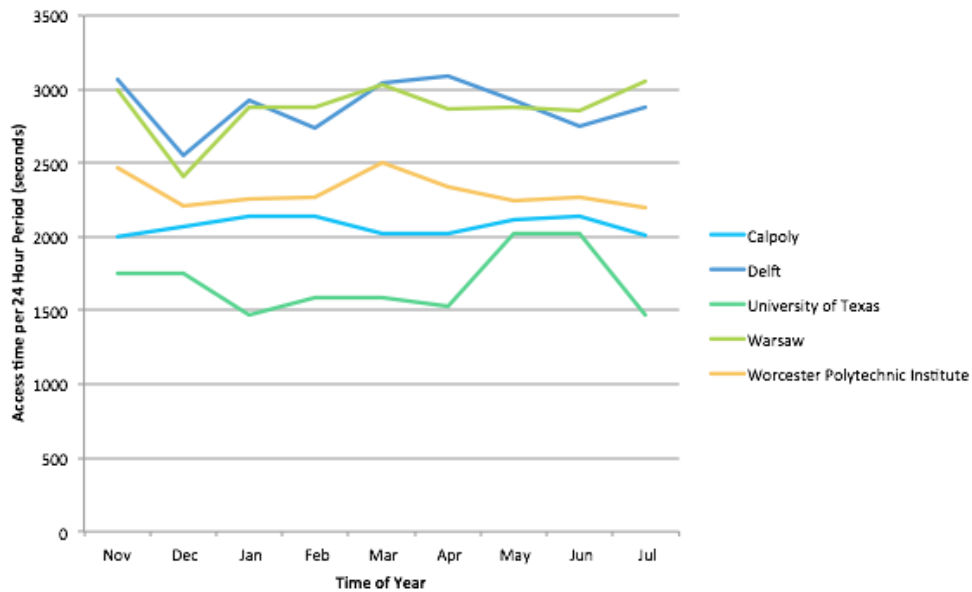


Figure 74: Annual Access Time per Ground Station

The average daily downlink budget for a particular year was determined to be 116Mb a day while the average daily uplink budget was determined to be 16Mb a day. The payload makes a very significant amount of data (approximately 700Mb a day) so these daily rates do not allow for the CubeSat to send all the scientific data that it will collect within a day

Once the GENSO network was found to be non-active, three ground stations were chosen to support the mission: UCLA, Warsaw, and a hypothetical WPI ground station. The preliminary

annual access time and downlink budget charts for these three ground stations can be seen in Figures 75 and 76, respectively.

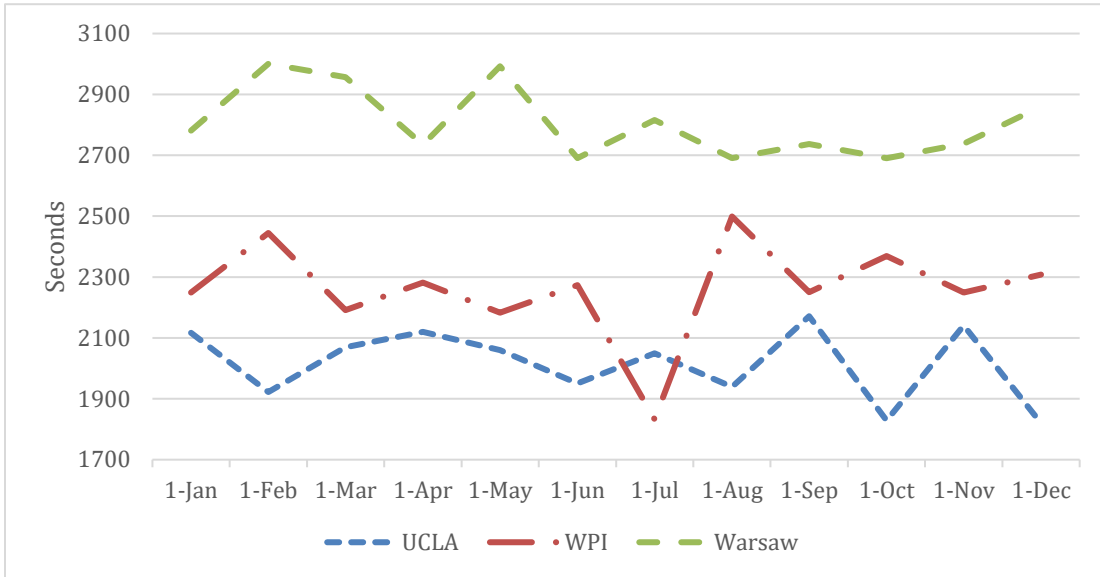


Figure 75: Annual Access Time per Station

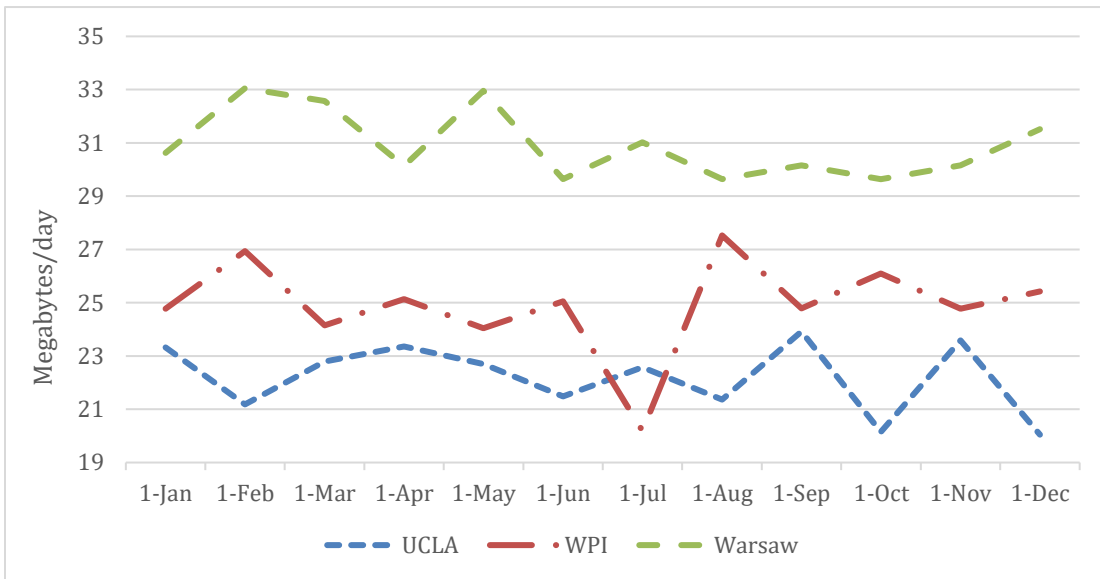


Figure 76: Annual Downlink per Station

Based on these three ground stations, the daily access time for the CubeSat is 7097s and the average daily downlink budget is 78.2Mb. This amount of data is insufficient for the mission to download all of the created payload data.

Mobile Ground Station

The individual components of a WPI-based Mobile Ground Station were selected and their associated costs recorded. A full line item cost estimate for the MGS can be found in Table 24.

Table 24: Mobile Ground Station Cost

Part	Category	Cost	Reference Number
Yaesu G-5500	Azimuth and Elevation Rotator	\$750	63
Yaesu GS-232B	Computer interface	\$550	64
NOVA	Tracking software	\$150	65
Yaesu FT-857D dual VHF/UHF	Earth Transceiver	\$800	66
SP7000	Low Noise Amplifier	\$350	67
Belden 8214 RG-8	Coaxial Cable	\$200	68
M2 436CP42 U/G	Antenna	\$450	69
Wood + Metal	Base	~\$250	N/A
N/A	Laptop	~\$500	N/A
Total Cost = ~\$4000			N/A

The total cost estimate was approximately \$4000 for a fully operational MGS. This cost breakdown is per mobile ground station and would be multiplied by two for a total cost, to account for a possible second mobile ground station to be added to another site.

Mobile Ground Station Case Study

The four chosen locations for a secondary mobile ground station were defined as part of an STK scenario for analysis purposes. The goal of this analysis was to find the site that would add the most access time, and in turn, downlinked data per day. Table 25 displays the added access time per day and data per day for each possible ground station.

Table 25: Added Access Time and Downlink Budget

	Bangkok, Thailand	Cape Town, South Africa	Melbourne, Australia	Asuncion, Paraguay
Access time/ day (s)	2550.45	3050.17	3230.09	2770.90
Data/day (bits)	2809580	3360068.174	3558269.81	3052427

Following the STK analysis, the station that added the most value in terms of access time and link budget was determined to be Melbourne, Australia. Adding in the fact that WPI students revisit the site twice a year in B and D term, it is the best candidate for the second mobile ground station. In total, adding in the Melbourne Mobile Ground Station brings approximately 22Mb of data per day, bringing the total data budget to 101Mb a day.

Now adding in the Melbourne, Australia site with the previous three-Ground Station configuration, the final data downlink and access time profiles could be created. Figure 77 displays the final downlink budget per ground station over a year's time and Figure 78 shows the final daily access time for the CubeSat.

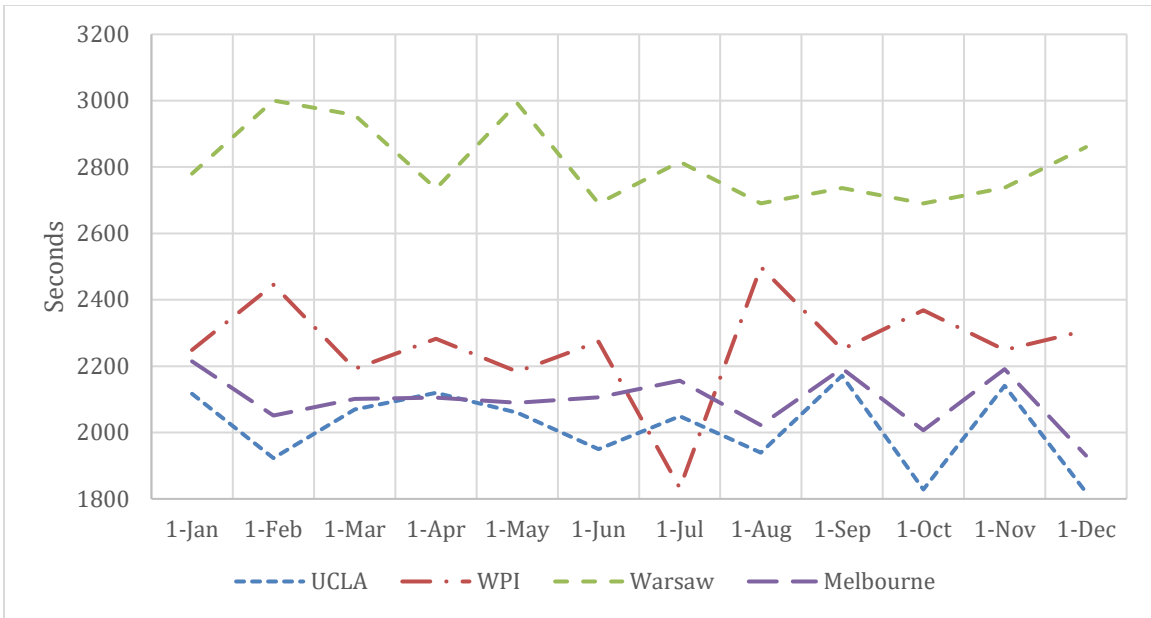


Figure 77: Final Annual Downlink Budget per Station

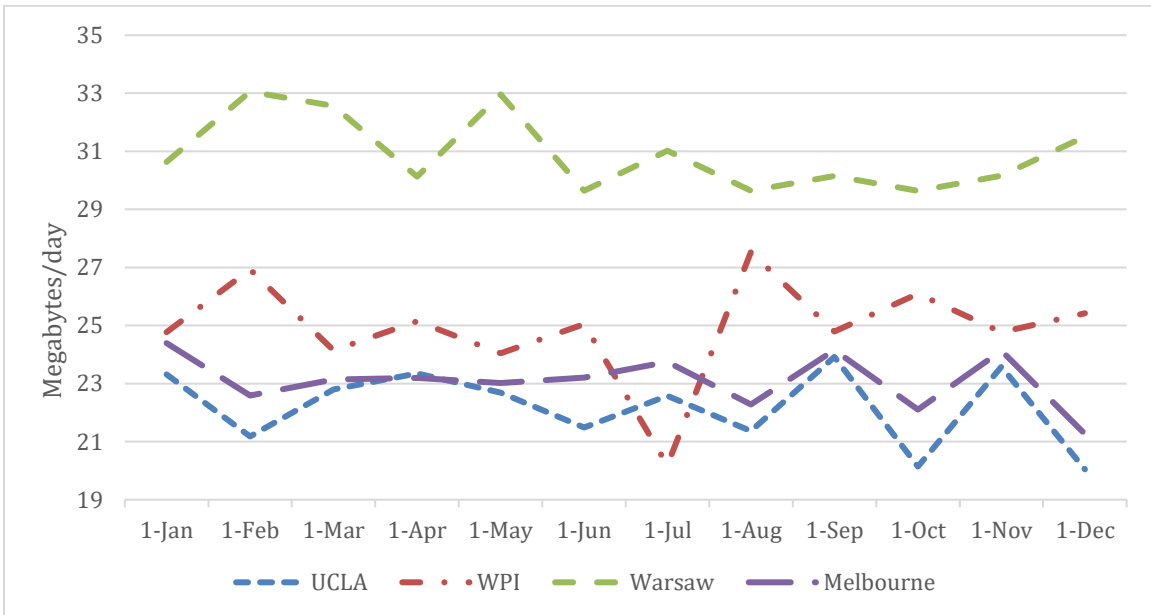


Figure 78: Final Annual Access Time per Station

Adding in the second MGS at Melbourne, Australia, the daily access time and downlink budget bumped up by approximately 30 percent. Now, the daily access time is 9185s and the

downlink budget is 101Mb. Even with a Melbourne Ground Station added, 101Mb/day still is insufficient to send all of the data which the payload creates in a day, so multiple passes will be needed to send down the scientific data.

4.3.2 Communication Hardware

The two pieces of hardware that needed to be selected for the telecommunications subsystem were the transceiver and the antenna. The selected transceiver for this mission is the Innovative Solutions in Space (ISIS) TRXUV VHF/UHF Transceiver due to its flight history, availability, and data rate [32]. The cost for this component is \$9000 [32]. The selected antenna for this mission is the Innovative Solutions in Space (ISIS) Deployable Dipole Antenna System for its flight heritage and compatibility with the previously chosen transceiver [35]. The cost for this antenna system is \$5000 [35].

4.4 Thermal Subsystem

4.4.1 CubeSat Thermal Limits

As described in previous sections, one of the main objectives of thermal control subsystem is to guarantee that the temperature of each internal component stays within its specified temperature ranges. Table 26 illustrates the specified operational and survival temperature ranges of components on CubeSat.

Table 26: Operational and Survival Temperature Range²

Part Name	Operational Max. (°C)	Operational Min. (°C)	Survival Max. (°C)	Survival Min. (°C)
Gyroscope	105	-40	125	-55

Magnetorquers	85 ¹	-40 ¹	85 ¹	-40 ¹
Magnetometer	85	-30	85 ¹	-40 ¹
GPS	50	-20	85 ¹	-40 ¹
OBC	80	-40	85	-40
EPS	85	-40	100	-50
Battery	50	-10	85 ¹	-40 ¹
Transceiver	45	-10	85 ¹	-40 ¹

¹ Components without specified operational or survival temperature range were assumed to have a range between 85°C to -40°C which is the standard thermal limit for industrial electronic parts [55]

² The temperature ranges were provided by other subsystems through weekly systems engineering meetings

The operational and survival temperature ranges of most components are equal to or close to a standard thermal limit for industrial electronic parts of between -40°C to 85°C, excluding the battery, transceiver, and GPS [55]. It was important that the temperature sensitive components, such as the battery, transceiver, and GPS, are observed carefully in the analysis. Furthermore, additional attention was paid to GPS and magnetorquers due to the fact that they are in direct contact with the frame of the CubeSat and thus experience relatively extreme temperatures via conduction.

4.4.2 Initial Result

Once the final CubeSat model was fully implemented into COMSOL and environmental inputs were gathered from STK, thermal simulation was conducted over five representative orbits. Figures 79, 80, 81, and 82 are snapshots of a 3-D surface plot of temperature distribution over the CubeSat and the circuit stack taken at arbitrary times over the five representative orbits

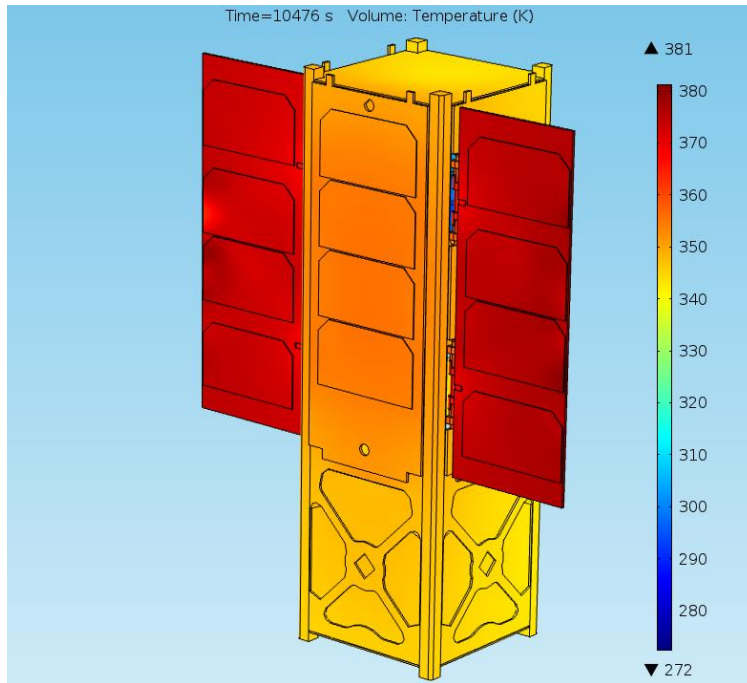


Figure 79: Snapshot of 3-D External Temperature Graph (t = 10476 sec)

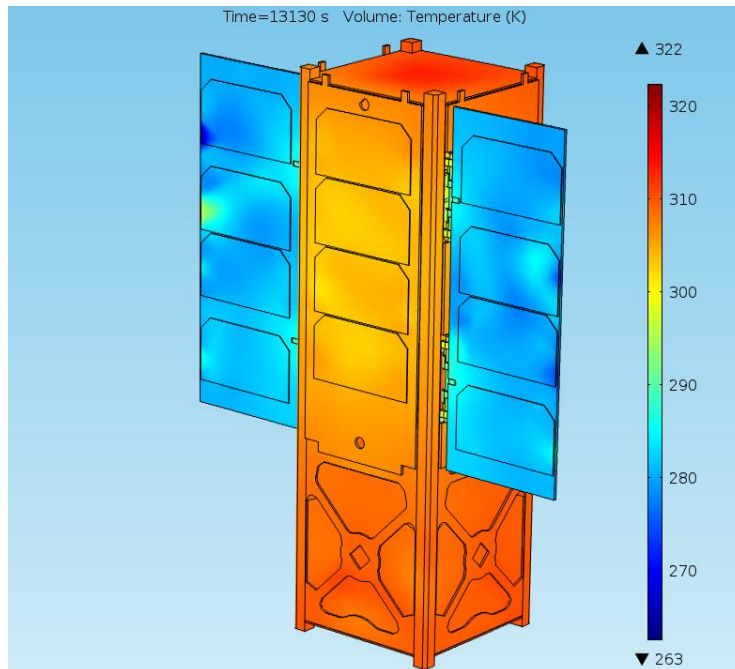


Figure 80: Snapshot of 3-D External Temperature Graph (t = 13130 sec)

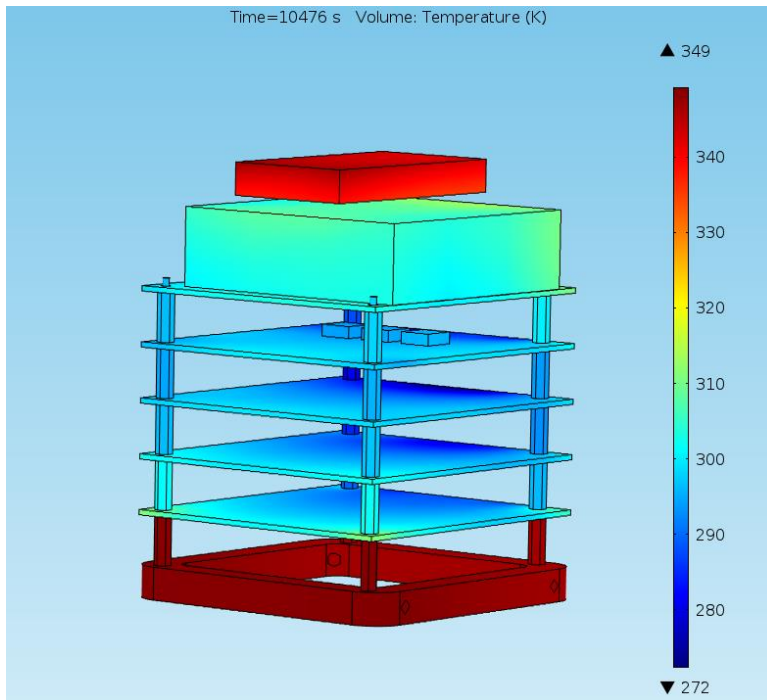


Figure 81: Snapshot of 3-D Circuit Stack Temperature Graph (t = 10476 sec)

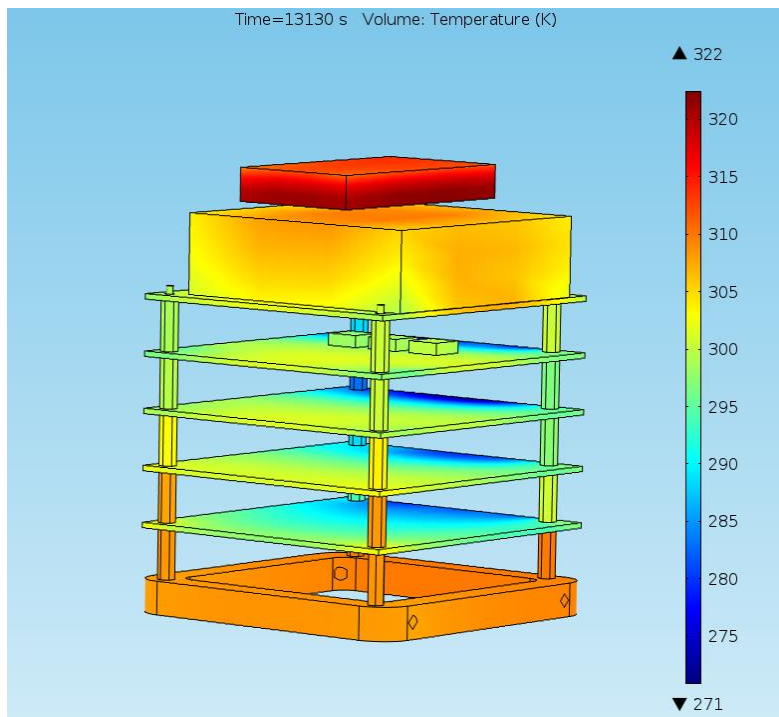


Figure 82: Snapshot of 3-D Circuit Stack Temperature Graph (t = 13130 sec)

Due to the material characteristics of the solar panel, they experienced relatively hot and cold temperatures over the five representative orbits. Additionally, due to the small dimensions of the hinges that are connecting the solar panels to the CubeSat structure, a thermal choke point is created near the hinges preventing nominal conduction between the structure and the solar panels.

Steady-State Temperatures

As the CubeSat orbits around the Earth, the time spent by the CubeSat in each the sunlight and in the eclipse is roughly the same over time, which means that the state of thermal environment experienced by the CubeSat is periodic. This is not necessarily true for a very long mission duration due to orbital precession and perturbations, which is discussed in more detail in Section 5.4, but the assumption is adequate for the purpose of this project. As a result, the maximum and minimum temperature experienced by the CubeSat is approximately the same for each orbit.

Steady-state temperature, in this context, refers to the range of temperature experienced by the CubeSat throughout the five representative orbits. For steady-state temperature analysis, two separate line graphs were generated where the x-axis represents the time since the beginning of the mission and the y-axis represents the average temperature of corresponding domain of the CubeSat. Figure 83 illustrates the average temperature of the frame, center solar panel, and side solar panels, Figure 84 illustrates the average temperature of all five circuit boards on the circuit stack, and Figure 85 illustrates the average temperature of the components on the circuit stack.

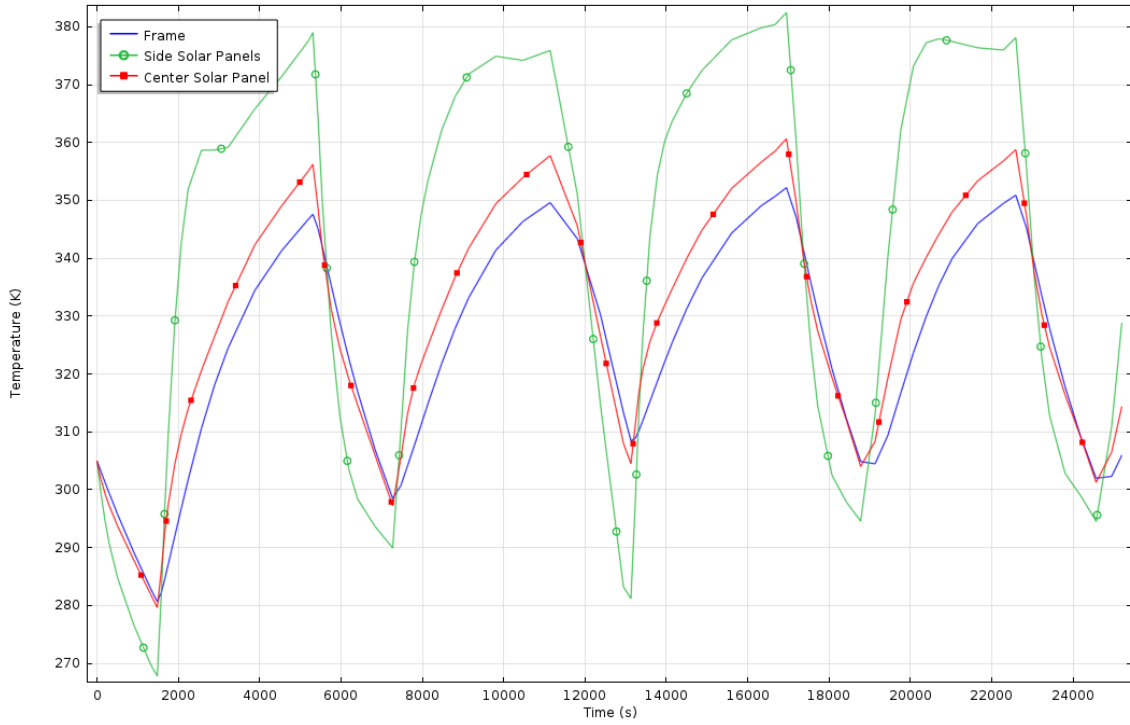


Figure 83: Average Temperature vs. Time for External Domains

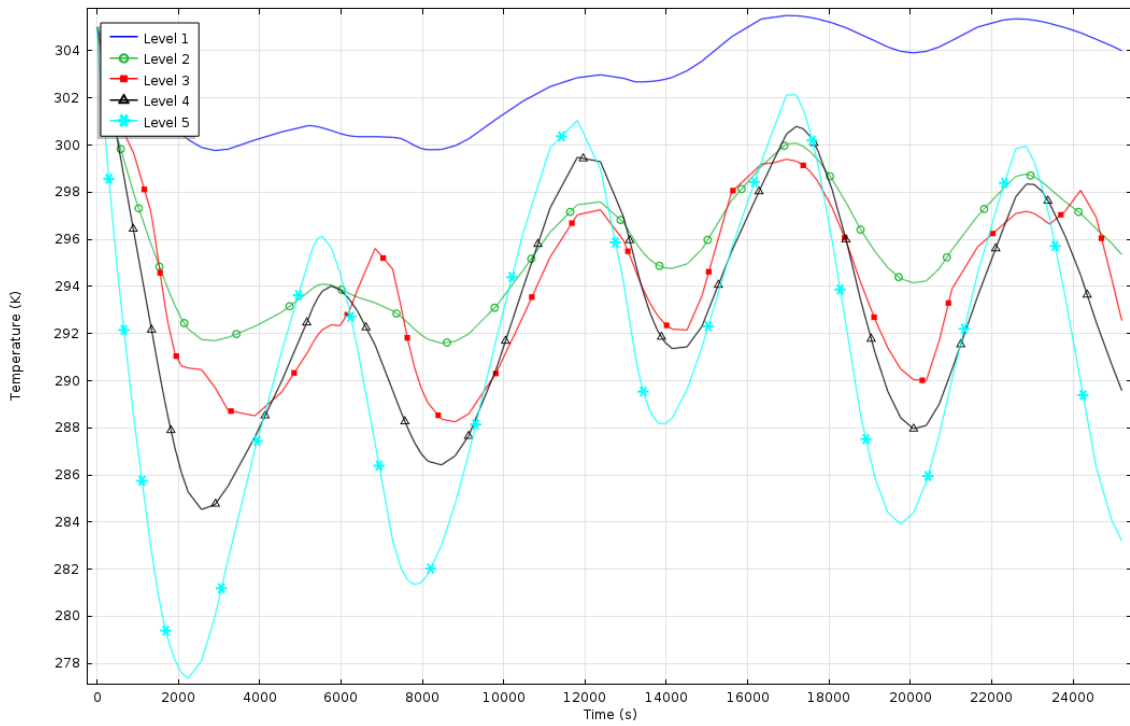


Figure 84: Average Temperature vs. Time for Circuit Boards

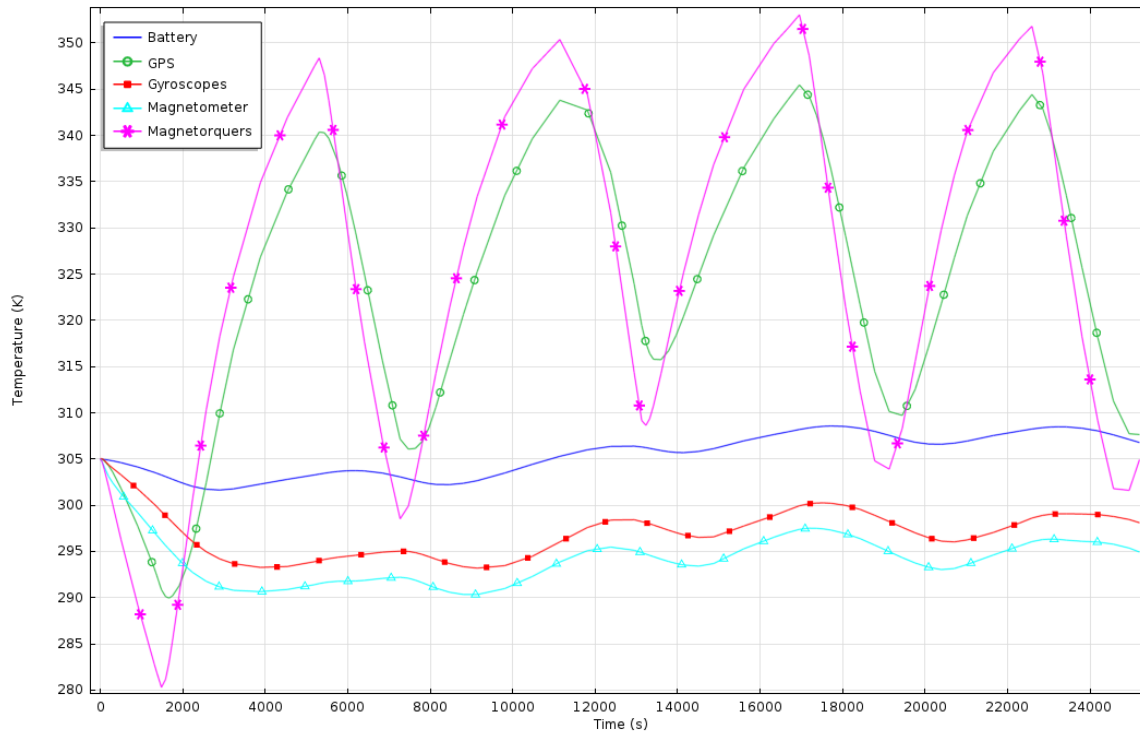


Figure 85: Average Temperature vs. Time for Components

Temperature Requirements

Throughout the five representative orbits, the maximum and minimum steady-state temperature experienced by the CubeSat’s components were approximated from the periodic trends illustrated in Figure 84 and Figure 85. The temperatures are shown in Table 27.

Table 27: Steady-State Temperatures of Components

Part Name	Steady-State Min (K)	Steady-State Max (K)
Gyroscope	290	300
Magnetorquers	300	355
Magnetometer	290	295
GPS	305	345
OBC (Level 5)	282	302

EPS (Level 4)	286	300
Battery	305	310
Transceiver (Level 3)	290	300

Figure 86 demonstrates the temperature range experienced by each component and its operational and survival limits.

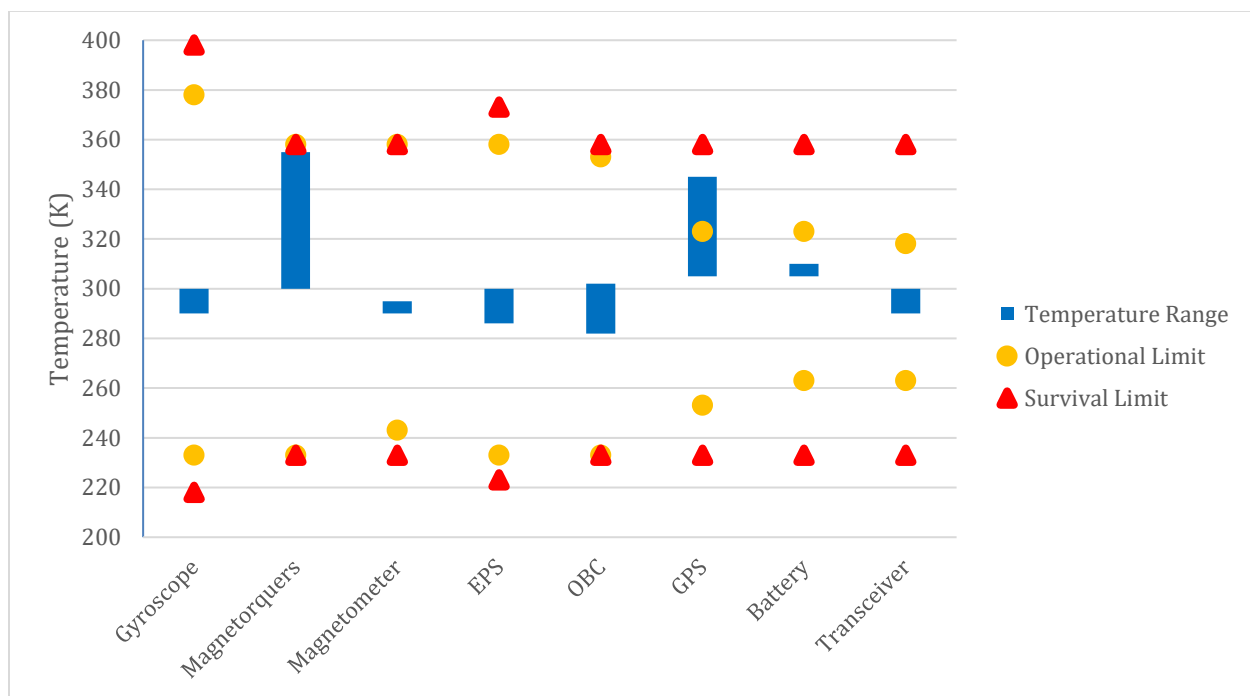


Figure 86: Temperature Range and Limits

The temperatures experienced by the components on the circuit board stack have very little difference between their maximum and minimum. This is because the circuit stack is protected from the Sun by center solar panel and the surface area of standoffs that are in contact with the circuit boards are small; therefore, the amount of heat that is conducted is relatively small. On the other hand the magnitude of and the difference between maximum and minimum temperatures of

GPS and magnetorquers, which are between 32°C and 72°C and 27°C and 82°C respectively, are relatively large because they are in direct contact with the CubeSat frame. As shown in Figure 86, the maximum temperature experienced by the magnetorquers is very close to the operational/survival limit; in addition, the maximum temperature experienced by GPS is below the survival limit, but beyond the operational limit.

Initial results demonstrate that the temperature requirements of the components are met with the exception of the GPS. The GPS is likely to have decreased performance or to generate inaccurate data throughout the mission due to the temperatures outside of the operational limit. To prevent this, introduction of some form of thermal control system was necessary.

4.4.3 Surface Finishes

As discussed in Section 2.4.3, surface finishes are very common type of passive thermal control used in numerous successful space missions. The purpose of surface finishes is to change the solar absorptivity, usually denoted as α , and the emissivity, usually denoted as ϵ . By changing the two values, the amount of heat absorbed from the sun and emitted by the spacecraft can be controlled to reach a desired steady-state temperature, preferably within the specified temperature limit.

In order to decrease the steady-state temperature range of GPS to be within its operational limits, surface finish was the first thermal control option considered. Four additional COMSOL simulations were conducted where the CubeSat frame had different value of surface emissivity in each simulation to represent some applied surface finish. The surface emissivity of the CubeSat frame was varied from 0.3 to 0.9 with 0.2 difference between simulations. Details of all four simulations are summarized in Table 28.

Table 28: Surface Finish Simulation Summary

Simulation	Surface Emissivity
Initial Result	0.115
Simulation 1	0.3
Simulation 2	0.5
Simulation 3	0.7
Simulation 4	0.9

The same procedure used to find the initial result of Section 4.4.2 was followed to analyze the results produced from the surface finish simulations. Figures 87, 88, 89, and 90 illustrate the average temperature of the CubeSat frame, side solar panels, and center solar panels for the surface emissivity values of 0.3, 0.5, 0.7, and 0.9. Figures 91, 92, 93, and 94 illustrate the temperature range, operational, and survival limits of the components for the surface emissivity values of 0.3, 0.5, 0.7, and 0.9.

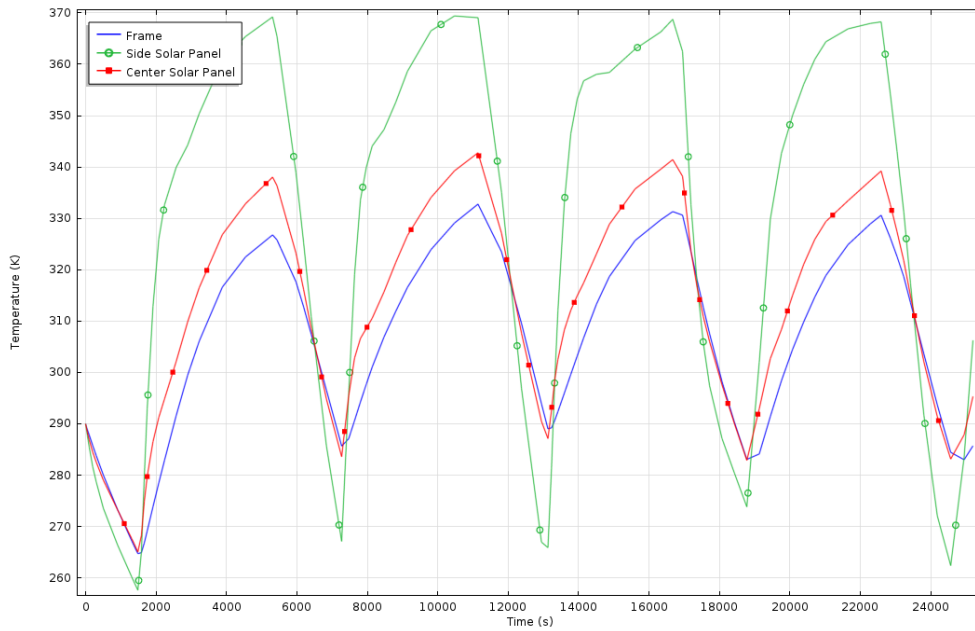


Figure 87: Average Temperature vs. Time for External Domains ($\epsilon = 0.3$)

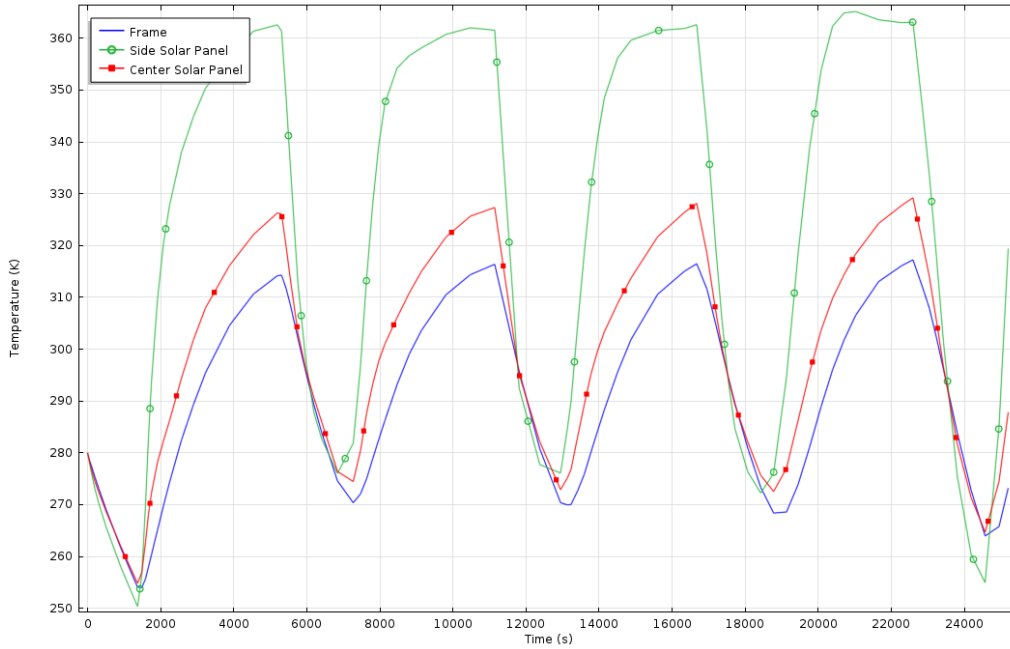


Figure 88: Average Temperature vs. Time for External Domains ($\epsilon = 0.5$)

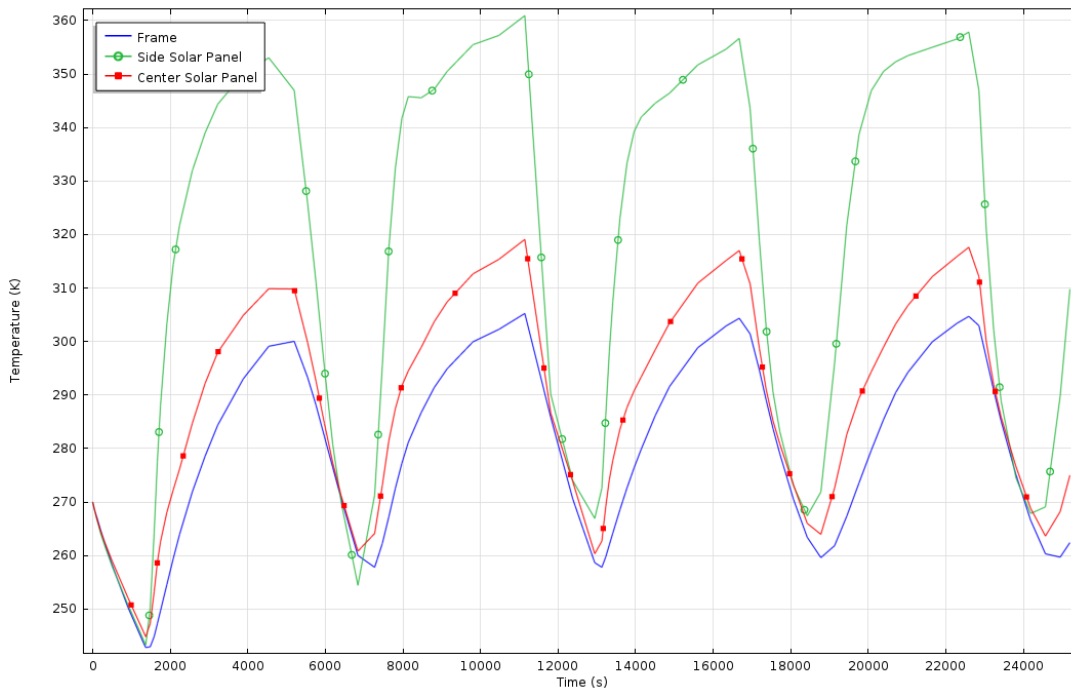


Figure 89: Average Temperature vs. Time for External Domains ($\epsilon = 0.7$)

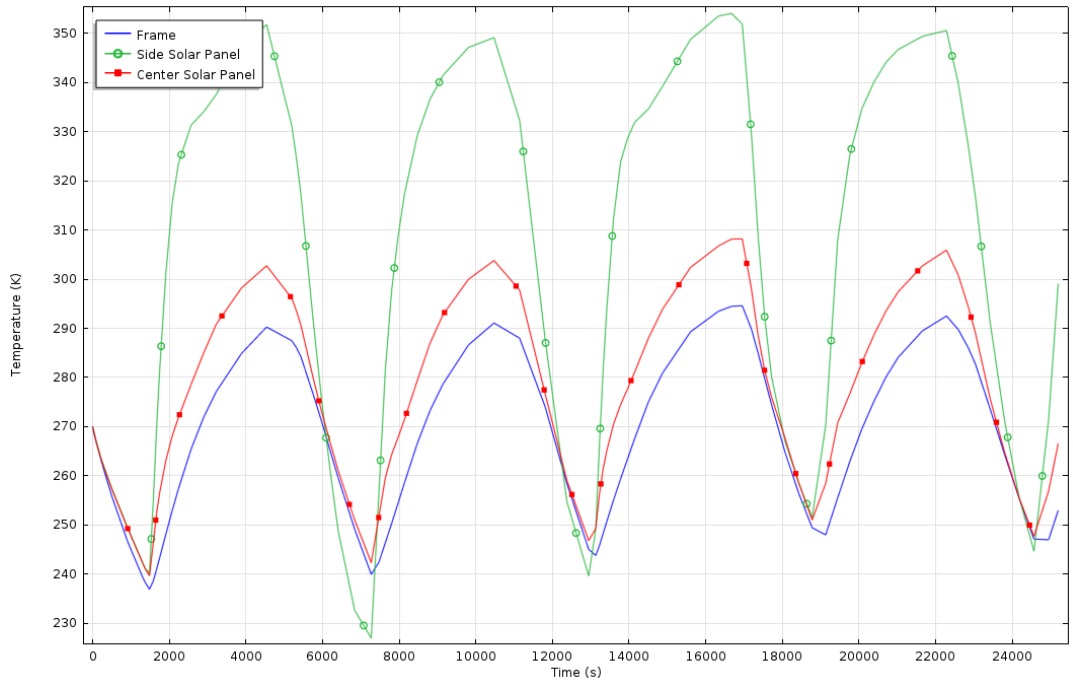


Figure 90: Average Temperature vs. Time for External Domains ($\epsilon = 0.9$)

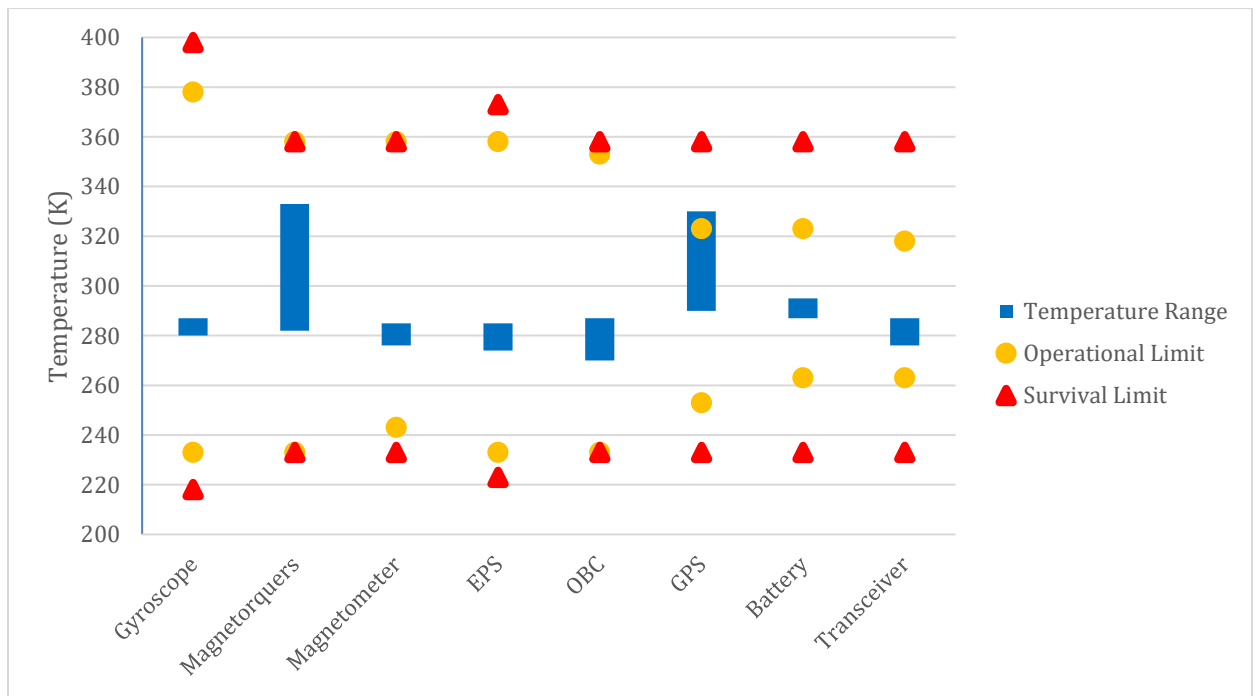


Figure 91: Temperature Range and Limits ($\epsilon = 0.3$)

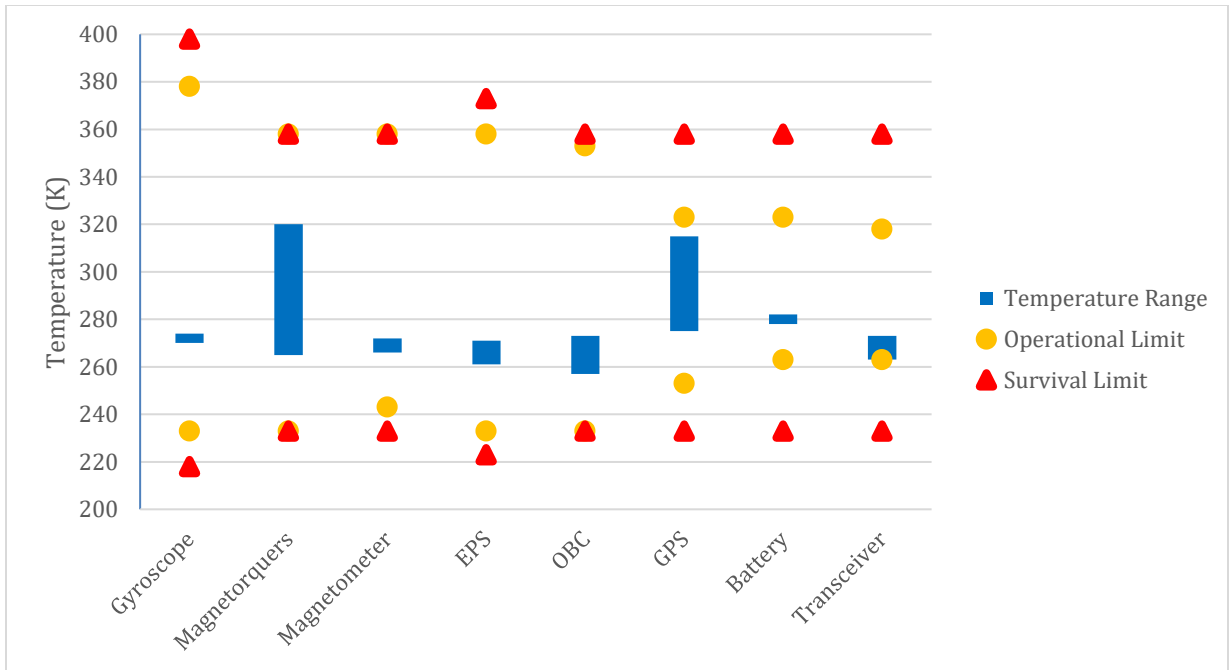


Figure 92: Temperature Range and Limits ($\epsilon = 0.5$)

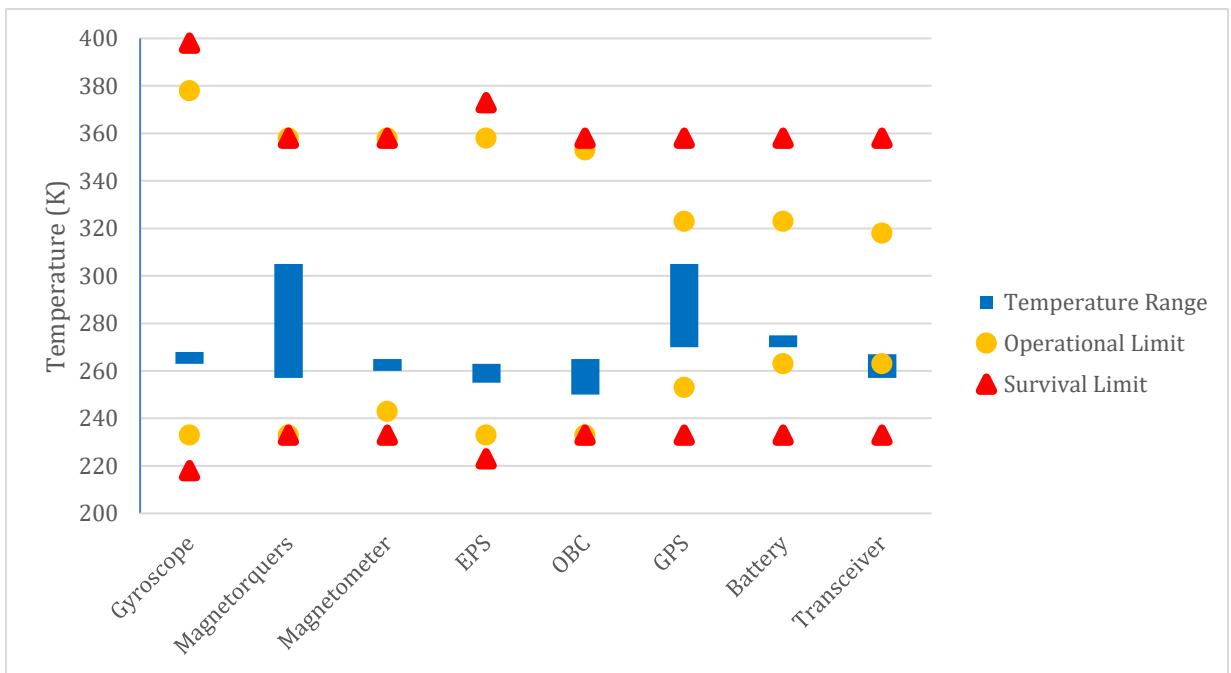


Figure 93: Temperature Range and Limits ($\epsilon = 0.7$)

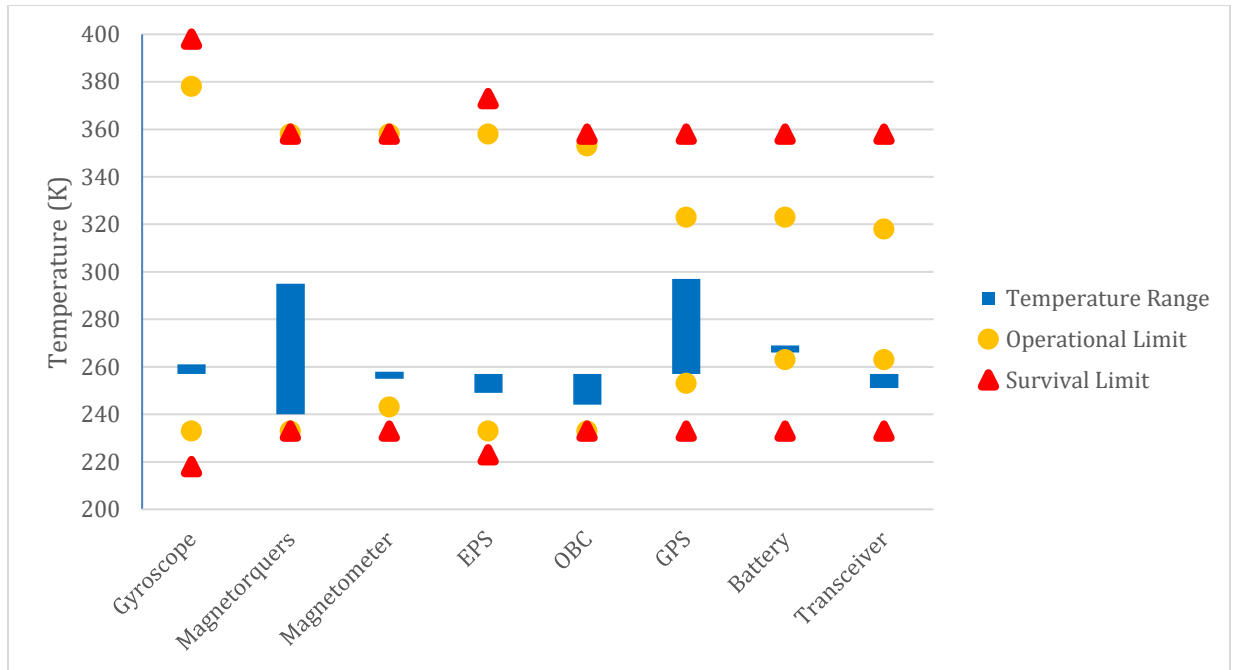


Figure 94: Temperature Range and Limits ($\epsilon = 0.9$)

A surface finish with surface emissivity of 0.5 or higher is required in order to keep the temperature range of GPS within its operational limit. However, it must be noted that surface emissivity of 0.7 or higher results the temperature range of the transceiver to be below its minimum operational range.

4.4.4 Recommended Thermal Control System Design

As shown in Figure 92 and 93 in Section 4.4.3, the temperature range of GPS is within its operational limit when the surface emissivity is equal to or higher than 0.5, but the temperature range of transceiver is within its operational limit only when the surface emissivity is equal to or lower than 0.7. Therefore, the recommended thermal control system design is to apply surface finish with surface emissivity of 0.5 ($\epsilon = 0.5$) and solar absorptivity equal to that of Al5052-H32 ($\alpha = 0.23$) to external surfaces of the CubeSat frame. As shown in Figure 14 in Section 2.4.3, a possible type of surface finish to achieve the recommended design is dielectric films.

5 Conclusions & Recommendations

5.1 Command & Data Handling Subsystem

To improve the results of the C&DH system's analysis, more accurate information regarding sensor and subsystem operation is needed. Knowing how much data is produced by each component in reality is critical to an accurate model of the system. Additionally, improved understanding of the scientific goals of the mission would be useful for determining what actions should be prioritized throughout CubeSat's lifespan. Such information would include which types of data should be sought for downlink first, and the resolution of data (i.e. time gaps between readings) sought in each downlink.

Eventually, physical modeling of this system should be performed, and the full software to enact all spacecraft operations requires development. Using actual flight software in place on an OBC model with artificial dependents would verify the conclusions made in Section 4.2, and would bring the C&DH subsystem to a level prepared for actual implementation. Throughout this, and all previous steps to develop the C&DH subsystem, interfacing with developers of other subsystems is necessary, and iterative adjustment to the particulars of the C&DH subsystem should be made.

A recommendation for establishing the subsystem functions is to start earlier in the project cycle when the subsystem architecture is still being developed. This would help catch problems and functional gaps earlier in the project when problems are easier to fix. It would also be worth it to spend some time with the each team working through various scenarios, checking for any consistencies in the system's abilities.

5.2 Power Subsystem

The most immediate next step in the development of the power subsystem would be to design the unifying board as described in Section 4.2.2. This would involve laying out the existing components as well as designing the magnetorquer control circuitry. Future teams could go further, and build a prototype of this unifying board as well. In addition, future work could focus on identifying the power connection for the Sphinx-NG and the serial connectors found on the GPS and fine sun sensor.

Additionally, should any of the currently selected hardware or mission requirements change in the future, the analysis that was carried out for the power profile will need to be reiterated using such new hardware specifications.

5.3 Telecommunications Subsystem

Although STK was used to calculate the link budget for the spacecraft-ground communications, increased fidelity to the STK model is necessary to correctly garner the outputted numbers. By having more accurate and complete modeling of the CubeSat and Ground Station hardware, the link budget calculations would be much more reasonable as currently, the calculated link budget parameters are not within the range of reason for a CubeSat's capabilities.

This project also established the importance of having established ground stations where the CubeSat can communicate with as the previously baselined ground station system, GENSO, was determined to be non-operational. Moving forward, further research needs to be conducted on which ground stations are available for communicative purposes.

Also researched in this project was the concept of WPI owned Mobile Ground Stations at WPI global project sites. If this is selected as a ground station option, there will need to be a significant amount of work with the university to develop the logistics needed to establish them.

5.4 Thermal Subsystem

During the course of this MQP, a number of challenges and lapses in information were encountered that could not be addressed due to time constraints. These are detailed as recommendations to future project groups as areas in the current thermal design that need improvement.

The first recommendation to future groups is to seek more accurate information on the energy dissipated as waste heat by electrical components in the CubeSat. In this MQP's thermal model we made the assumption that 10% of the power draw of a component is radiated as waste heat, which means that all parts were exactly 90% efficient. Although it's possible that this may not be the case in reality but due to time constraints further research into part specifications was not viable. The specification sheets that part providers have readily available lack the needed efficiency values; communication with the manufacturers may be required.

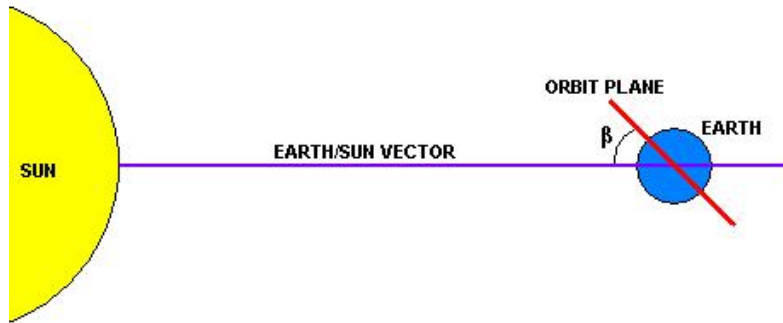
The second recommendation is similarly rooted in a lack of information about some of the parts being used. Though manufacturers have CAD models available of the circuit boards that we used, they do not specify what each displayed component of the board is. A CAD model of a board may clearly display that there is a part at a certain location but we are unsure of which part it is. This means that the team did not know where on the boards things like the gyroscopes were. Considering the variation of temperature seen between different areas of the circuit boards, this could mean the difference between a part being functional or not. Additional communications with

manufacturers is recommended to gain this extra level of detail. This will also broaden the opportunities to create more detailed thermal models, since by knowing what each part of the board is, heat dissipation values can be assigned to as many parts as future teams deem necessary. It is recommended that the future teams work more closely with the mechanical teams to resolve this uncertainty

The next recommendation is that future teams account for the x-axis slip away from the direction of sun that occurs during eclipse. The current model assumes that the sun is always normal to the solar panels of the spacecraft, however during eclipse the spacecraft does not currently use the magnetorquers to perform attitude control [9]. The control algorithm only resumes once the sun vector can again be determined on the sunward side of the Earth. This means there may be a significant amount of time that the nadir constraint would not be preserved. Further analysis in STK is needed to determine how far out of sun alignment the spacecraft will drift in eclipse, and the future team will need to communicate with the ADC team to perform such analysis to determine how long it will take for the spacecraft to reorient itself [9].

Another recommendation is that future teams conduct hot case, cold case analysis on the thermal properties of the spacecraft. Over time the orbit of the spacecraft will shift and the beta angle, the angle formed between the orbital plane and the vector between the sun and the earth, will vary due to the changing seasons and orbital precession [70].

This directly impacts the duration that the satellite is in illumination, creating new hot and cold cases that all components will need to endure. In Figure 96 the fraction of orbit spent in sunlight is displayed for a satellite in a 408 km orbit around the earth as the Beta angle varies. It clearly shows how the amount of sunlight and therefore the peak temperatures increase as the Beta angle approaches 90 degrees.



View from above Earth, looking down on N Pole (orbit $i = 90^\circ$)

Figure 95: Beta Angle of Satellite [70].
 Copyright © 2005 Colorado Center for Astrodynamics Research.

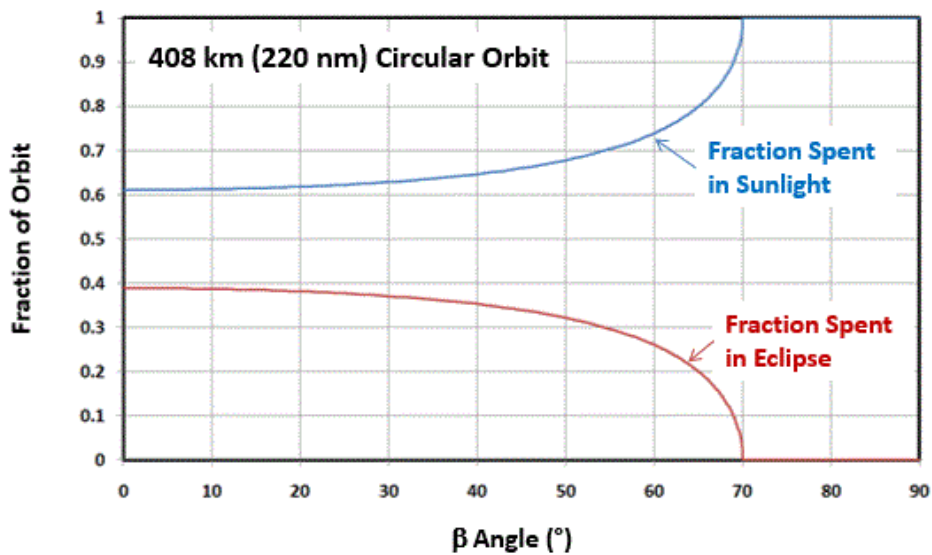


Figure 96: Beta Angle Effect on Illumination of Spacecraft [71].
 Copyright © 2016 NASA Engineering and Safety Center

The simulation that the team performed used the initial orbit that the orbital team deemed a likely candidate, the team did not account for variations over time in the orbit. Teams in the future should investigate how the orbit of a satellite is likely to drift over the course of its mission, and from those results create maximum sunlight and minimum sunlight simulations of the thermal profile.

The next recommendation for future teams is to further define the y and z axis orientation. Currently the only defined axis orientation of the spacecraft is its x-axis, which points towards the sun. In the model it was assumed that the z axis would be pointing towards the earth, and so the Earth's infrared radiation and albedo radiation primarily affect those surfaces on the spacecraft that are perpendicular to the z axis. Discussion with the ADC team [9] to determine the orientation of the other axes of the spacecraft will be required to ensure that the radiation from the Earth is affecting the correct faces of the spacecraft.

Works Cited

- [1] MQP JB3-CBS3, Jenifer Hanley, Brian Joseph, Martha Miller, Samantha Monte, Joshua Trudeau, Racheal Weinrick, Advisor: J. Blandino, "Thermal, Telecommunication Power Systems for a CubeSat", Worcester Polytechnic Institute, 2013.
- [2] MQP NAG-1102, Celena Dopart, Robert Morlath, Erik Oliver, Jake Schomaker, Advisor: N. Gatsonis, "Design and Analysis for a CubeSat Mission", Worcester Polytechnic Institute, 2012.
- [3] MQP MAD-D11A, Assad Farhad, Jig Ivase, Ye Lu, Allan Snapp, Advisor: M. Demetriou, "Attitude Determination and Control System for CubeSat", Worcester Polytechnic Institute, 2012.
- [4] MQP JB3-CBS2, Joe Bauer, Michael Carter, Kaitlyn Kelley, Ernie Mello, Sam Neu, Alex Orphanos, Tim Shaffer, Andrew Withrow, Advisor: J. Blandino, "Mechanical, Power, and Thermal Subsystem Design for a CubeSat Mission", Worcester Polytechnic Institute, 2012.
- [5] MQP NAG-1204, Dylan Billings, Ilea Gradel, Francis Hoey, Peter Lavallee, Nicolas Martinez, Advisor: N. Gatsonis, "Design and Analysis for a CubeSat Mission", Worcester Polytechnic Institute, 2013.
- [6] MQP MAD-2013, Elizabeth Dawson, Nelly Nassiff, Diana Velez, Advisor: M. Demetriou, "Determination and Control System Design For A CubeSat Mission", Worcester Polytechnic Institute, 2013.
- [7] MQP NAG-1701, Emily Curci, Jarrett Jacobson, Weston Schlack, Kelley Slabinski, Advisor: N. Gatsonis, "Design and Analysis of the Sphinx-NG CubeSat", Worcester Polytechnic Institute, 2017
- [8] MQP JB3-1701, Dong Hyun Ko, Steven Laudage, Matthew Murphy, Daniel Pelgrift, Sam Young, Advisor: J. Blandino, "Design and Analysis of the Sphinx-NG CubeSat", Worcester Polytechnic Institute, 2017
- [9] MQP MAD-1701, Jack Agolli, James Gadoury, Andrew Rathbun, Advisor: M. Demetriou, "Design and Analysis of the Sphinx-NG CubeSat", Worcester Polytechnic Institute, 2017
- [10] Blandino, J.J., Martinez, N., Demetriou, M. A., Gatsonis, N. A., Paschalidis, N., "Feasibility for Orbital Life Extension of a CubeSat Flying in the Lower Thermosphere", *Journal of Spacecraft and Rockets*, Vol. 53, No. 5, pp. 864-875, 2016. DOI:10.2514/1.A33462
- [11] Gatsonis, N.A., Ye, L., Blandino, J.J., Demetriou, M., Paschalidis, N., "Micro Pulsed Plasma Thrusters for Attitude Control of a Low Earth Orbiting CubeSat," *Journal of Spacecraft and Rockets*, Vol. 53, No. 1, pp. 57-73, 2016. DOI: 10.2514/1.A33345.
- [12] Kewen Z., Gatsonis, N.A., Blandino, J. J., Demetriou, M. A., "Nanosat Orbit Raising and Rendezvous Using a Continuous-Thrust Controller," AIAA 2017-0163, 55th AIAA Aerospace Sciences Meeting, Grapevine TX, Jan. 9-13, 2017, DOI 10.2514/6.2017-0163
- [13] Blandino, John J. Personal Communication. 16 September 2016.
- [14] Clyde Space, "On Board Computer Interface Control Document," 08 September 2016.

- [15] Consultative Committee for Space Data Systems, "CCSDS File Delivery Protocol (CFDP)," CCSDS Secretariat Office of Space Communication, Washington, DC, October 2013.
- [16] L.J. Hansen, R.W. Hoksen, and C.H. Pollock, "Spacecraft Computer Systems," in *Space Mission Analysis and Design (3rd Edition)*, Microcosm Press, 1999, pp. 645-684.
- [17] I2C Info, "I2C Info – I2C Bus, Interface and Protocol," 2016. [Online]. Available: <http://i2c.info/>. [Accessed 08 October 2016].
- [18] C.M.L. Burnett, "SPI Three Slaves," 19 December 2006. [Online]. Available: https://commons.wikimedia.org/wiki/File:SPI_three_slaves.svg. [Accessed 08 October 2016].
- [19] Byte Paradigm, "Introduction to I²C and SPI protocols," 2016. [Online]. Available: <http://www.byteparadigm.com/applications/introduction-to-i2c-and-spi-protocols/>. [Accessed 08 October 2016].
- [20] Sparkfun, "Serial Communication," 18 December 2012. [Online]. Available: <https://learn.sparkfun.com/tutorials/serial-communication> [Accessed 26 January 2017].
- [21] R.T. Berget, "Command and Data Handling," in *Space Mission Analysis and Design (3rd Edition)*, Microcosm Press, 1999, pp. 395-407.
- [22] Wertz, J. R., & Larson, W. J. (Eds.). (1999). *Space Mission Analysis and Design (3rd Edition ed.)*. New York, NY; Hawthorne, CA: Springer; Microcosm Press.
- [23] Clyde Space, "3rd Generation 3U EPS," clyde.space, [Online]. Available: <https://www.clyde.space/products/5-3rd-generation-3u-eps>. [Accessed 27 September, 2016].
- [24] Cal Poly SLO, "Launch Services Program: Program Level Poly-Picosatellite Orbital Deployer (PPOD) and CubeSat Requirements Document," National Aeronautics and Space Administration, John F. Kennedy Space Center, Florida, LSP-REQ-317.01 Rev. A 2011.
- [25] National Aeronautics and Space Administration, "Standard Materials and Processes Requirements for Spacecraft," Launch Services Program, Washington DC, NASA STD-6016 2013.
- [26] National Aeronautics and Space Administration, "NASA Procedural Requirements for Limiting Orbital Debris (w/ Change 1 - 5/14/09)," NASA, 2009.
- [27] CubeSats Need Coordination Too - SpaceNews.com. (2013, October 28). Retrieved October 12, 2016, from <http://spacenews.com/37890editorial-cubesats-need-coordination-too/>
- [28] Amateur apparatus licences. (n.d.). Retrieved January 24, 2017, from <http://www.acma.gov.au/Industry/Spectrum/Radiocomms-licensing/Apparatus-licences/amateur-apparatus-licence-information-paper>
- [29] Federal Register of Legislation - Australian Government. (n.d.). Retrieved January 24, 2017, from <https://www.legislation.gov.au/Details/F2016C00286>
- [30] Radio HF/VHF/UHF. (n.d.). Retrieved October 12, 2016, from <https://www.ito-inc.com/tech7.html>

- [31] ESA. (n.d.). Satellite frequency bands. Retrieved October 12, 2016, from http://www.esa.int/Our_Activities/Telecommunications_Integrated_Applications/Satellite_frequency_bands
- [32] VHF downlink/UHF uplink Full Duplex Transceiver. (n.d.). Retrieved January 24, 2017, from <https://www.cubesatshop.com/product/isis-vhf-downlink-uhf-uplink-full-duplex-transceiver>
- [33] Antenna Design Overview. (n.d.). Retrieved October 12, 2016, from <http://ardupilot.org/copter/docs/common-antenna-design.html>
Winder, S., & Carr, J. (n.d.). Newnes Radio and RF Engineering Pocket Book. Retrieved January 24, 2017, from https://books.google.com/books?id=3b_InpSowcC&pg=PA4&dq=%22simplest%2Bpractical%2Bbradiator#v=onepage&q=%22simplest%20practical%20radiator&f=false
- [34] Winder, S., & Carr, J. (n.d.). Newnes Radio and RF Engineering Pocket Book. Retrieved January 24, 2017, from https://books.google.com/books?id=3b_InpSowcC&pg=PA4&dq=%22simplest%2Bpractical%2Bbradiator#v=onepage&q=%22simplest%20practical%20radiator&f=false
- [35] Dipole antenna system. (n.d.). Retrieved January 24, 2017, from <https://www.isispace.nl/product/dipole-antenna/>
- [36] ESA Bulletin 149. (n.d.). Retrieved January 24, 2017, from <http://esamultimedia.esa.int/multimedia/publications/ESA-Bulletin-149/pageflip.html>
- [37] Communications System. (n.d.). Retrieved October 12, 2016, from <http://www.qrg.northwestern.edu/projects/vss/docs/communications/1-what-are-uplink- and-downlink.html>
- [38] *Space primer*. (2009). Retrieved from <http://www.au.af.mil/au/aupress/digital/pdf/book/AU-18.pdf>
- [39] Lyatt Jaeglé , "Planetary Energy Balance," <http://www.atmos.washington.edu> [Online]. Available:<http://www.atmos.washington.edu/2002Q>
- [40] Eric Coates, "Power in Resistors," [learnabout-electronics.org](http://www.learnabout-electronics.org)[Online]. Available http://www.learnabout-electronics.org/Resistors/resistors_15.php. [Accessed 2 October, 2016].
- [41] Gilmore, D. G., Stuckey, W. K., and Fong, M., "Spacecraft Thermal Control Handbook Volume I: Fundamental Technologies," 2nd edition, 139-141. Retrieved from http://matthewwturner.com/uah/IPT2008_summer/baselines/LOW%20Files/Thermal/Spacecraft%20Thermal%20Control%20Handbook/04.pdf
- [42] Gilmore (ed), David G.. (© 2002). "Spacecraft thermal control handbook, volume I: fundamentals technologies," [Books24x7 version] Retrieved from <http://common.books24x7.com.ezproxy.wpi.edu/toc.aspx?bookid=10788>.
- [43] COMSOL Multiphysics, Ver. 5.0, COMSOL AB, Stockholm, Sweden, 2014 Retrieved from <https://www.comsol.com/products>
- [44] Gianni, D., D'Ambrogio, A., & Tolk, A. (2015). *Modeling and simulation-based systems engineering handbook*. Boca Raton: Taylor & Francis.

- [45] Spangelo, S. C., Kaslow, D., Delp, C., Cole, B., Anderson, L., Fosse, E., . . . Cutler, J. (2012). Applying Model Based Systems Engineering (MBSE) to a standard CubeSat. *2012 IEEE Aerospace Conference*. doi:10.1109/aero.2012.6187339
- [46] The sequence diagram. (2004, February 16). Retrieved February 25, 2017, from <http://www.ibm.com/developerworks/rational/library/3101.html>
- [47] Visio Pro for Office 365. (n.d.). Retrieved February 25, 2017, from https://products.office.com/en-us/Visio/microsoft-visio-pro-for-office-365?wt.srch=1&wt.mc_id=AID522514_SEM_BqRzTA2v
- [48] PC/104 Embedded Consortium. "PC/104 Specification Version 2.6," pc104.org [Online]. Available: https://pc104.org/wp-content/uploads/2015/02/PC104_Spec_v2_6.pdf
- [49] STK. (n.d.). Retrieved January 25, 2017, from <https://www.agi.com/products/stk/>
- [50] *MODULAR GROUNDSTATION DEVELOPMENT* (Rep.). Retrieved December 15, 2016, from http://www.spacegrant.hawaii.edu/reports/16_SUM06-FA06/Ichikawa_Dylan_FA06.pdf
- [51] Rodrigues Capela, C. J. (2012, April). *PROTOCOL OF COMMUNICATION S FOR VORSAT SATELLITE* (Rep.). Retrieved December 15, 2016, from <http://paginas.fe.up.pt/~ee97054/Link Budget.pdf>
- [52] Fantino, E., "14. Thermal Control Subsystem," Polytechnic University of Catalonia, 2013. Retrieved from http://projectehermes.upc.edu/Enginyeria_Aeroespacial/4A/Enginyeria%20espacial/Teoria/14.%20Thermal%20control%20subsystem.pdf
- [53] 7329873 Canada Ltd., "5052-H32 Aluminum," MakeItFrom.com, August 16, 2016, Retrieved from <http://www.makeitfrom.com/material-properties/5052-H32-Aluminum>
- [54] Aalco Metals Ltd., "5052-H32 Sheet and Treadplate", 2017, Retrieved from http://www.aalco.co.uk/datasheets/Aluminium-Alloy-5052-H32-Sheet-and-Treadplate_138.ashx
- [55] Coker, R., "Thermal Modeling and Testing of the Edison Demonstration of Smallsat Networks Project," International Conference on Environmental Systems, July 2014, Retrieved from <https://ntrs.nasa.gov/archive/nasa/casi.ntrs.nasa.gov/20140012465.pdf>
- [56] Peake, N., "CubeSat Component Thermal Modeling," Worcester Polytechnic Institute, Worcester, 2014
- [57] Spectrolab, "28.3% Ultra Triple Junction Solar Cells", 2010.
- [58] Pavlovskis, E., "User Manual: 3rd Generation CubeSat Battery Family," Clyde Space, 14 July, 2014.
- [59] Clyde Space, "40 Whr CubeSat Battery," clyde.space [Online]. Available: <https://www.clyde.space/products/49-40whr-cubesat-battery>. [Accessed 27 September 2016].
- [60] Clyde Space, "2U Single-Deployable Solar Array (Long Edge)," clyde.space [Online]. Available: <https://www.clyde.space/products/33-2u-singledeployable-solar-array-long-edge>
- [61] Pumpkin, "CubeSatKit ProtoBoard Data Sheet Rev. B." cubesatkit.com [Online]. Available from:

- http://www.cubesatkit.com/docs/datasheet/DS_CSK_Protoboard_711-00303-B.pdf
- [62] "Pulse Width Modulation," sparkfun.org [Online] Available from: <https://learn.sparkfun.com/tutorials/pulse-width-modulation>
- [63] Yaesu G-5500. (n.d.). Retrieved February 26, 2017, from https://www.gigaparts.com/Yaesu-G5500.html?gclid=CjwKEAiAg5_CBRDo4o6e4o3NtGAB-IatYAU1F1wriJxyaV2gjcJP0aqk_wJvcSJsthuBk4nII4BoCFivw_wcB
- [64] Yaesu GS-232B. (n.d.). Retrieved February 26, 2017, from <https://www.gigaparts.com/yaesu-gs-232b.html>
- [65] AMSAT - Satellite Related Software. (n.d.). Retrieved February 26, 2017, from <http://www.amsat.org/amsat-new/tools/software.php>
- [66] Yaesu FT-857D. (n.d.). Retrieved February 26, 2017, from https://www.gigaparts.com/Yaesu-FT-857D.html?gclid=CjwKEAiAg5_CBRDo4o6e4o3NtG0JAB-IatY-V-fGpvoeFv_h6ejsj4m8iRf6GeDe9L4sEh_o8TcTRoCEXvw_wcB
- [67] Ordering and Pricing ***UPDATED 03/05/2016*** 570-868-5643 570- 868-6917 FAX. (n.d.). Retrieved February 26, 2017, from <http://www.ssbusa.com/ordering.html>
- [68] BELDEN | 8214 0101000 Coax - RG-8/U Type RG-8/U Type Coax Black. (n.d.). Retrieved February 26, 2017, from https://www.anixter.com/en_us/products/8214-0101000/BELDEN/Coaxial-Cable/p/B8214
- [69] 436CP42UG, 420-440 MHz. (n.d.). Retrieved February 26, 2017, from <http://www.m2inc.com/amateur/436cp42ug-420-440-mhz/>
- [70] Orbital Description- ccar.colorado.edu, September 21, 2006 Retrieved February 23, 2017, from http://ccar.colorado.edu/asen5050/projects/projects_2004/uchida/orbit.html
- [71] Introduction to On-Orbit Thermal Analysis- nescacademy.nasa.gov Retrieved February 24, 2017, from <https://www.google.com/url?sa=t&rct=j&q=&esrc=s&source=web&cd=3&cad=rja&uact=8&ved=0ahUKEwjlmKeDrKvSAhVq74MKHRvBCUgQFggpMAI&url=https%3A%2F%2Fnescacademy.nasa.gov%2Freview%2Fdownloadfile.php%3Ffile%3DOnOrbitThermalEnvironmentsPart3.pptx%26id%3D25%26distr%3DPublic&usg=AFQjCNF20mLQLcrCq3aD9FyPuNae7Hi4Ig&sig2=8syrAVKnpdj9YkAr9yFV8A>
- [72] Cal Poly SLO, "Launch Services Program: Program Level Poly-Picosatellite Orbital Deployer (PPOD) and CubeSat Requirements Document," National Aeronautics and Space Administration, John F. Kennedy Space Center, Florida, LSP-REQ-317.01 Rev. A 2011.
- [73] Cal Poly, "DNEPR Safety Compliance Requirements," August 5, 2004, pp. 2-3,10.
- [74] NASA, "General Environmental Verification Standard (GEVS)," 2005, pp. 2.6-1,2,4.

- [75] L. C. P. M. Solie, "Launch Safety Requirements For Air Force Space Command Organizations," Air Force Space Command, AFSPCMAN91-711 2007.
- [76] COMSOL Multiphysics, "COMSOL_ReferenceManual," Documentation within Software Package, Ver. 5.0, COMSOL AB, Stockholm, Sweden, 2014
- [77] COMSOL Multiphysics, "Heat Transfer Module User's Guide," Documentation within software Package, Ver. 5.0, COMSOL AB, Stockholm, Sweden, 2014
- [78] Bejan, A. (ed.), Kraus, A.D. (ed.), "Heat Transfer Handbook", John Wiley & Sons, Hoboken, NJ, 2003.
- [79] Datta, S., "Piezoelectric Materials: Crystal Orientation and Poling Direction," COMSOL Blog, COMSOL Inc., 2014
- [80] Analog Devices, "ADXRS453 Data Sheet Rev. B," analog.com [Online]
Available from: <http://www.analog.com/media/en/technical-documentation/data-sheets/ADXRS453.pdf>
- [81] Honeywell, "3-Axis Digital Compass IC HMC5883L," honeywell.com [Online]
Available from:
https://aerocontent.honeywell.com/aero/common/documents/myaerospacecatalog-documents/Defense_Brochures-documents/HMC5883L_3-Axis_Digital_Compass_IC.pdf
- [82] Surrey Satellite Technology, "SGR-05U Product Sheet," sst-us.com [Online]
Available from: <https://www.sst-us.com/shop/satellite-subsystems/global-positioning-systems-gps-receivers/sgr-05u-space-gps-receiver>

Appendices

Appendix A: GENSO Ground Stations [34]

ORGANIZATION (country)	COMPONENT (satellite)
Aalto University (Finland)	GSS
California Polytechnic State University (United States)	GSS
Delft University of Technology (Netherlands)	MCC (Delft)
ESOC (Germany)	GSS
ESTEC (Netherlands)	GSS
Swiss Federal Institute of Technology in Lausanne (EPFL), Space Centre (Switzerland)	MCC (SwissCube)
Swiss Federal Institute of Technology in Lausanne (EPFL), Space Centre (Switzerland)	GSS
Graz University of Technology (Austria)	GSS
International Space University (France)	GSS
Isis Space (Netherlands)	GSS
MyGroundStations.com (UK)	GSS

Polytechnic University of Catalonia (Spain)	GSS
Radio Amateur – G3VZV (UK)	GSS
Radio Amateur – G4DPZ (UK)	GSS
Radio Amateur – KA0SWT (United States)	GSS
Sergio Arboleda University (Colombia)	GSS
University of Applied Sciences, Heidelberg (Germany)	GSS
University of Kentucky (United States)	GSS
University of Montpellier (France)	GSS
University of New Mexico, Configurable Space Microsystems Innovations & Applications Centre (United States)	GSS
University of Surrey, Surrey Space Centre (UK)	GSS
University of Texas at Austin (United States)	MCC (FASTRAC 1)
University of Texas at Austin (United States)	MCC (FASTRAC 2)
University of Texas at Austin (United States)	GSS
University of Valladolid (Spain)	GSS

University of Vigo (Spain)	AUS
University of Vigo (Spain)	MCC (Test Satellites)
University of Vigo (Spain)	MCC (Xatcobeo)
University of Vigo (Spain)	GSS
University of York (UK)	GSS
University of La Reunion, LIM, ESIROI IT Dept (Réunion/France)	GSS
Stanford Research Institute International & University of Michigan, College of Engineering	MCC (RAX-2)
University of Michigan (United States)	MCC (M-CUBED)
Sapienza University of Rome	MCC (UniCubeSat-GG)
Warsaw University of Technology & Space Research Centre of Polish Academy of Sciences	MCC (PW-Sat)
Politecnico di Torino (Italy)	MCC (E-st@r)
Hungary	MCC (MaSat-1)
IDeTIC-ULPGC (University of Las Palmas de Gran Canaria) (Spain, Canary Islands)	GSS

Appendix B: Subsystem and Sensor Computing Requirements

Subsystem Name & Person of Contact:	PMAD, Dan Pelgrift	ADCS, Andrew Rathbun
Date:	09/18/16	09/20/2016
Sensor/System Name:	Electrical Power System	Fine Sun Sensor
Quantity of Sensor/System:	1	1
What does the computer need to do for this sensor/system? e.g. store data in memory and then send to telecom system; calculate ephemeris; control whether or not the system itself is on <i>Note: the computer can be required to do multiple things for a sensor/system</i>	Contains 24 switches that can be turned on and off by the OBC. The status and current through each switch can also be retrieved at any time by the OBC. Also provides telemetry and health information on the solar panels, battery, and other components.	TBD
When is this sensor/system on? e.g. when the s/c can see the sun; 40% of the time; always; once per orbit	Always	In view of Sun
When the system/sensor is interacting with the computer, how frequently will the computer need to perform each operation listed in Row 3? (Preferably answer in Hz, i.e. times per second) e.g. calculate new orbital propagation estimate at 10 Hz; send sun sensor readings at 4 Hz		10HZ
How much data will be generated by this sensor/system? e.g. 1KB per orbit; 0.5KB per reading		-
How long will this data need to be stored? e.g. until calculations have been performed on it, then it can be overwritten; until it can be relayed to a ground station; for the life of the s/c		Until Calc Performed
Does the processing of this data need to be done in space? e.g. the ACDS system does need to be controlled in space, since time delays would introduce errors in performance, while s/c health information could be relayed to a ground station for processing		Yes
How does this sensor/system connect to the computer? e.g. it must be wired directly into the bus; it has a certain kind of plug that must be accounted for	Connected through Inter Integrated Circuit (I2C) network, data rate of 100kbps	9-Way Female Nano-D

ADCS, Andrew Rathbun	ADCS, Andrew Rathbun	ADCS, Andrew Rathbun	ADCS, Andrew Rathbun
09/20/2016	09/20/2016	09/20/2016	09/20/2016
Coarse Sun Sensor	Magnetometer	Magnetic Torquer	Gyroscope
4	1	3	1

TBD	TBD	TBD	TBD
In view of Sun	Always	Always	Always

NA, Limited by ADC Board	75 Continuous, 160 Single	-	77.5HZ
-	-	-	-

Until Calc Performed	Until Calc Performed	Until Calc Performed	Until Calc Performed
Yes	Yes	Yes	Yes

Flying Leads Two-Wire Serial Flying Leads 14-Lead/16-Lead Pin

Subsystem Name:

ADCS

ADCS

Date:

What operations can your subsystem be commanded to perform?

e.g. ADCS has a control algorithm which can be commanded to execute by the OBC; the EPS might be able to be commanded to turn on/off other subsystems; or apply a certain voltage or current

Note: there can be multiple such operations per subsystem

What inputs are needed to perform this operation?
e.g. ADCS might need magnetic field and sun vector information; the EPS might need the target pin and voltage

ADCS Detumble Algorithm (BDOT)

- Magnetic field reading from magnetometer
- Angular velocities from gyros

ADCS Attitude Maintenance Algorithm (EKF/TRIAD)

- Magnetic field reading from magnetometer
- Sun vector from sun sensors

What outputs are the result of this operation?

e.g. the ADCS algorithm might input currents that need to be applied to magnetorquers; the EPS might have turned a target subsystem off

- Currents to magnetorquers

- Currents to magnetorquers

What triggers this operation to be performed?

e.g. the EPS might take over and force the battery to be recharged by the solar panels when the battery reaches 20% charge remaining

Note: an operation could be triggered by being in a certain Operational State (which can be seen below), by an event, or by something else

Operational State = Detumbling

When triggered, how frequently must this operation be performed?

e.g. the EPS simply might turn something on and then it's done; the ADCS algorithm might update every second

~0.5 s

What is the total time it takes for this operation to be completed?

e.g. 1000s to detumble, or however long it takes until it is commanded to stop (if this is the case, note why it would be commanded to stop)

~3000s

Are there any other subsystems/sensors which you know cannot be active while your subsystem is performing this operation?

e.g. a magnetorquer might cause interference with magnetometer readings, or something to that effect

Similarly, is there any subsystem which must be concurrently operating in order to make this operation successful?

e.g. the telecom transmitter might require the ADCS algorithm to be concurrently operating to ensure optimal antenna pointing

Appendix D: Subsystem and Sensor Data Processing Calculations

Subsystem Name & Person of Contact:	OBC	PMAD, Dan Pelgrit	ADCS, Andrew Rathbun
Sensor/System Name:	OBC	Electrical Power System	Fine Sun Sensor
What does the computer need to do for this sensor/system?	Contains 24 switches that cal	TBD	
Does the processing of this data need to be done in space?	Yes	Connected through Inter Intel	Yes
How does this sensor/system connect to the computer?		9-Way Female Nano-D	
Quantity of Sensor/System:	1	1	1
When is this sensor/system on?	Always	Always	In view of Sun
Time Modifier	1	1	0.67
How frequently will the computer need to perform each operation listed in Row 3? (Hz)			10
How much data?			
How long will this data need to be stored?			Until Calc Performed
SIMAD ESTIMATES (Tables 16-13 & 16-15)	Autonomy, Fault Monitoring, Fault	Power Management	Sun Sensor
Size (Kwords)			
Code	23	1.2	0.5
Data	27.5	0.5	0.1
Typical Throughput (KIPS)	50	5	1
Typical Execution Frequency (Hz)	10	1	1
Throughput (KIPS)	500	5	6.7
Number of I/O Ports	n/a	24	1
Number of Functions per Second	10	1	10
Number of Scheduled Tasks per Second (n)			

Application Functions									
ADCS, Andrew Rathbun	ADCS, Andrew Rathbun	ADCS, Andrew Rathbun	ADCS, Andrew Rathbun	ADCS, Andrew Rathbun	ADCS, Andrew Rathbun	ADCS, Andrew Rathbun	ADCS, Andrew Rathbun	ADCS, Andrew Rathbun	ADCS, Andrew Rathbun
Coarse Sun Sensor	Magnetometer	Magnetic Torquer	Gyroscope	Command Board	GPS	Transfer Data between GPS	TBD	TBD	TBD
TBD	TBD	TBD	TBD	TBD	TBD	TBD	TBD	TBD	TBD
Yes	Yes	Yes	Yes	Yes	Yes	Yes	Yes	Yes	Yes
Flying Leads	Two-Wire Serial	Flying Leads	14-Lead/16-Lead Pin	-	-	-	-	-	-
these don't actually deal with data, they just need to be off/for RS-422, RS-485 & SPI interfacing									
4	1	3	1	1	1	1	1	1	1
In view of Sun	Always	Always	Always	Always	Always	Always	Always	Always	Always
0.67	1	1	1	1	1	1	1	1	1
N/A, Limited by ADC Board	75 Continuous, 160 Single	-	-	77.5	-	-	-	-	-
-	-	-	-	-	-	-	-	-	-
Until Calc Performed	Until Calc Performed	Until Calc Performed	Until Calc Performed	Until Calc Performed	-	-	-	-	-
Sun Sensor	Magnetometer	Magnetic Control	Rate Gyro	Kine. Integration, Error Det., Epi Command Processing	-	-	-	-	-
0.5	0.2	1	0.8	26	1	1	1	1	1
0.1	0.1	0.2	0.5	5.6	4	4	4	4	4
1	1	1	9	129	7	7	7	7	7
1	2	2	10	10	10	10	10	10	10
2.68	75	6	697.5	1290	70	70	70	70	70
4	1	3	16	1	2	2	2	2	2
4	75	6	77.5	10	10	10	10	10	10

SUBTOTALS	Accounting for Uncertainty/ On-Orbit Spare	TOTAL ESTIMATE OF COMPUTER REQUIREMENTS		
69.6 Kwords of code	69.6	139.2	278.4 Kwords of code	285081.6 words of code
47.9 Kwords of data	47.9	95.8	191.6 Kwords of data	196198.4 words of data
3089.08 KIPS throughput	3089.08	6178.16	12356.32 KIPS throughput	12.35632 MIPS
52 I/O Ports			52 I/O Ports	
193.5 Functions Per Second			193.5 Functions Per Second	
774 Scheduled Tasks per Second			774 Scheduled Tasks per Second	

Assuming 16 bit memory:

4561305.6 bits of code	0.54375 megabytes of code
3139174.4 bits of data	0.37421875 megabytes of data
	0.91796875 Megabytes (MB) of software storage

Appendix E: CubeSat Main Header Connections

Header Diagram Legend

	not being used
	stack connection only
	user connections

Header 1

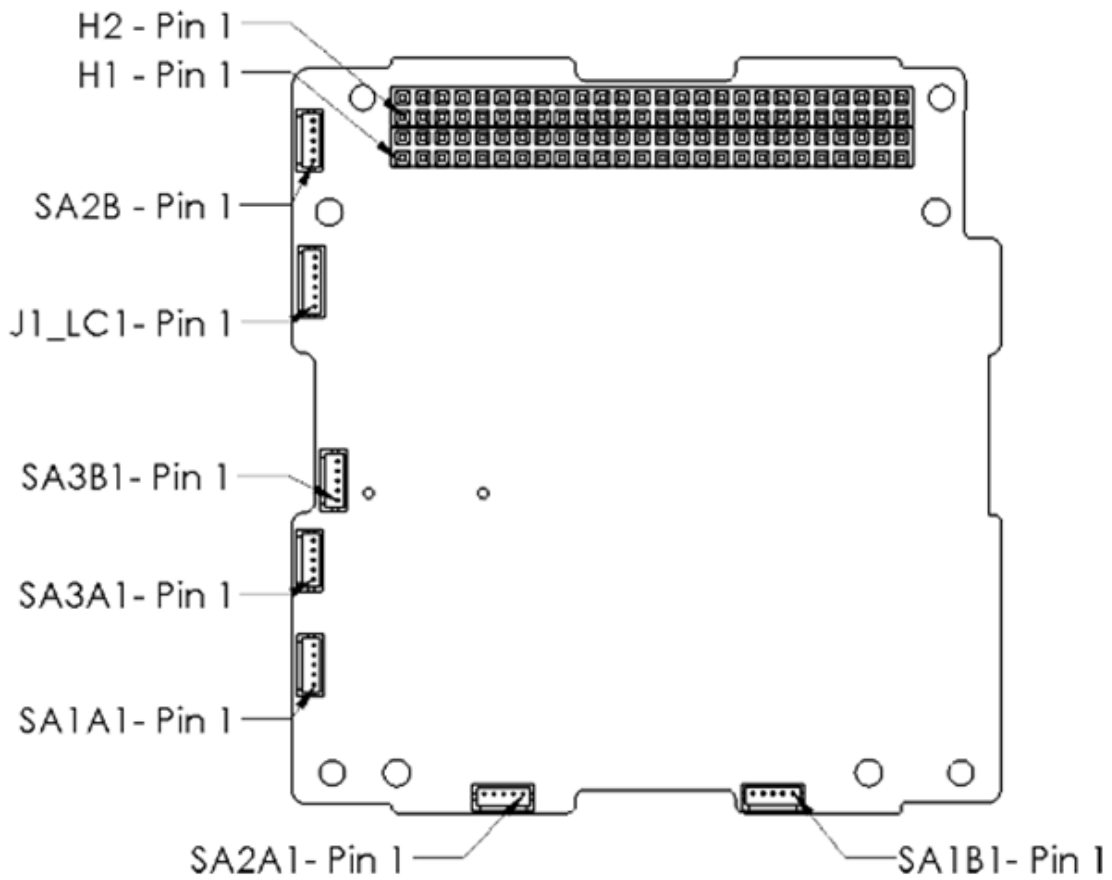
pin	name	use	volt	Connected	pin	name	use	volt	Connected
1	GPIO_A		3.3	-	2	GPIO_B		3.3	-
3	GPIO_C		3.3	-	4	GPIO_D		3.3	-
5	GPIO_E		3.3	-	6	GPIO_F		3.3	-
7	GPIO_G		3.3	-	8	GPIO_H		3.3	-
9	SPI_CS_A	SPI BUS		-	10	SPI_CS_B	SPI BUS		-
11	SPI_CS_C	SPI BUS		-	12	SPI_CS_D	SPI BUS		-
13	SPI_CS_E	SPI BUS		-	14	SPI_CS_F	SPI BUS		-
15	GPIO_J		3.3	-	16	GPIO_K		3.3	-
17	GPIO_L		3.3	-	18	GPIO_M		3.3	-
19				-	20				-
21	SPI_CLK	SPI BUS		Gyroscope	22	SPI_MISO	SPI BUS		Gyroscope
23	SPI_MOSI	SPI BUS		Gyroscope	24	SPI_CS	SPI BUS		Gyroscope
25				-	26				-
27	GPIO_R		3.3	-	28	GPIO_S		3.3	-
29	GPIO_T		3.3	-	30	GPIO_U		3.3	-
31	GPIO_V		3.3	-	32	5VUSB_CHG (EPS)	5V USB Charge		EPS
33	RS232_RXA			-	34	RS232_RXB			-
35	RS232_TXA			-	36	RS232_TXB			-
37	RS422_RXC+			-	38	RS422_TXC+			-
39	RS422_RXC-			-	40	RS422_TXC-			-
41	I2C_DATA/SDA_A	I2C DATA	3.3	Transceiver	42	CANH	Controller Area Network		-
43	I2C_CLK/SCL_A	I2C CLOCK	3.3	Transceiver	44	CANL	Controller Area Network		-
45	SDA_B	I2C DATA	3.3	-	46				-
47	SCL_B	I2C CLOCK	3.3	-	48				-
49				-	50				-
51				-	52				-

Header 2

pin	name	use	volt	Connected	pin	name	use	volt	Connected
1	-			-	2	-			-
3	-			-	4	-			-
5	-			-	6	-			-
7	-			-	8	SW1	PDM 1 Output	12	EPS 12V PDM
9	GND	Ground		-	10	SW2	PDM 2 Output	12	EPS 12V PDM
11	SW3	PDM 3 Output	8.3	EPS BAT PDM (BATT)	12	SW4	PDM 4 Output	8.3	EPS BAT PDM (BATT)
13	SW5	PDM 5 Output	5	EPS 5V PDM, Magnetorquers	14	GND	Ground		-
15	SW6	PDM 6 Output	5	EPS 5V PDM, GPS	16	SW7	PDM 7 Output	5	EPS 5V PDM, Gyroscope
17	GND	Ground		-	18	SW8	PDM 8 Output	3.3	EPS 3V3 PDM, Magnetometer
19	SW9	PDM 9 Output	3.3	EPS 3V3 PDM	20	SW10	PDM 10 Output	3.3	EPS 3V3 PDM
21	GND	Ground		-	22	GND	Ground		-
23	12VBUS	12V Bus		-	24	12VBUS	12V Bus		-
25	5VBUS	5V		-	26	5VBUS	5V		-
27	3V3BUS	3.3V		-	28	3V3BUS	3.3V		-
29	GND	Ground		CSS, Transceiver	30	GND	Ground		Magnetometer, Transceiver
31	-			-	32	GND	Ground		Gyroscope, Transceiver
33	Reserved	-		Do Not Connect	34	Reserved	-		Do Not Connect
35	PCM_IN (EPS)	PCM Input		Deployment Switch 1 & 2, input to PCM's	36	PCM_IN (EPS)	PCM Input		deployment switch 1 & 2: switch on
37	Reserved	-		-	38	Reserved	-		-
39	Reserved	-		-	40	Reserved	-		-
41	BCR_OUT	BCR Output		-	42	BCR_OUT	BCR Output		-
43	BCR_OUT	BCR Output		-	44	BCR_OUT	BCR Output		-
45	BatVBUS	Unregulated Battery Bus	8.3 (BATT)	Transceiver, OBC	46	BatVBUS	Unregulated Battery Bus	8.3 (BATT)	Transceiver, OBC
47	GND	Ground		-	48	GND	Ground		-
49	DTMF1	DTMF Interface	3.3	OBC	50	DTMF2	DTMF Interface	3.3	OBC
51	DTMF3	DTMF Interface	3.3	OBC	52	DTMF4	DTMF Interface	3.3	OBC

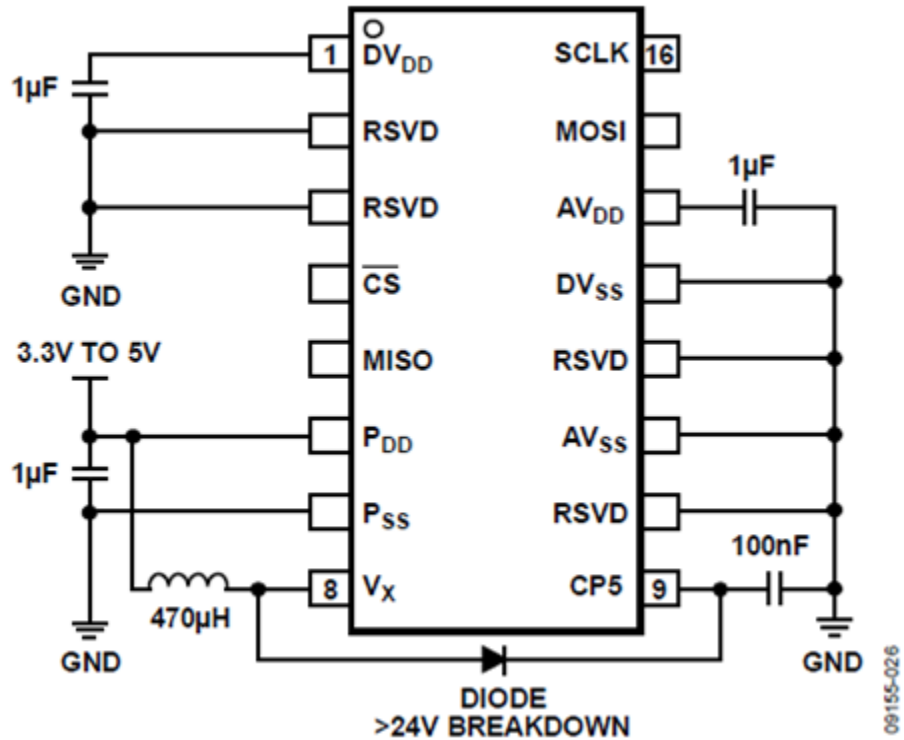
Appendix F: CubeSat Wiring Diagrams

EPS



EPS Solar Array & CubeSat Header Connections [23]

Gyroscope

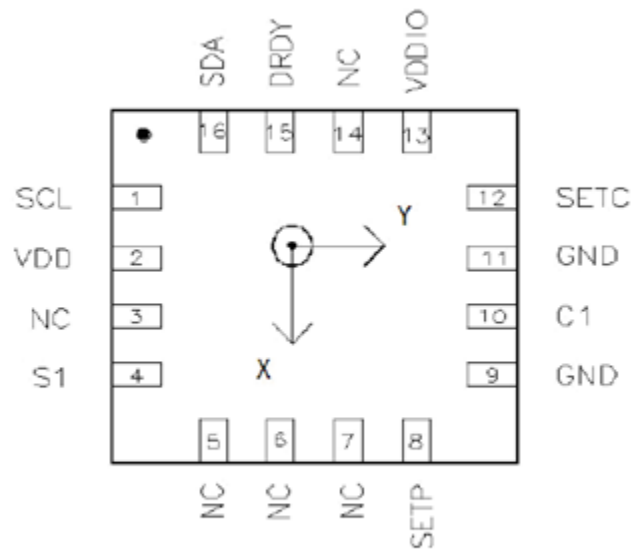


Gyroscope Application Circuit [80]

Gyroscope Header Connections

pin	name	Connected	Notes
1	DV_DD		Digital Regulated Voltage
2	RSVD	H2:32	Reserved
3	RSVD	H2:32	Reserved
4	CS	H1:24	Chip Select
5	MISO	H1:22	Master In/Slave Out
6	P_DD	H2:16	Supply Voltage
7	P_SS		Switching Regulator Ground
8	V_X		High Voltage Switching Node
9	CP5		High Voltage Supply
10	RSVD	H2:32	Reserved
11	AV_SS	H2:32	Analog Ground
12	RSVD	H2:32	Reserved
13	DV_SS	H2:32	Digital Signal Ground
14	AV_DD		Analog Regulated Voltage
15	MOSI	H1:23	Master Out/Slave In
16	SCLK	H1:21	SPI Clock

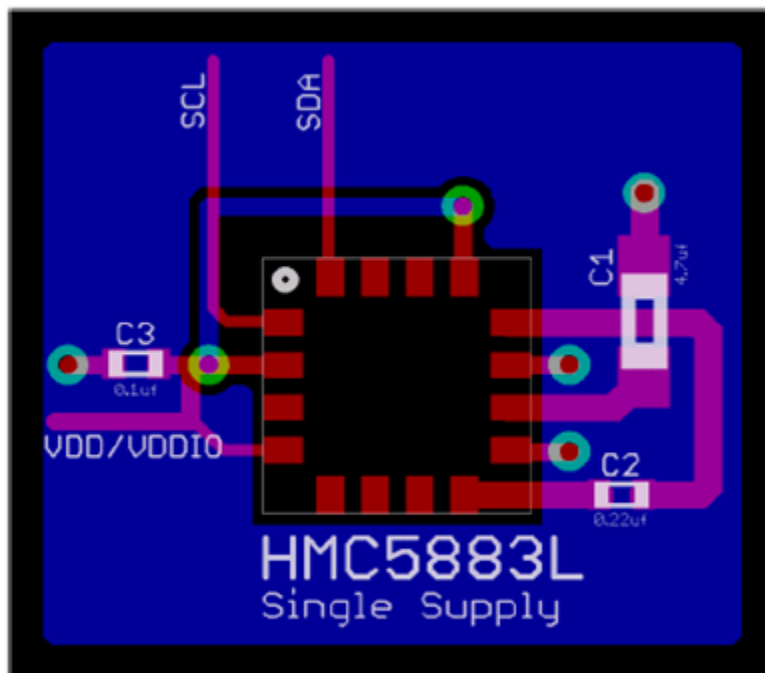
Magnetometer
HMC5883L



TOP VIEW (looking through)

Arrow indicates direction of magnetic field that generates a positive output reading in Normal Measurement configuration.

Magnetometer Pinout Schematic [81]



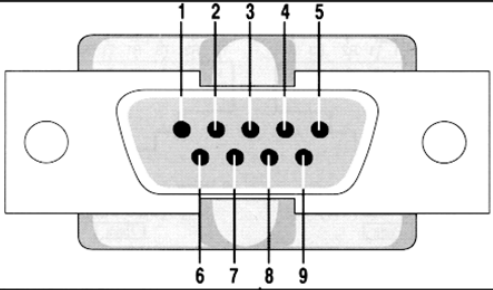
Magnetometer Application Circuit [81]

Magnetometer Header Connections

pin	use	Connected
1	SCL	H1:43
2	VDD	H2:18
3	NC	-
4	S1	VDDIO
5	NC	-
6	NC	-
7	NC	-
8	SETP	SETC
9	GND	H2:30
10	C1	(C1) Cap
11	GND	H2:30
12	SETC	SETP
13	VDDIO	VDD
14	NC	-
15	DRDY	-
16	SDA	H1:41

GPS

number	name	description	level	Dir.	Etc.
1	DCD	Data Carrier Detect	RS232	Input	Mandatory
2	RXD	Receive Data	RS232	Input	Mandatory
3	TXD	Transmit Data	RS232	Output	Mandatory
4	DTR	Data Terminal Ready	RS232	Output	Optional
5	GND	Ground	Ground	-	Mandatory
6	DSR	Data Set Ready	RS232	Input	Optional
7	RTS	Request To Send	RS232	Output	Optional
8	CTS	Clear To Send	RS232	Input	Optional
9	RI	Ring Indicator	RS232	Input	Optional



Pin	Signal	Pin	Signal
1	Data Carrier Detect	6	Data Set Ready
2	Received Data	7	Request to Send
3	Transmitted Data	8	Clear to Send
4	Data Terminal Ready	9	Ring Indicator
5	Signal Ground		

GPS Connector Pin Designation [82]